Correlation between *Mycobacterium avium* ssp. *paratuberculosis* infection and colitis

Von der Fakultät für Lebenswissenschaften

der Technischen Universität Carolo-Wilhelmina

zu Braunschweig

zur Erlangung des Grades

eines Doktors der Naturwissenschaften

(Dr. rer. nat.)

genehmigte

D i s s e r t a t i o n

von Abdulhadi Suwandi
aus Bandung/Indonesien

1. Referent: Privatdozent Dr. Gerhard Gross
2. Referent: Professor Dr. Stefan Dübel
eingereicht am: 23.10.2013
mündliche Prüfung (Disputation) am: 18.12.2013

Druckjahr 2014

Vorveröffentlichungen der Dissertation

Teilergebnisse aus dieser Arbeit wurden mit Genehmigung der Fakultät für Lebenswissenschaften, vertreten durch den Mentor der Arbeit, in folgenden Beiträgen vorab veröffentlicht:

Publikationen

Suwandi, A., Bargen, I., Roy, B., Pils, M.C., Krey, M., Zur Lage, S., Basler, T., Rohde, M. , Falk, C.S., Hornef, M.W., Goethe, R., Weiß, S.: Experimental colitis is exacerbated by concomitant infection with *Mycobacterium avium* subsp. *paratuberculosis* (submitted).

Suwandi, A., Bargen, I., Pils, M.C., Krey, M., Zur Lage, S., Singh, A.K., Basler, T., Falk, C.S., Seidler, U., Hornef, M.W., Goethe, R., Weiß, S.: Role of CD4+ T cells inducing colitis after secondary challenge with *Mycobacterium avium* subsp. *paratuberculosis* in mice (in preparation).

Tagungsbeiträge

Suwandi, A., Bargen, I., Hornef, M.W., Goethe, R., Weiß, S.: Correlation between MAP infection and colitis (Poster). 1st Public Retreat HZI Graduate School, Quedlinburg (2010).

Suwandi, A., Bargen, I., Hornef, M.W., Goethe, R., Weiß, S.: Correlation between MAP infection and colitis (Poster). 4th International PhD Symposium, HZI, Braunschweig (2010).

Suwandi, A., Bargen, I., Hornef, M.W., Goethe, R., Weiß, S.: Correlation between MAP infection and colitis (Poster). National Symposium on Zoonoses Research, Berlin (2011).

Suwandi, A., Bargen, I., Hornef, M.W., Goethe, R., Weiß, S.: Correlation between MAP infection and colitis (Oral presentation). ZooMAP meeting, Braunschweig (2011).

Suwandi, A., Bargen, I., Hornef, M.W., Goethe, R., Weiß, S.: Correlation between MAP infection and colitis (Oral presentation). 2nd Public Retreat HZI Graduate School, Hahnenklee (2011).

Suwandi, A., Bargen, I., Hornef, M.W., Goethe, R., Weiß, S.: Correlation between MAP infection and colitis (Poster). 5th International PhD Symposium, HZI, Braunschweig (2011).

Suwandi, A., Bargen, I., Pils, M.C., Hornef, M.W., Goethe, R., Weiß, S.: Correlation between MAP infection and colitis (Poster). 8th Spring School on Immunology, Ettal (2012).

Suwandi, A., Bargen, I., Pils, M.C., Hornef, M.W., Goethe, R., Weiß, S.: Correlation between MAP infection and colitis (Poster). EMBO/EMBL Symposium: New Perspective on Immunity and Infection, Heidelberg (2012).

Suwandi, A., Bargen, I., Pils, M.C., Hornef, M.W., Goethe, R., Weiß, S.: Correlation between MAP infection and colitis (Oral presentation). National Symposium on Zoonoses Research, Berlin (2012).

Suwandi, A., Bargen, I., Pils, M.C., Hornef, M.W., Goethe, R., Weiß, S.: Correlation between MAP infection and colitis (Oral presentation). 3rd Public Retreat HZI Graduate School, Bad Bevensen (2012).

Suwandi, A., Bargen, I., Pils, M.C., Hornef, M.W., Goethe, R., Weiß, S.: Correlation between MAP infection and colitis (Oral presentation). Workshop "ZooMAP: From Johne’s disease to Crohn’s disease: still more questions than answers", Hannover (2013).

Suwandi, A., Bargen, I., Pils, M.C., Hornef, M.W., Goethe, R., Weiß, S.: Correlation between MAP infection and colitis (Poster). 16th International Congress of Mucosal Immunology (ICMI), Vancouver, Canada (2013).

Suwandi, A., Bargen, I., Pils, M.C., Hornef, M.W., Goethe, R., Weiß, S.: Correlation between MAP infection and colitis (Poster). 43. Jahrestagung der Deutschen Gesellschaft für Immunologie, Mainz (2013).

Table of Content

Table of Content

1 Introduction

Bacterial pathogens interact with the mammalian immune system that could lead to bacterial clearance or pathology. Mycobacteria are one of the well-known examples of bacteria that cause disease.

1.1 Mycobacteria

The genus *Mycobacterium* belongs to the family of Mycobacteriaceae. They are acid-fast, aerobic, rod shaped, Gram positive bacteria and have a lipid-rich cell envelope (Figure 1.1). One of the characteristic of mycobacteria is the cell wall which is differing from other Gram positive bacteria. It is thicker than any other Gram positive bacteria. The plasma membrane of mycobacteria contains phosphatidylinositol mannoside which is glycosylated to lipoarabinomannan (LAM) and lipomannan (LM) in some of the species. The cell wall skeleton is composed of a peptidoglycan layer linked to polysaccharide side chains consisting of arabinogalactan. These chains are substituted with myolic acids. The complexity of mycobacterial cell wall results in difficulties for many compounds to penetrate to the cell wall thus causing multidrug resistance. Another characteristic that can differentiate the genus *Mycobacterium* from other closely related genera such as *Nocardia, Rhadococcus* and *Corynebacterium* is the molecular predominance of 61 to 71 % of guanine + cytosine content in the genome (Over et al., 2011).

More than 100 different *Mycobacterium* species have been described. The majority of mycobacteria species are non-pathogenic environmental bacteria. However, some of them are clinical important because they are animal and human pathogens. The pathogenic mycobacteria usually exhibit slow growth in comparison to environmental mycobacteria and have the ability to establish residence and to proliferate inside host macrophages. These pathogenic bacteria could survive although the cells have antimicrobial properties. The firstly described pathogenic mycobacteria were *M. tuberculosis* and *M. leprae* being the cause of tuberculosis and leprosy in humans (Cosma et al., 2003).

Pathogenic mycobacteria can generally be divided into several groups; *M. tuberculosis* complex, *M. marinum* and *M. ulcerans*, *M. leprae*, and *M. avium* complex (MAC).

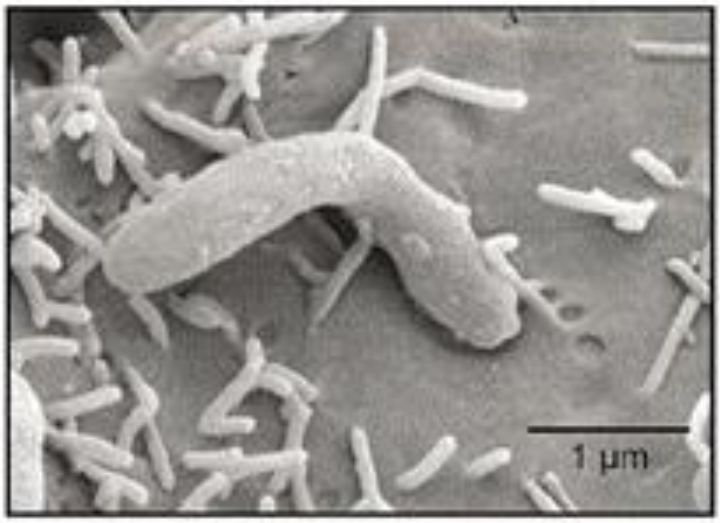

Figure 1.1 Scanning electron microscope image of MAP

Scanning electron microscope image of MAP attaching to murine intestinal epithelial cell line mICcl2 showed the rod shaped of MAP (Pott et al., 2009).

M. bovis, M. africanum, M. mircroti, M. canettii and M. tuberculosis which are the member of *Mycobacterium tuberculosis* complex can cause tuberculosis in humans and animals. Humans are the only natural host for *M. tuberculosis*. In contrast, *M. bovis* has a broad host range in mammals including humans and cattle. Another important mycobacteria species is *M. marinum*, because it is the closest relative of *M. tuberculosis* complex organism. *M. marinum* causes a tuberculosis-like granulomatous infection and disease in fish and frogs as theirs natural hosts. Zebrafish (*Dario rario*) is a particularly model system that is often being used to study this type of tuberculosis.

1.1.1 Mycobacterium avium complex

The other group of mycobacteria is *Mycobacterium avium complex* (MAC). MAC is an environment related mycobacteria and known as nontuberculous

mycobacteria or atypical mycobacteria. These bacteria have been isolated from environment including water, soil, dust and plants (Falkinham et al., 2001). MAC has been known as an opportunistic respiratory infection in immune compromised individuals, particularly in AIDS patients and in elderly individuals. MAC may cause progressive parenchymal lung disease and bronchiectasis in patients.

MAC consists of *M. avium*, *M. intracellulare, M. lepraemurium* and *M. silvaticum*. *M. avium* comprises subspecies such as *M. avium* ssp. *avium* (MAA), *M. avium* ssp. *hominissuis* (MAH) and *M. avium* ssp. *paratuberculosis* (MAP) (Over et al., 2011) which infect different host. MAA is the causative agent of tuberculosis in birds, but also in patients with AIDS, cervical lymphadenitis in children and chronic lung disease in cystic fibrosis patients. Whereas MAH is an opportunistic pathogen found in human and swine (Bruijnesteijn van Coppenraet et al., 2008). Importantly, MAP is a significant pathogen of livestock causing Johne's disease and has been discussed to be involved in Crohn's disease (Cosma et al., 2003).

1.1.2 Mycobacterium avium ssp paratuberculosis

Mycobacterium avium ssp. paratuberculosis (MAP) is the only etiological agent of chronic inflammatory bowel disease in ruminants, known as Johne's disease (JD)(Harris and Barletta, 2001). MAP also has been implicated in Crohn's disease in humans. MAP is an extremely slow growth bacterium that forms colonies after several months or even years (Bull et al., 2003). MAP is clumping in the culture (Merkal and Curran, 1974) and depends on iron chelating mycobactin (Merkal and McCullough, 1982). By polymerase chain reaction (PCR), insertion element (IS) 900 is usually used to distinguish MAP from other mycobacteria (Green et al., 1989). However, the waxy materials contained in the MAP cell wall renders the cells particularly difficult to disrupt to release DNA for PCR (Grant, 2005). Three main groups of MAP strains are distinguished based on the molecular characterization. The groups are called sheep or Type I,

cattle or Type II and intermediate or type III. Types I and III are being sometimes grouped as type I/III due to their close genetic homology (Carta et al., 2013).

MAP is a host-dependent organism which differentiates it from other members of MAC (Olsen et al., 2002). It can survive over a long period of time in the environment like in soil and water, but MAP can only replicate inside macrophages (Grant, 2005). Interestingly, some studies found that MAP is more resistant to heat treatments than other mycobacteria including *M. avium*, *M. chelonae*, *M. xenopi* and *M. scrofulaceum* (Schulze-Röbbecke and Buchholtz, 1992). Strikingly, MAP exhibits a high tenacity and can survive after low-temperature holding treatment at 63^{o}C for 30 minutes and high temperature-short time (HTST) treatment at 72^{o}C for 15 seconds (Millar et al., 1996; Sung and Collins, 1998). In addition, another study constructed thermal death curves for MAP and concluded that pasteurization process was not sufficient to ensure the complete destruction of the organism (Grant et al., 1996). These studies are important since milk might be involved in the transmission of MAP from infected animals to other animals or humans.

1.2 Inflammatory bowel disease

Inflammatory bowel disease (IBD) in humans consists of Crohn's disease (CD) and ulcerative colitis (UC). Although they share many clinical symptoms, they have distinct characteristics. The location of the inflammation in CD occurs anywhere along the digestive tract from mouth to the anus. In UC, the colon is typically the only site that is affected. However, only CD will be discussed in more detail due to its correlation with MAP. Furthermore, Johne's disease is known as an inflammatory bowel disease that affects animals.

1.2.1 Johne's disease

Johne's disease (JD) or paratuberculosis is a chronic, progressive and ultimately fatal disease in the intestines affecting domestic and wild ruminants like cattle, sheep, goats and deer. It was firstly described by German scientist H.A Johne and L. Frothingham in 1895 (Harris and Barletta, 2001). F. W. Twort

was able to culture MAP in the laboratory and transmit the infection thus meeting Koch's postulates in 1912. As described previously, JD is caused by MAP and characterized by regional lymphangitis and lymphadenitis and chronic granulomatous enterocolitis. In the infected host, large lesions, segmental or diffuse are usually seen in the intestines and mesenteric lymph nodes (Olsen et al., 2002). One study described the pathological finding from MAP infected goats showed transmural granulomatous enteritis and often was found with abundant acid-fast bacilli (Lybeck et al., 2013). These were more evident in the proximal jejunum and jejunal lymph nodes (Figure 1.2).The clinical symptoms of JD are loss of body weight, diarrhea, decreased in milk production and death in the later stage (Clarke, 1997). Dairy industry is affected significantly due to productivity loss, infertility and direct cost of diagnosis and control. The infected animals show decreased milk production and need to be culled because they shed large amounts of MAP in feces and milk which can transmit the bacteria.

The bacteria most likely transmit via the fecal oral route either through contaminated milk, colostrum, feces or surfaces and residence in the upper gastrointestinal tract, especially in the mucosa-related lymphoid tissue. Other route of transmitting the bacteria is via intrauterine transfer to the unborn fetus. After first exposure to MAP, animals like cattle need 2 to 5 years incubation phase until the clinical phase starts (Collins, 1997; Grant, 2005). During incubation phase or subclinical phase, there is no clinical symptoms can be detected.

The diagnosis of JD is not simple due to lack of reliable diagnostic tools. Culture of MAP from feces as a gold standard requires at least 6 week incubation due to bacterial slow growth. This is not only due to the long period of incubation, but also the sensitivity, especially for fecal culture of subclinical infected animals, render the culture method not a reliable method for diagnostics. In addition, certain MAP types or form may be more difficult or even impossible to isolate *ex vivo* (Chiodini et al., 1986; Stabel, 1998). Serological assays have been turned out to be unreliable because animals do not develop antibodies during the subclinical phase. MAP specific antibodies can only be detected during the clinical stages of the disease (Stabel, 1998).

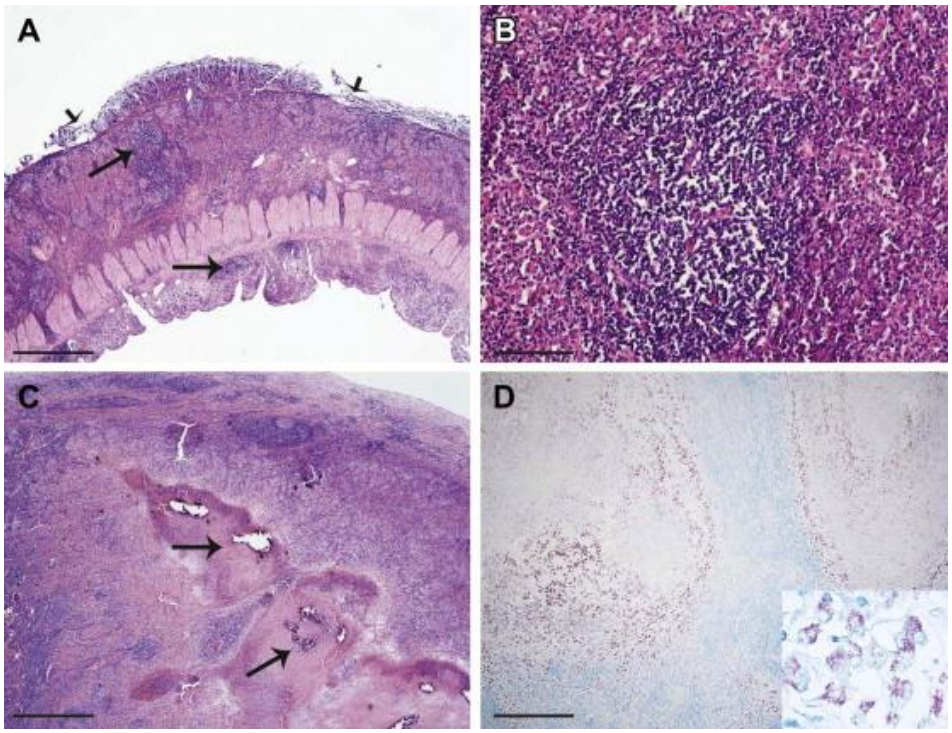

Figure 1.2 Microscopical lesion in the jejenum and jejunal lymph node of MAP infected goat.

A.H&E staining of transmural granulomatous enteritis in the proximal jejenum with aggregation of lymphocytes in submucosa and serosa (arrow). B. Higher magnification of (A) showing infiltration of macrophages and lymphocytes. C. H&E staining of jejunal lymph node with granulomatous lesions and necrosis (arrows). D. Ziehl-Neelsen staining within the necrotic lesion showed acid-fast bacteria in macrophages. Bars, 1,000 µm (A and C), 500 µm (D), 100 µm (B) (Lybeck et al., 2013).

To control MAP, vaccinations are available commercially including killed whole-cell-based vaccines and live-attenuated whole-cell based vaccines. The current vaccination was found to slow the rate of occurrence of clinical paratuberculosis. However, this measure could not prevent infection, since is no protective immunity conferred. In addition, complications in diagnosing infected animals may arise from the use of vaccines due to false-positive serological test results (Over et al., 2011).

1.2.2 Crohn's disease

As described above, Crohn's disease (CD) is a relapsing inflammatory bowel disease (IBD) in humans involving mucosal ulceration and inflammation with uncertain etiology. CD can affect any part of the gastrointestinal tract from mouth to anus, but manifest itself primarily in the terminal ileum and colon (Hermon-Taylor and Bull, 2002). Recently, the prevalence of CD rapidly increased in developed countries which seriously impact the quality of life in patients (Kappelman et al., 2007; Loftus, 2004). The clinical symptoms of CD are chronic inflammation, abdominal pain, loss of body weight, bloody diarrhea and malnutrition (Hermon-Taylor and Bull, 2002). Transmural inflammation of entire bowel wall in CD leads to atrophy of ileal villi, fibrosis, hypertrophy of smooth muscle and an inflammatory response.

The pathogenic mechanisms of CD are still poorly understood. Genetic dispositions (Consortium, 2007; Rioux et al., 2007), autoimmunity (Cerf-Bensussan and Gaboriau-Routhiau, 2010), an inappropriate immune response to the intestinal microbiota (Chassaing and Darfeuille-Michaud, 2011), certain pathogenic bacteria (Greenstein, 2003; Selby, 2004) and combinations of such factors (Cadwell et al., 2010) have been proposed as the cause of CD.

Current understanding of the genetics in CD is that the genes associated with CD regulate innate immune responses, mucosal barrier function and bacterial killing (Sartor, 2006) play an important role in susceptibility of the disease. Recently, genome-wide association studies (GWAS) have revealed more than 100 genetic loci that show significant association with IBD (Franke et al., 2010). Genetic variation in intracellular pattern recognition receptor gene CARD15 or known as NOD2 and an autophagy gene ATG16L1 are the examples of gene associated with CD. Additionally, variation in genes encoding interleukin-23 (IL-23) receptor subunit, IL12B, STAT3 and NKX2-3 also showed their association with CD (Cho, 2008).

Loss tolerance and autoinflammatory disorder apparently contributes to the progression of CD. Highly activated innate and acquired immune responses were detected in CD patients. Effector macrophages as well as neutrophils

representing innate immune system and T cells of acquired immune system accumulate in the inflamed intestine. They are the producers of proinflammatory cytokines which are the characteristics of pathogenesis of CD. The best established mechanism is the dysregulation of T effector cells responding to the commensal intestinal. A disturbed balance between regulatory T cells (Tregs) and T effector cells which results in a disable immune homeostasis leads to development of the disease (Maynard and Weaver, 2009).

Certain pathogenic bacteria were suggested as one of the causing of CD. *Mycobacterium avium* ssp. *paratuberculosis* (MAP) as the focus in this thesis has been postulated involving in pathogenesis of CD, since CD shares clinical symptoms and histopathological appearance with an Johne's disease (Figure 1.3) (Greenstein and Collins; Hermon-Taylor and Bull, 2002). However, studies to reveal the presence of MAP in the intestine of CD patients have given contradictory results (Abubakar et al., 2008; Chiodini et al., 2012). Several meta-analyses revealed a positive correlation between intestinal presence of MAP and CD (Feller et al., 2007). Difficulties in cultivating MAP from clinical isolates might be one explanation for the controversial reports, as many MAP strains need months or even years to form colonies on solid media (Bull et al., 2003). Interestingly, cell wall deficient MAP called spheroplast were found in tissue of CD patients that could not be stained with conventional dyes and failed to grow in hypertonic media (Chiodini et al., 1986). Alternatively, MAP might be situated in anatomical locations like the mesentery that are usually not examined by standard techniques, as suggested recently (Pierce, 2009). Hence, the question whether MAP plays a causative or disease promoting role in CD is still remaining unanswered.

CD is such a complex disease that makes discussion of the etiology controversial. However, understanding the complex interplay between genetic and environmental factors might help to understand the etiology of CD. Interestingly, one study demonstrated that an interaction between a specific virus infection and a mutation in the CD susceptibility gene ATG16L1 can induce intestinal pathologies in mice. This study provided an example that a virus and host susceptibility gene, in combination with environmental factors

such as microbiota, can generate the phenotype that is prone to inflammatory disease (Cadwell et al., 2010).

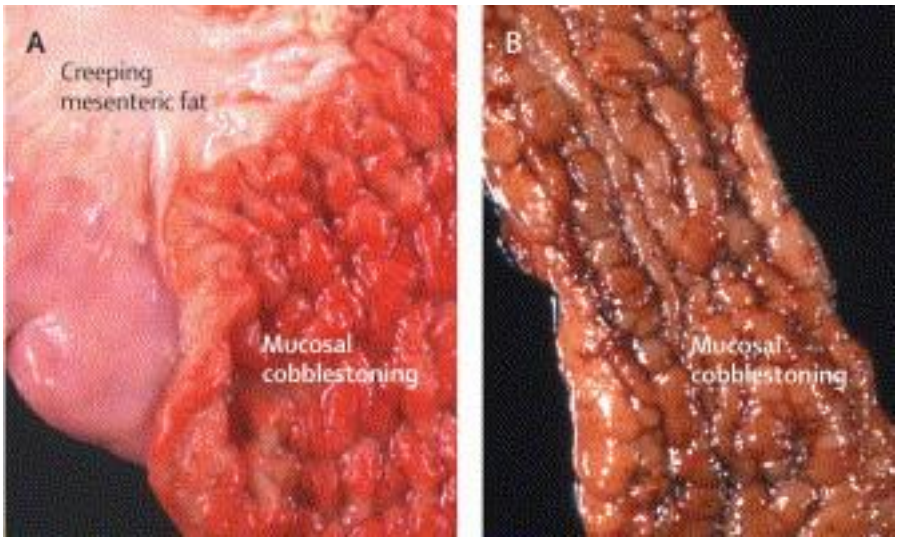

Figure 1.3 Mucosal cobblestoning in Johne's and Crohn's disease.

Creeping mesenteric fat as the characteristic of Crohn's disease, can be seen on serosal surface in Johne's disease. A. bovine Johne's disease. B. Crohn's disease (Greenstein and Collins).

Treatments for CD depend in the specific symptoms and individual severity. Aminosalicylates (sulfasalazine and mesalamine), antibiotics (rifampin, ciprofloxacin and metronidazole), conticosteroids (budesonide and prednisone) and immunomodulators (azathioprine, 6-mercaptopurine and methotrexate) are used for the treatment of mild to moderate disease activity. This is the condition that the patients are still able to tolerate oral alimentation. For severe symptoms, intravenous corticosteroids or anti TNF (infliximab) were used (Baumgart and Sandborn, 2007; Over et al., 2011). Nevertheless, development of new drugs with better efficacies and less adverse effect is still needed.

Animal models are important to provide fundamental insight into the pathogenesis of IBD in general, CD in particular. This could assist the development of new and better therapies against the disease. Mouse represent the most commonly used animals for such models due to the availability of

distinct inbred strains as well as the access to genetic deficient and transgenic animals that allow to investigate host mechanisms in detail. Many mouse models have been established to study the disease. Interleukin (IL)-10 and transforming growth factor (TGF)-β deficient mice were often used because those mice develop colitis which is the clinical symptoms of CD (Li and Flavell, 2008). Both cytokines have been known as a regulatory cytokines which down regulate immune activation and are important in immune tolerance. Transfer of a subpopulation of T cells ($CD4^+CD45RB^{hi}$) to lymphopenic mice which leads to colitis which represents an important model to study specific T cells involvement in dysregulation (Powrie et al., 1994). Interestingly, another study that utilized previously described mouse model combined with co-transfer of $CD4^+CD25^+$ T cells could suppress colitis development (Sakaguchi et al., 1995). This study is important in proving the anti-inflammatory role of $FoxP3^+$ regulatory T cells which is a therapeutic option for CD treatment.

The dextran sulfate sodium (DSS) mouse model was also frequently used to study inflammatory bowel disease. Administration of DSS in drinking water exerts a direct cytotoxic effect on enterocytes and the protective mucus layers resulting in barrier damage and translocation of commensal bacteria associated with an inflammatory response (Johansson et al., 2013; Saleh and Elson, 2011). In the DSS model, the innate immunity such as TLRs and inflammasomes are important for tissue repair and host protection from translocation of commensal bacteria (Kirkland et al., 2012; Saleh and Elson, 2011). Even though the adaptive immunity does not play an essential role in this model, both T helper (Th)1 and Th2 cells have been shown the influence the disease at the later phases.

1.3 Immunology of MAP infection

It is important to study immune response in MAP infection to cure the disease. However, detail studies about immune response of the host against mycobacteria have been carried out mostly in *M. tuberculosis* infection. Nevertheless, the course MAP infection is beginning to be understood. Upon

oral exposure of the host to MAP, the pathogen enters the intestinal mucosa via M cells in the epithelium that lines the dome areas of Peyer's patches or via enterocytes (Figure 1.4) (Bermudez et al., 2010). MAP is recognized by resident macrophages or dendritic cells then phagocytosed and persists within subepithelial macrophages (Momotani et al., 1988). Other immune cells including polymorphonuclear cells (PMNs), DC and natural killer cells are recruited to the site of infection. The dissemination of MAP is thought by using macrophages as vehicles from the infected sites (Valentin-Weigand and Goethe, 1999). It has been shown in one study that MAP was able to disseminate from intestinal tissues into liver and lymph nodes. Both ileum and mesenteric lymph nodes were infected with MAP, albeit fecal shedding of MAP was not observed in this initial phase (Wu et al., 2007).

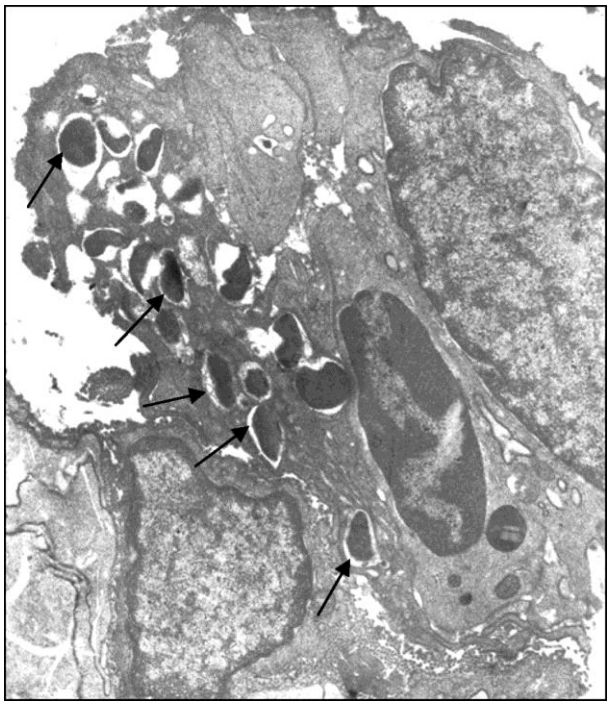

Figure 1.4 Transmission electron micrograph of MAP in mouse intestine.

Transmission electron micrograph from a mouse orally infected with MAP. MAP can be observed within enterocytes (arrows). Magnification, x10,000 (Bermudez et al., 2010).

Cytokines and chemokines production was induced at the site of of infection. The adaptive immune system represented by $CD4^+$ and $CD8^+$ T cells were recruited to the site of infection and activated. This leads to inflammation and

granuloma formation. Granulomas were formed because the immune cells could not eliminate mycobacteria from infected macrophages. These structures are established, because the immune cells were continuously recruited to the site of infection and try to restrict the bacteria from dissemination (Figure 1.5).

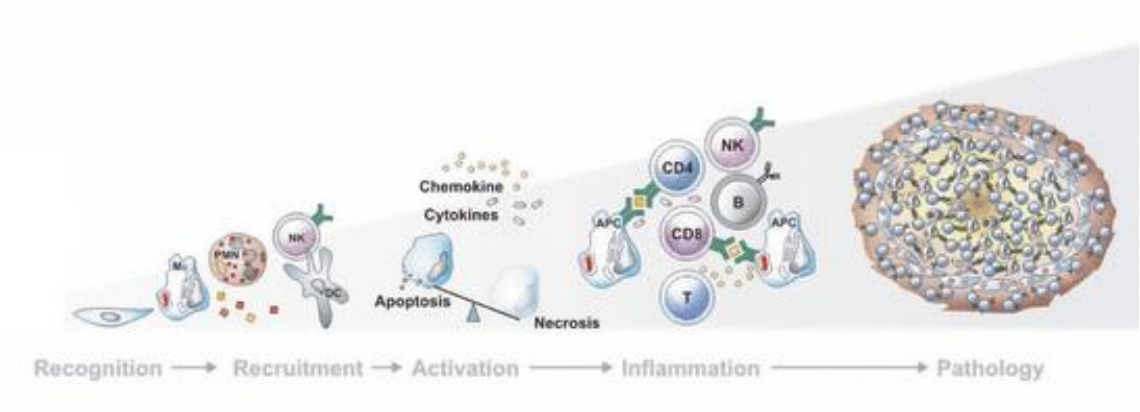

Figure 1.5 The host cellular immune response during Mycobacteria infection.

Summary of current knowledge in host cellular immune response against mycobacterial infection, starting from bacterial recognition, recruitment of innate immune cells, activation of adaptive immune system, inflammation and granuloma formation (Dorhoi et al., 2011).

1.3.1 Early response to MAP infection

The mechanisms how MAP can survive inside of macrophages are still poorly understood. However, monocytes infected with live MAP showed reduction of phagolysosome fusion in comparison to monocytes that had ingested killed MAP. In addition, one study showed that live MAP showed higher percentage of colocalization with LAMP-1 in comparison to heat-killed MAP within macrophages (Figure 1.6). This result showed that live MAP could delay the phagolysosome fusion (Ghosh et al., 2013). It also showed that $Ca2^{+}$ and phosphatidylino 3-kinase dependent pathways are required for MAP elimination (Woo et al., 2007). Additionally, acidification and maturation of phagolysosome were increased in macrophages stimulated *in vitro* by IFN-γ and LPS. This leads to higher killing activity of the macrophages against MAP (Hostetter et al., 2002). Interestingly, MAP uses Jun N-terminal kinase/stress activated protein kinase pathway to regulate cytokines expression in bovine monocytes to inhibit

phagosome acidification (Souza et al., 2006). Therefore, MAP could survive and reside within the host cells.

To activate the innate response to MAP, toll like receptors (TLRs) and nucleotide-binding oligomerization domain-containing protein 2 (NOD2) are important. One study showed that sonicated MAP can only be recognized by TLR2 in peripheral blood mononuclear cells (PBMCs), but not TLR4. In contrast, TLR4 is important to activated cytokines in live MAP infected human mononuclear cells. Furthermore, HEK cells transfected with NOD2 could be stimulated by sonicated MAP in dose-dependent manner, suggesting NOD2 to recognize MAP (Ferwerda et al., 2007).

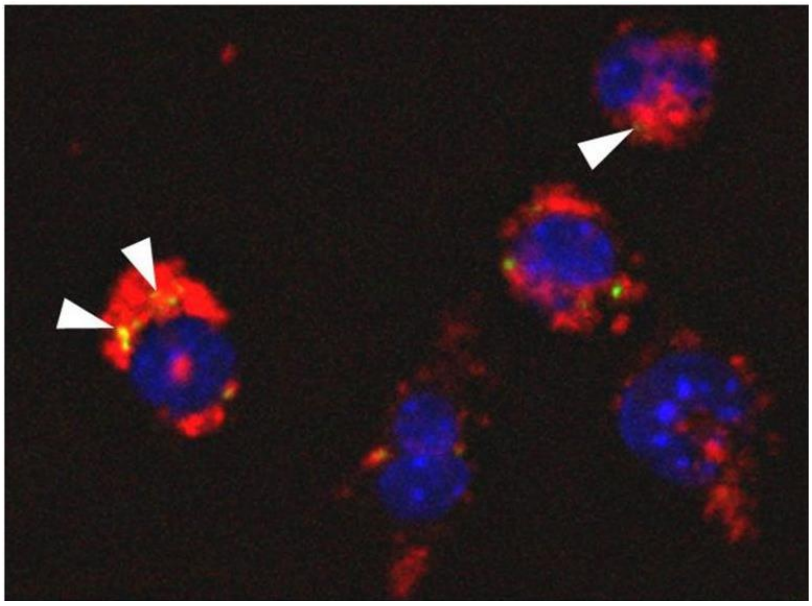

Figure 1.6 Confocal microscopic examination of MAP-lysosome colocalization.

MAP could delay the maturation of phagolysosome. Blue, DAPI-stained nuclei; red, LAMP-1 (marker for lysosome); green- auramine-stained MAP. Yellow showed co-localization of MAP and LAMP-1 (arrowhead) (Ghosh et al., 2013).

1.3.2 Adaptive immune response to MAP infection

Activation of adaptive immunity is also important for the elimination of MAP. Antigen presentation is initiating the adaptive immune response. After ingestion of MAP, antigen presenting cells (APC) express Major Histocompatibility Complex (MHC) class II molecules that present mycobacterial antigens (Sohal

et al., 2008). This then leads to the activation of specific $CD4^+$ T cells. On the other hand, MHC class I molecules expressed in all nucleated cells present the antigen to activate specific $CD8^+$ T cells. Both specific $CD4^+$ and $CD8^+$ T cells are important in elimination mycobacteria. MHC molecules are upregulated by pro-inflammatory cytokines such as IFN-γ, TNF-α and IL-1. Anti-inflammatory cytokines such as IL-10 can inhibit both MHC expressions. The productions of cytokines on the site of infections are also important for recruitment of T cells and other immune cells. Interestingly, MAP could downregulate the expression of MHC I and MHC II expression which leads to lower activation of T cells and higher survival of MAP (Weiss et al., 2001; Zur Lage et al., 2003). This could be because MAP can inhibit pro-inflammatory cytokines expression resulting lower expression of MHC.

Granuloma is one of the hallmarks in mycobacteria infection. As described previously, formations of granulomas are considered as an accumulation of inflammatory mononuclear cells directed by T cells which capable of limiting growth of mycobacteria (Ehlers and Schaible, 2012). Macrophages, $CD4^+$ and $CD8^+$ T cells and other immune cells are consistently present in surrounding of MAP granulomas. In subclinical MAP infection, TNF-α induces MAP-infected macrophages and other cells to release cytokines and chemotactic factors including IL-8 and MCP-1 to the site of infection. This could maintain mycobacteriostasis within persistently infected macrophages and activation newly recruited macrophages at site of MAP infection.

The humoral response to mycobacteria infection has beneficial effects to the host including prolonged survival, CFU reduction and antigen clearance. Efficient antigen processing and presentation of B cells to activate T cells against MAP infection could be significant for the early response. Recognition of MAP antigen by surface IgM on B cells leads to clone specific activation and expansion which results in plasma cells producing MAP specific antibody (Sohal et al., 2008). In subclinical phase, antibody titers against MAP are only detected in mid to late stage, which is associated with increasing number of MAP detected in feces. At this stage of infection, anti-MAP antibodies of the IgG1 subclass is dominant (Whitlock and Buergelt, 1996).

1.4 Animal models of MAP infection

Animal models are needed to experimentally study in more detail the host-pathogen interaction, host immune response, and to evaluate vaccine candidates and therapeutics. Cattle, goats, sheep, cervids and mice have been used as animal models for previously described purpose in MAP infection. Although mouse models may not entirely reflect the disease in cattle, sheep and goats, it is beneficial to study MAP infection in this small animal model. The availability of distinct inbred strain as well as transgenic mice and knockout mice allows investigating pathogenicity of microorganism as well as defense mechanism of the host in more detail. The information acquired might lead to novel therapies.

Many mouse experiments have been done with regard to MAP infection. A comparison of i.p infection in different mouse strains showed that BALB/c were the most susceptible and C57BL/10 were the least susceptible (Chiodini and Buergelt, 1993). However, another study demonstrated that C57BL/6 mice are more susceptible than C3H/HeN mice after i.p infection (Veazey et al., 1996). None of these mouse strains could be infected orally. Oral infection was performed successfully in SCID/beige mice deficient in B, T and NK cells (Mutwiri et al., 1992). However, in one study using B-cell deficient mice that lack of Peyer's patches it was demonstrated that MAP could translocate across the mucosal barrier via M cells and enterocytes (Bermudez et al., 2010). The reason why such experimentals leaded controversial results is unclear. Experimental set up or more likely bacterial strain differences could account for it.

1.5 Aim of the work

In general, little is known about the infection process of MAP, its persistence in the host and the elicited immune responses. To a large extend, this is due to the absence of an appropriate small animal model. Although mouse models for

Introduction

MAP infection have previously been developed, a suitable model that reflects the situation in JD or even CD is still missing.

Prompted by the controversy on the presence of MAP in intestinal tissues of CD patients as well as the ubiquitous exposure of humans to environmental MAP, it was hypothesized that MAP might not cause CD but rather exacerbate a preexisting intestinal inflammation. In JD, animals are usually infected with MAP early in life and have long disease progression from subclinical phase to the clinical phases. It has been discussed that MAP could survive in milk, soil and water which could be possible sources for MAP transmission. Accordingly, it was hypothesized that infected animals will reveal the clinical JD symptoms after secondary exposure to MAP. This might be also the case in CD. Based upon both hypotheses; dextran sulfate sodium-induced colitis was combined with MAP infection in mice. A secondary challenge with MAP was also tested.

The establishment of mouse infection model for MAP should give important hints to understand Johne's disease in ruminants as well as the association between MAP and Crohn's disease in human. It will allow establishing immune parameters and ultimately leading to the development of new treatment strategies for patients.

2 Materials and Methods

2.1 Bacterial strains and cultures

Cultivation of bacteria was done at the University of Veterinary Medicine Hannover (TiHo). *M*. *avium* ssp. *paratuberculosis* (MAP) strain DSM 44135 was grown on Watson Reid medium supplemented with mycobactin J (1 mg/L) at 37^0C (Kuehnel et al., 2001). *M. avium* ssp. *avium* (MAA) strain DSM 44156 or ATCC 25291 and *M. avium* ssp. *hominissuis* (MAH) strain 04A/1287 were grown in the same medium without mycobactin J.

2.2 Mouse strains

$TLR2^{-/-}$ and $RAG2^{-/-}$ mice were bred at the animal facility of the Helmholtz Centre for Infection Research (HZI) under specific pathogen-free conditions (SPF). C57BL/6J wild type mice were purchased from Janvier (Le Genest-saint-Isle, France). Female mice aged between 8-10 weeks were used at the beginning of all experiments. Animal studies were carried out under good animal practice conditions in strict accordance with the German law for animal protection (Tierschutzgesetz, §7-9) from Okt.1. 2006. In particular, experimental procedures were performed under the approval of the ethics committee of the local authority, Niedersächsisches Landesamt für Verbraucherschutz und Lebensmittelsicherheit (LAVES). Permit number for this study is Nr.:33.14.42502-04/090/08. All efforts were made to minimize the number of animals used and their suffering.

2.3 Induction of DSS induced colitis and MAP infection

DSS treatment: 4% DSS (35-50,000 kDa; MP Biomedical) was administered via the drinking water from day 1 until day 5. For infection, mice were intraperitoneally (i.p) injected with 10^8 MAP, MAA or MAH in endotoxin free

Dulbecco's phosphate-buffered saline (PAA) two days after DSS administration. This application route was chosen since oral application did not lead to reproducible infection rates in our hands. Body weight was monitored 2-3 times weekly.

Mice were sacrificed at day 1 post infection (1d p.i.), 1 week post infection (1wk p.i.) and 3 week post infection (3wk p.i.). For secondary challenge, mice were re-injected at 5 week post infection (5wk p.i), and then were sacrificed at day 1 after secondary challenge. The total weight of liver and spleen were measured and the organs were harvested for histology and homogenization for serial dilution and plating. The length of colon was measured, a 1-2 cm section was then separated for histology, and the rest was homogenized for plating after washing with PBS. Small intestine and mesentery were collected similarly for plating and histology.

To deplete CD4 and $CD8^+$ T cells, 150µg/mL anti-CD4 antibody (Clone GK1.5, Molecular Immunology, HZI), anti-CD8 (Clone 53-6.7, Molecular Immunology, HZI) or Rat IgG2b isotype control (eBR2a, eBioscience) were administered i.p 3 days before secondary challenge.

2.4 Organ plating

Liver, spleen, colon, small intestine and mesentery tissues were homogenized with sterile PBS supplemented by 0.1% Triton-X100 (Sigma) with sterile 3 mm glass beads 2 times for 20 seconds using the homogenizer FastPrep-24 (MP Biomedicals). The liver, spleen and mesentery homogenates were plated on Middlebrook 7H10 agar (Difco TM) containing Mycobactin J (IDVet Innovative Technology). The colon and small intestine homogenates were also plated on Middlebrook 7H10 agar containing Mycobactin J and antibiotics (Vancomycin, 5mg/mL, Roth; Amphotericin B, 39 mg/mL, Roth and; Nalidixin Acid, 10 mg/mL, Sigma). The plates were incubated at 37^oC for up to 8 weeks.

2.5 Pathology and Histology

Histology was performed in the Mouse Pathology platform at HZI Braunschweig. Organs were fixed in 10% formaldehyde, dehydrated with ethanol, and embedded in paraffin. Paraffin sections (0.5 µm) were stained with hematoxylin-eosin (H&E) and Ziehl-Neelsen (ZN) staining according to standard laboratory procedures. Scoring of histopathological changes of both colon and mesenteric tissue was performed in a blinded fashion. For scoring of colonic tissue, a combined score of severity, ulceration, edema and area involved was applied. Grades applied for severity were 0 = no alteration, 1 = mild, 2 = moderate, 3 = severe alterations. For ulceration score, the graded were 0 = no ulcer, 1 = 1-2 ulcers (involving up to a total of 20 crypts), 2 = 1-4 ulcers (involving a total of 20-40 crypts) and 3 = any ulcers larger than 40 crypts. For edema score, the grades were 1 = only mild epithelial or submucosal edema, 2 = mild epithelial edema associated with mild submucosal edema or more moderate submucosal edema, and 3 = every edema more extensive that the previous. For area involved in the inflammatory process, the grades were 0 = 0%, 1 ≤ 30%, 2 = 40%-70%, 3 ≥ 70%.

For scoring of mesenteric tissue, only a combined score of severity, area involved and the existence of mycobacteria in ZN staining was applied. The severity and area involved were graded similar to the colon tissue. For the existence of mycobacteria in ZN staining, the grades were 0 = no bacteria, 1 = small amounts of bacteria, 2 = moderate amounts (clearly seen in 20x magnification), and 3 = high amounts (massive colonies were clearly seen in 10x magnification). Granuloma, number and area, in liver section were analyzed in 0.2 cm2 fields per section and quantified using AxioVision software (Carl Zeiss, Germany). The following antibodies were used for immunohistochemistry of mesentery: Myeloperoxidase (Clone Ab-1, Medac), Mac-2 Antibody (M3/38, Biozole) and CD3 Antibody (SP7, Thermo Fischer Scientific).

2.6 Transmission electron microscopy

Electron Microscopy was carried out in the imaging platform of the HZI. Mesenteric tissue were excised and fixed in with 2% glutaraldehyde/5% formaldehyde in HEPES buffer containing 10 mM $MgCl_2$, 10 mM $CaCl_2$ and 0.09M sucrose, pH 6.9, for 1 hour on ice, washed with buffer, and further fixed with 1% aqueous osmium for 1 hour at room temperature. Samples were then dehydrated with a graded series of acetone (10, 30, and 50%). At the 70% dehydration step samples were left over night in 70% acetone containing 2% uranylacetate, and further dehydrated with 90% and 100% acetone. Samples were then embedded in the epoxy resin Spurr (hard formular) according to described procedures (Spurr, 1969). Ultrathin sections were cut with a diamond knife, picked up with butvar-coated grids, counterstained with uranyl acetate and lead citrate, and examined in a TEM 910 transmission electron microscope (Carl Zeiss, Oberkochen) at an acceleration voltage of 80 kV. Images were recorded digitally at calibrated magnifications with a Slow-Scan CCD-Camera (ProScan, 1024x1024, Scheuring, Germany) with ITEM-Software (Olympus Soft Imaging Solutions, Münster, Germany).

2.7 ELISA

For collection of sera, blood was collected into Microvette 500 serum gel (Sarstedt), and then centrifuged for 5 minutes at 10000g in room temperature. The supernatants were collected and stored at -20 °C. For collection of intestinal lavage, small intestines were washed with 300 µl intestinal wash buffer (PBS including 0.1 mg/ml Trypsin-inhibitor, 50 mM EDTA, and 0.1 % BSA). The flow through was collected into 1.5 ml tubes, centrifuged for 10 min at 1000 rpm in room temperature. The supernatants were collected and stored at -80 °C. For colon supernatant, colon were flushed with cold PBS, opened along longitudinal axis, cut into 0.5 cm pieces and incubated for 24 h in RPMI 1640 supplemented with 10% FCS. Colon supernatant were collected and kept at -20^{o}C.

Immunoglobulin (Ig) concentrations in intestinal lavage and sera and IFN-γ level in sera were measured using ELISA. In brief, goat anti-mouse IgA (Sigma), goat anti-mouse IgG (Sigma), rat anti-mouse IgM (BD Pharmingen) or rat anti-mouse IFN-γ (Molecular Immunology, HZI) in coating buffer were incubated in 96 well plates (MaxiSorb TM Immunoplates, Nunc) overnight at 4^{o}C. The 96 well plates were then blocked for 1 hour, with 3% BSA in 0.05% Tween 20. Diluted sera/intestinal lavages were distributed to the wells and incubated for 2 hours at room temperature. Ig was detected with biotinylated rat anti-mouse IgA (Sigma), peroxidased goat anti-mouse IgG (Jackson Immunoresearch), biotinylated rat anti-mouse IgM (AbD Serotec) or biotinylated anti-mouse IFN-γ antibodies (Molecular Immunology, HZI). Biotinylated antibodies were bound with horseradish peroxidase (HRP) conjugated streptavidin (BD). Bound HRP was determined using o-Phenylendiamin (OPD) as substrate and the results were read using an ELISA-reader (BioRad 3550- UV microplate reader) at a wavelength of 490 nm.

TNF-α level from sera and colon supernatant were detected using Mouse TNF-α ELISA kits (Biolegend) according to manufacturer's protocol. Mouse cytokines and chemokines from sera were analyzed using Bio-plex Pro Mouse Cytokines 23-plex Assay (Bio-Rad) according to manufacturer's protocol.

2.8 Flow cytometry

Spleen cells were prepared by gently flushing the spleen with IMDM containing antibiotics (100 U/mL penicillin and 100 µg/mL streptomycin), 10% FCS, 50 µM β-ME, 2 mM L-glutamine. Cells from mesenteric lymph nodes were prepared by mechanical dissociation. Cells suspension was passed through 50 µm nylon filter. Red blood cells were lysed for 2 minutes in ACK buffer (0.15 M NH_4Cl, 10 mM $KHCO_3$, and 0.1 mM EDTA) and were then blocked with 1 µg/mL FcR block (rat anti-mouse CD16/CD32, BD Pharmingen).

Isolation of colonic lamina propria leukocytes were performed according to described procedure with slightly modification (Zigmond et al., 2012). In brief,

colons were flushed their luminal content with cold PBS, opened longitudinally and cut into 0.5 cm pieces and incubated 3x in HBSS (Ca and Mg free) with 5% FCS, 2mM EDTA, 1mM DTT and 10mM HEPES at 37^{o}C shaking at 250rpm for 15 minutes to remove epithelial cells and mucus. Tissue was then digested in RPMI 1640 with 10% FCS, 1.5 mg/mL collagenase type VIII, and 0.1mg/mL DnaseI at 37^{o}C shaking at 250rpm for 45 minutes. Percoll (GE Healthcare) gradients using 40/80% were performed to purify the leukocytes.

The following antibodies were used for flow cytometry analysis: anti-CD45 APC-Cy7 (30-F11, Biolegend), anti-CD3 FITC (17A2, eBioscience), anti-CD4 APCeFluor780 or APC (RM4-5, eBioscience), anti-CD11c Pe-Cy7 or FITC (N418, eBioscience), anti-CD19 APC or PerCP-Cy5.5 (1D3, BD Pharmigen), anti-CD8 PerCP-Cy5.5 or PE (53-6.7, eBioscience), anti-Ly6C APC (AL-21, BD Pharmigen), anti-Gr-1 APC-Cy7 (RB6-8C5, BD Pharmigen), anti-Ly6G PE-Cy7 (1A8, Biolegend), anti-F4/80 PerCP-Cy5.5 (BM8, eBioscience) and anti-CD11b FITC or PE (M1/70, eBioscience). DAPI (Sigma) were used for live and dead discrimination.

To quantify MAP binding IgG, IgM and IgA antibodies, a similar volume containing 10^{8} CFU/mL MAP and serum were mixed and incubated for 30 minutes. The bacteria were washed in PBS/5mM EDTA/2% FCS before resuspension in anti-IgM PE (BD Pharmingen), anti-IgG FITC (Caltag lab) or anti-IgA Biotin (Maltechab). Flow cytometry was performed using a LSR II analyzer (BD, NJ, USA). The data were analyzed using FACSDiva software (BD) and FlowJo (TreeStar).

2.9 Quantitative Real Time PCR

RNA from colon tissues was isolated with RNeasy Mini kit (Qiagen) according to manufacturer's protocol. cDNA synthesis was performed using Revert Aid First Strand cDNA Synthesis Kit (Fermentas) according to manufacturer's protocol. Power SYBR® Green PCR Master Mix (AB Applied Biosystems) was used according to the manufacturer's instructions. The following primers were used

for quantitative PCR: 5'-TGG GAG TAG ACA AGG TAC AAC CC-3', 5'-CAT CTT CTC AAA ATT CGA CTG ACA A-3' for TNF-α; 5'-TTG ACG GAC CCC AAA AGA TG-3', 5'-AGA AGG TGC TCA TGT CCT CA-3' for IL-1β; 5'-TGG CTC TGC AGG ATT TTC ATG-3',5'-TCA AGT GGC ATA GAT GTG GAA GAA-3' for IFN-γ; 5'-CTG GAC AAC ATA CTG CTA ACC GAC TC-3', 5'-ATT TCT GGG CCA TGC TTC TCT GC-3' for IL-10; 5′-CTG GAC GAG GGC AAG ATG AAG C-3′, 5′-TGA CGT TGG CGG ATG AGC ACA-3′ for ribosomal protein S9 (RPS9) as standard. Relative fold changes were normalized against housekeeping gene RPS9. qRT-PCR were performed on 7500 Real Time PCR System (Applied Biosystem).

2.10 Measurement of fluid absorption in colon

Fluid absorption measurement was performed at Department of Gastroenterology, Hepatology, and Endocrinology, Hannover Medical School according to previously published protocol (Singh et al., 2010). Animals had free access to food and water before the experiment. Induction of anesthesia was achieved by spontaneous inhalation of isoflurane (Forene; Abbott Germany, Wiesbaden, Germany). The inhalation gas contained a mixture of ~10–15% oxygen, ~85–90% air, and ~2.0 ± 0.2% isoflurane with the use of an isoflurane pump (Univentor 1250 Anaesthesia Unit; AgnTho, Lidingö, Sweden) and was administered continuously through a breathing mask. The depth of the anesthesia was tested by probing the pedal withdrawal reflex and breathing rate of the mice. The gas flow through the cylindrical mask (2 cm long with an inner diameter of 1.2 cm) was ~200 ml/min, which minimized rebreathing of exhaled CO_2 by the animals. To minimize the anesthesia level and pain during surgery, all the mice received subcutaneous injection of 500 mg/kg body weight of Novalgin 30 min. before the surgery was started. Body temperature was maintained using a heating pad. A catheter was placed in the left carotid artery for continuous infusion of (in mM) 200 Na^+ and 100 CO_3^{-2} at a rate of 0.30 ml/h to prevent anesthesia induced acidosis. Lower abdomen was opened by one small central incision, and whole colon was used for measurement. A small

polyethylene tube (PE100) with a distal flange was advanced into the proximal colon through an opening in cecum and secured by a ligature that served as an inlet tube. PE200 flanged tubing was secured by ligature to allow for drainage through the anus in the distal part of the colon. The isolated colonic segment with an intact blood supply was gently flushed and then perfused (Perfusor compact; BRAUN, Bethlehem, PA, USA) at a rate of 3 ml/h with 150 mmol/l NaCl. Effluents from the isolated segment were visually free of blood throughout all experiments. After an initial 30-min. washout and recovery period, fluid absorption was measured for another 1 hour. At the end of the experiments, mice were killed by cervical dislocation. The perfused segment was excised from in situ position, and its length was measured. The perfusate was collected in a pre-weighed 4.5-ml collecting tube. After a 30-min period, the tube was weighed again and the difference of the two up to four places of decimal was taken as the amount of fluid recovered after 30 min (taking density of fluid roughly at about 1 g/ml). The difference was further subtracted from 1.5 ml, which was the original volume recovered after 30 min. in case of no fluid absorption. All values were represented in milliliters of fluid absorbed per centimeter colon length per hour (ml/cm/h).

2.11 Statistics

All data were analyzed with GraphPad Prism software. In some figures statistical difference between groups were determined by 1-way Anova and followed by Tukey's multiple comparison tests. In some figures statistical difference between groups were determined by Student t-test. The data considered statistically significant when p values were less than 0.05. * = p values < 0.05, **= $p \leq 0.01$,***= $p < 0.001$, n.s = not significant.

3 Results

All the following experiments were carried out under the premises that a MAP infection will exacerbate an existing inflammation in the gut. Thus inflammatory bowel disease was chemically induced in mice and the animals were subsequently infected intraperitoneally (i.p) with MAP.

3.1 MAP infection after colitis induction

In the drinking water of adult female C57BL/6J mice, 4% DSS was added from day 1 until day 5. After two treatment-free days, 10^8 MAP were injected i.p. The experimental schedule is illustrated in Figure 3.1A. Body weight was measured as a read out for the general health condition (Figure 3.1B). Mice infected with MAP only (H_2O+MAP) showed reduction of body weight at 1 day p.i. and started to regain weight at 2 days p.i.. In contrast, both MAP infected (DSS+MAP) and non-infected DSS pretreated mice (DSS+PBS) started to lose weight after DSS administration and showed bloody diarrhea.

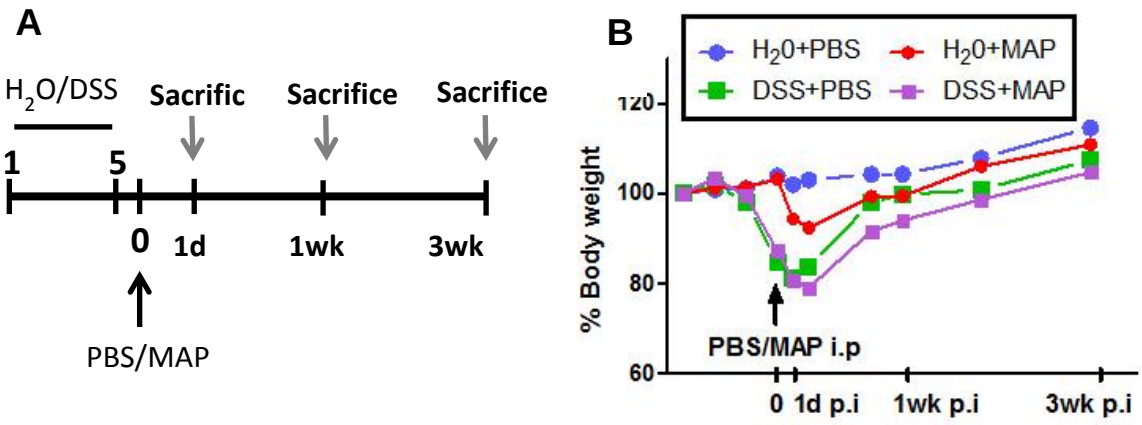

Figure 3.1 Experimental set-up and body weight measurement.

A. Overview of the experimental schedule. H_2O or 4% DSS were administered to the drinking water from day 1 until day 5, followed by normal drinking water afterwards. PBS or 10^8 CFU MAP in 200 µL i.p. was administered two days after DSS treatment finished (day 0). Mice were sacrificed at day 1, 1 week and 3 weeks p.i.. B. Weight change during experiment, expressed as percentage change from day 1 of DSS treatment. The results shown are representative of more than three independent experiments (n= 5-15).

Dramatically elevated levels of cytokines were observed in the serum of mice after MAP administration (Figure 3.2 and Table 3.1). Interestingly, the kinetic of enhanced cytokine levels differed between H_2O+MAP and DSS+MAP mice. H_2O+MAP mice showed higher TNF-α serum level at 2 hours and 6 hours after infection than DSS+MAP mice but decreased to normal at 24 hours p.i.. Conversely, levels of TNF-α in DSS+MAP mice remained constitutively increased until 24 hours p.i. (Figure 3.2). These results suggest that a differential response to MAP infection takes place between untreated and DSS-treated mice. The DSS+PBS group showed low TNF-α serum level and H_2O+PBS control group showed TNF-α serum level below detection limit.

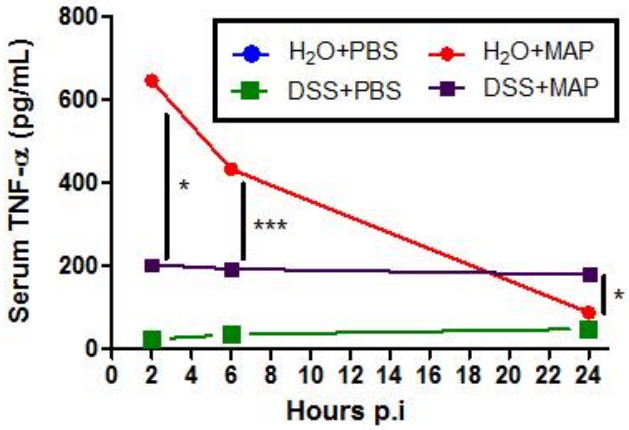

Figure 3.2 Kinetics of TNF-α serum level from 2, 6 and 24 hours post infection.

At 2h and 6h p.i., TNF-α serum level was significantly higher in H_2O+MAP (2h = *, 6h = **) and DSS+MAP (2h = ***, 6h = **) group in comparison to DSS+PBS. TNF-α serum level of H_2O+MAP showed higher at 2h (*) and 6h (***) p.i. in comparison to DSS+MAP. At 24h p.i., DSS+MAP showed higher TNF-α serum level then H_2O+MAP (*) and DSS+PBS (**). H_2O+MAP and DSS+PBS showed no different TNF-α serum level at 24h p.i. TNF-α serum level of H_2O+PBS was below detection limit. The results shown are representative of at least two independent experiments (n=3-5). *p<0.05, **p<0.01, ***p<0.0001.

3.2 Enlargement of spleen and liver in DSS+MAP mice

At 1 week p.i., DSS+PBS, H_2O+MAP and DSS+MAP mice showed higher total spleen weight compared to H_2O+PBS mice. This effect was most pronounced in DSS+MAP mice. Such mice exhibited significantly more enhanced spleen weight at 3 weeks p.i. compared to H_2O+MAP or DSS+PBS mice (Figure 3.3A). Similarly, a significant enlargement of the liver was observed in DSS+MAP mice

at 3 weeks p.i. (Figure 3.3B). Independent of MAP infection, DSS treated mice displayed a significant shortening of the colon length at 1 day p.i. but had recovered by 1 week p.i. (Figure 3.3C).

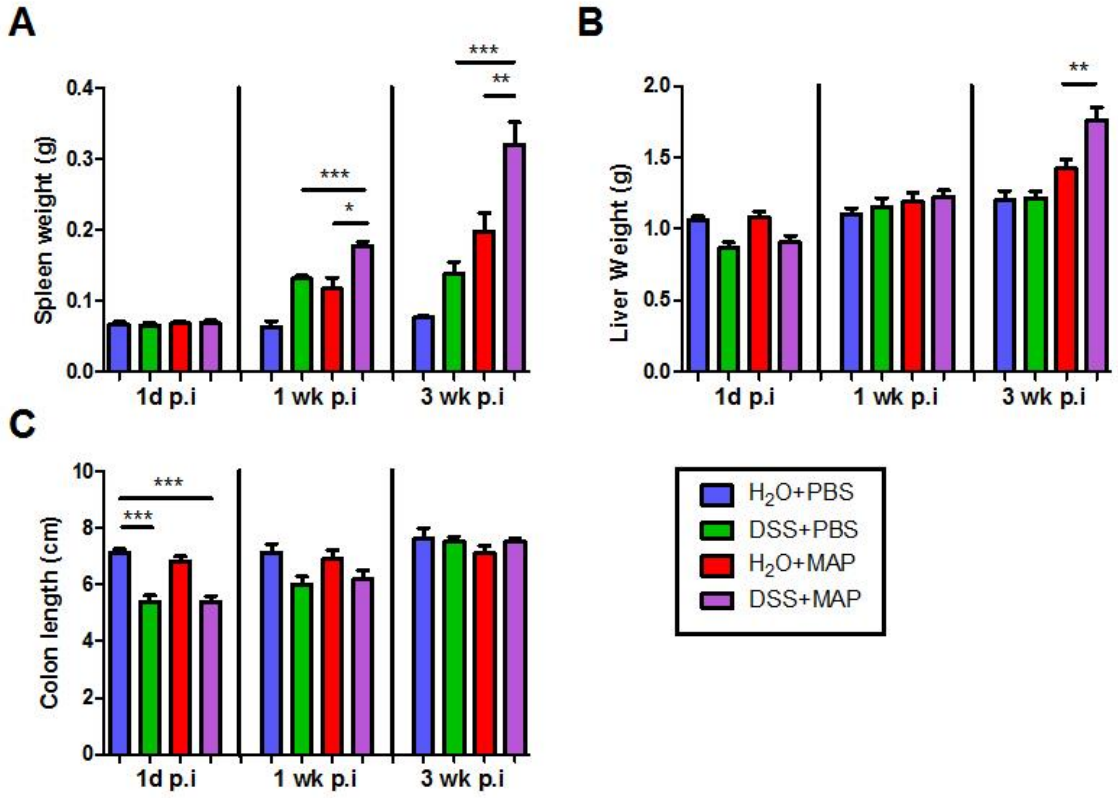

Figure 3.3 Measurement of total spleen and liver weight and colon length at 1d, 1 week and 3 weeks p.i.

A. Total spleen weight in Gram. B. Total liver weight in Gram. C. Colon lengths in cm. Data are representative of at least three independent experiments (n=3-15). *p<0.05, **p<0.01, ***p<0.0001

3.3 Cellularity of spleen

The significant enlargement of the spleen observed at 1 and 3 weeks p.i. in DSS+MAP treated mice was not accompanied by a significant enhancement of bacterial organ counts (Figure 3.4A). Since the enlargement of spleen tissue was most likely due to the immigration or accumulation of immune cells we analyzed the composition of splenic cells at 3 weeks p.i. by flow cytometry. Polymorphonuclear cells (PMN; $CD11b^{+}Gr1^{hi}Ly6C^{int}$) and monocyte

($CD11b^{+}Ly6C^{hi}Gr1^{int}$) numbers were higher in DSS+MAP compared to H_2O+PBS and H_2O+MAP spleen tissue but similar to DSS only treated animals (Figure 3.4B-C). The elevation of the myeloid compartment was therefore most likely induced by the DSS induced damage of the colon. Penetration of the intestinal mucosal barrier and spread of commensal bacteria from the enteric microbiota might be responsible for the inflammatory response observed in the spleen. We could not see any difference in lymphocytes population between the groups examined (data not shown).

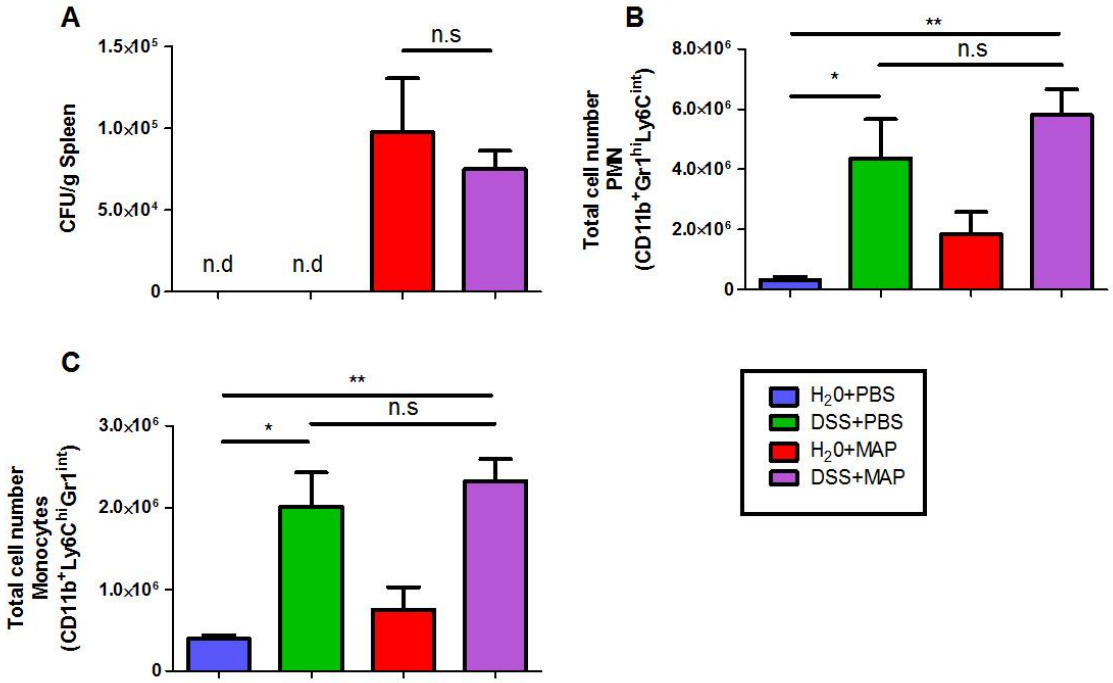

Figure 3.4 DSS+MAP treated mice show an increase in splenic PMN and monocyte population.

A. Bacterial loads in spleen were analyzed at 3 weeks p.i. by plating tissue on Middlebrook agar (n=3-9). B-C. Spleen cells were isolated and stained with DAPI and analyzed by Flow cytometry. B. Total number of PMN ($CD11b^{+}Gr1^{hi}Ly6C^{int}$). **C**. Total number of monocyte ($CD11b^{+}Ly6C^{hi}Gr1^{int}$). Data are representative of at least two independent experiments (n=3-5). *p<0.05, **p<0.01, n.s = not significant.

3.4 Increased granuloma formation in the liver of DSS+MAP mice

To understand the underlying cause of the liver enlargement in DSS+MAP mice at 3 weeks p.i. (Figure 3.3B), a detailed analysis was carried out. Severe granuloma formation was observed in both infected groups by histological examination, which was never found in uninfected animals (Figure 3.5A-B). Granuloma formation represents the histopathological hallmark of mycobacterial infection in general and represents both protective immunity and inflammatory tissue destruction. Strikingly, number (Figure 3.6A) and size of granulomas (Figure 3.6B) in DSS+MAP mice were significantly enhanced compared to H_2O+MAP mice. More polymorphonuclear cells (PMN) and macrophages were visible in these areas in the DSS+MAP group (Figure 3.5B). Even though, no significant difference in CFU/g liver between H_2O+MAP and DSS+MAP mice could be observed (Figure 3.6C). Despite granuloma formation, MAP could be hardly visualized in liver tissue using Ziehl Neelsen staining (data not shown). This might be due to the low number of total MAP in liver. An enhanced immunoreactivity of the liver tissue, however, could be detected in DSS+MAP mice illustrated by the enhanced frequency and extent of granuloma formation.

3.5 Elevated antibody levels in DSS+MAP mice

Since a marked immune activation was observed in mice treated with DSS and infected with MAP, we next wanted to know whether an antibody response was induced under these circumstances. Therefore, we monitored the immunoglobulin levels in serum and intestinal washing fluid at 1 day, 1 week and 3 weeks p.i. Total serum IgM increased over time in all groups which was most likely due to the increasing age of the animals (Figure 3.7A). Nevertheless, there were no differences in serum IgM level in all of the groups. In addition, flow cytometry-based quantification of MAP specific IgM antibodies showed no significant difference between the groups examined (Figure 3.7C).

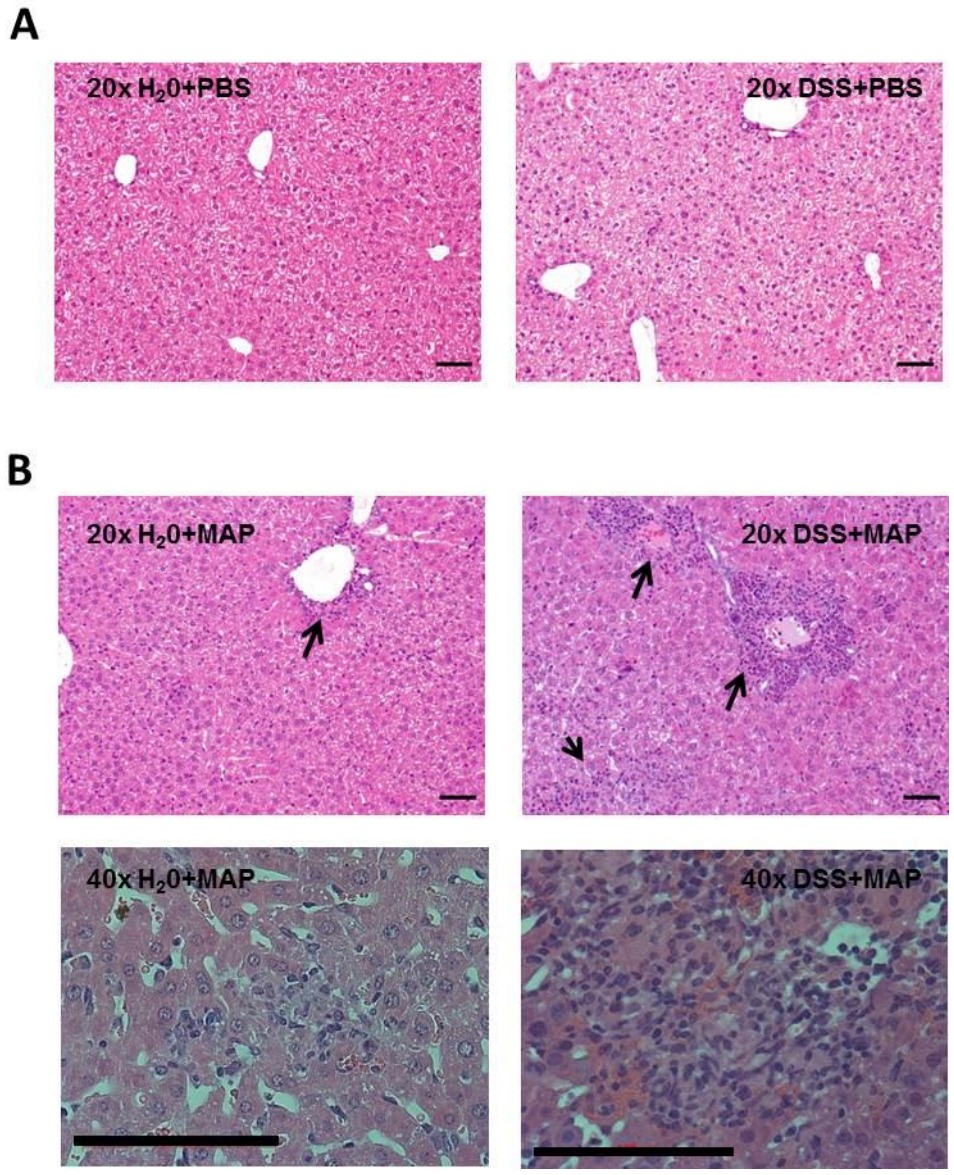

Figure 3.5 H&E staining of liver tissue sections at 3 weeks p.i.

A. Normal liver tissue (20x magnification) was observed in H_2O+PBS (left) and DSS+PBS (right). Scale bars, 50 µm. B. Granuloma formation (black arrow) was observed in infected mice H_2O+MAP (upper left) and DSS+MAP (upper right) in 20 x magnifications. Scale bars, 50 µm. Larger granuloma was observed in DSS+MAP (bottom right) compares to H_2O+MAP (bottom left) in 40x magnifications. Scale bars, 100 µm.

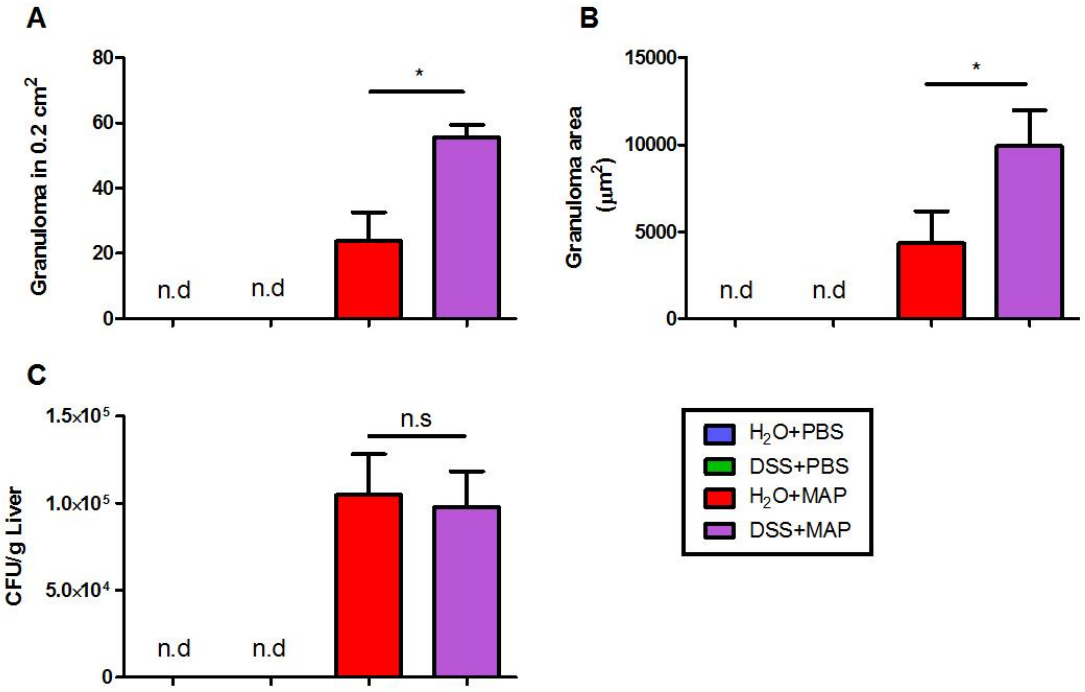

Figure 3.6 Histological determination of granuloma numbers and size and bacterial loads in liver at 3 weeks p.i.

A. Number of granuloma in an area 0.2 cm^2. B. Size of granuloma, expressed in μm^2 (n=3-5) C. Bacterial loads in liver were analyzed at 3 weeks p.i. by plating tissue on Middlebrook agar. Data are representative of at least two independent experiments (n=3-11). *p<0.05, n.d = not detectable.

In a similar fashion, total serum IgG levels also increased over the time in all groups (Figure 3.7B). However, at 1 day p.i., animals of the DSS+PBS, H_2O+MAP and DSS+MAP groups showed significantly lower total serum IgG levels in comparison to mice of the H_2O+PBS group. These results might be due to inflammation elicited by DSS treatment and/or MAP infection in line with the observed reduced body weight. However, at 1 week p.i. total serum IgG level in all groups showed similar levels. Interestingly, at 3 weeks p.i. only animals of the DSS+MAP group showed significantly higher ($p<0.05$) total serum IgG levels as compared to H_2O+PBS and DSS+PBS animals. Additionally, MAP specific IgG levels in animals of the DSS+MAP group were significantly elevated ($p<0.01$) as compared to uninfected animals (Figure 3.7D). In contrast, total intestinal IgA and total serum IgA were not significantly altered (Figure 3.7E-F).

Thus, the inflammation associated with DSS-treatment led to an increase in total serum IgG levels, and also to a significant increase of MAP specific IgG.

3.6 Colonization of mesenteric tissue and granuloma formation by MAP

In our mouse model, viable MAPs were found in liver (Figure 3.6C), spleen (Figure 3.4B) and intestine (see below) although at relatively low numbers. Colonization of the mesenteric tissue was previously postulated to explain inconsistencies of MAP detection in mucosal biospies from CD patients. Therefore, we investigated the possibility of colonization of mesenteric tissue by MAP under our experimental conditions. Indeed, high numbers of viable MAP could be detected by serial dilution platings of homogenized mesenteric tissue from MAP infected mice 3 weeks p.i (Figure 3.8A). Evidently, the MAP colonization led to accumulation of extremely high numbers of inflammatory cells which resulted in severe granuloma formation, tissue destruction and necrosis (Figure 3.8C). This was illustrated by the elevated histopathological score in both MAP infected groups (Figure 3.8B). Accumulation of neutrophils, macrophages and T cells in granulomas could be observed by immunohistochemistry in mesenteric tissue (Figure 3.9). Additionally, transmission electron microscopy demonstrated MAP inside host cells of the mesenteric tissue most likely representing macrophages (Figure 3.10).

Colonization of the mesenteric tissue by MAP was not significantly different in the DSS treated and untreated group (Figure 3.8A). Similarly, the histological score did not reveal any significant difference between both groups (Figure 3.8B). Importantly, no tissue alterations were found in DSS+PBS mice (data not shown). Thus, DSS treatment appears not to influence bacterial colonization and destruction of the mesenteric tissue. Taken together, the colonization of mesenteric tissue by MAP attracted immune cells, which subsequently led to severe granuloma formation.

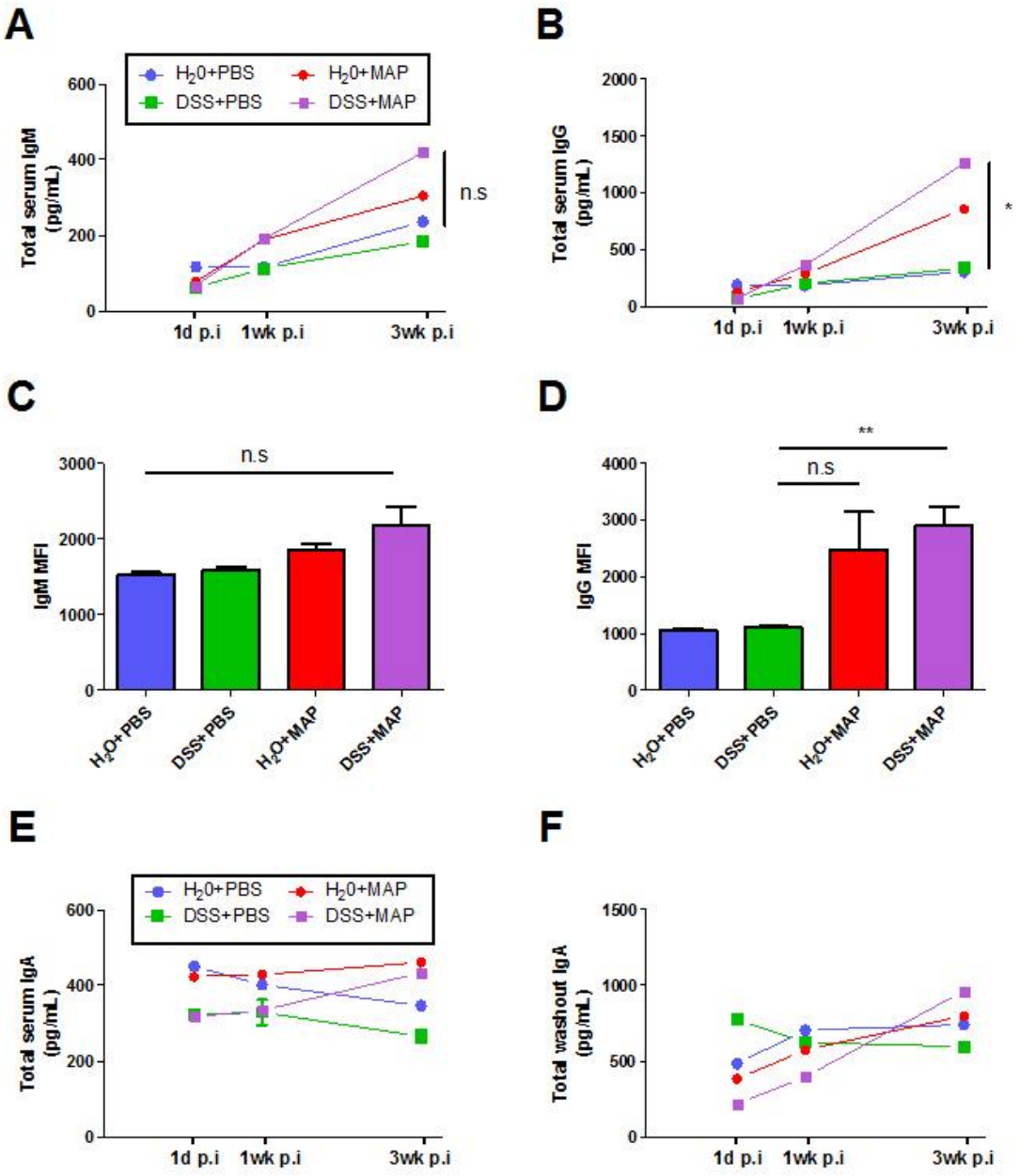

Figure 3.7 Elevated antibody levels in DSS+MAP mice.

A. Total serum IgM, B. Total serum IgG at day 1, 1 week and 3 weeks p.i. were determined by ELISA. C. Mean fluorescence intensity (MFI) IgM and D. IgG bound MAP at 3 weeks p.i. was determined by flow cytometry. E. total serum IgA. F. total intestinal washout IgA at day 1, 1 week and 3 weeks p.i. were determined by ELISA. Data are representative from at least two independent experiments (n=3-5). *p<0.05, **p<0.01, ***p<0.0001, n.s = not significant.

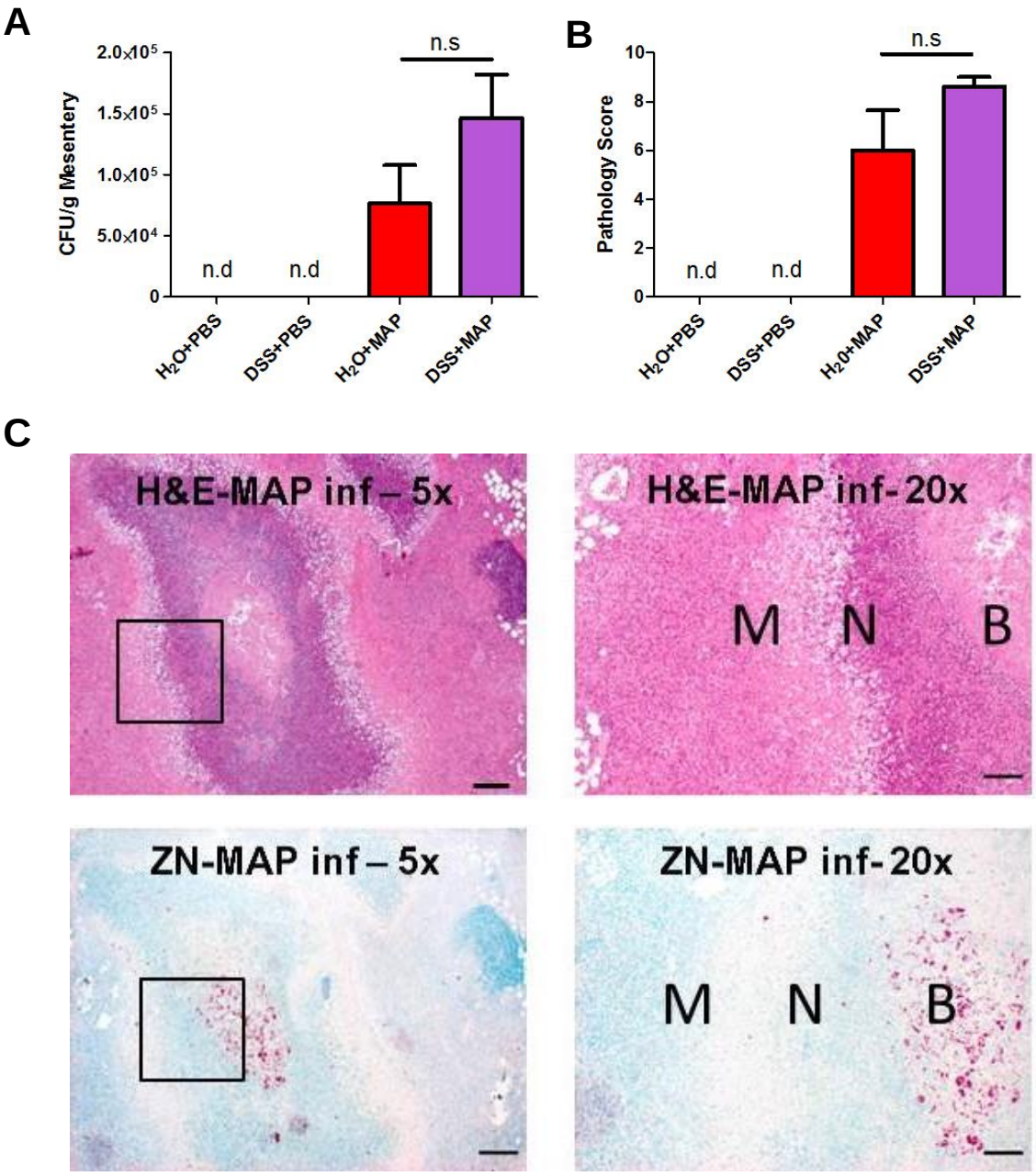

Figure 3.8 MAP was found in mesenteric tissue generating granuloma.

A. Bacterial loads in mesentery were analyzed at 3 weeks p.i. by plating tissue on Middlebrook agar (n=3-8). B. Histology changes in mesentery were analyzed at 3 weeks p.i.(n=3-5). n.s = not significant, n.d = not detectable. C. H&E staining and Ziehl-Neelsen staining (ZN) of mesentery at 3 weeks p.i. MAP infected showed granuloma and huge number of inflammatory cells in 5x (upper left) and 20x magnifications (upper right). ZN staining of mesentery at 3 weeks p.i. showed positive ZN staining in MAP infected group in 5x (bottom left) and 20x magnifications (bottom right). Scale bars, 200 µm (5x) and 50 µm (20x).

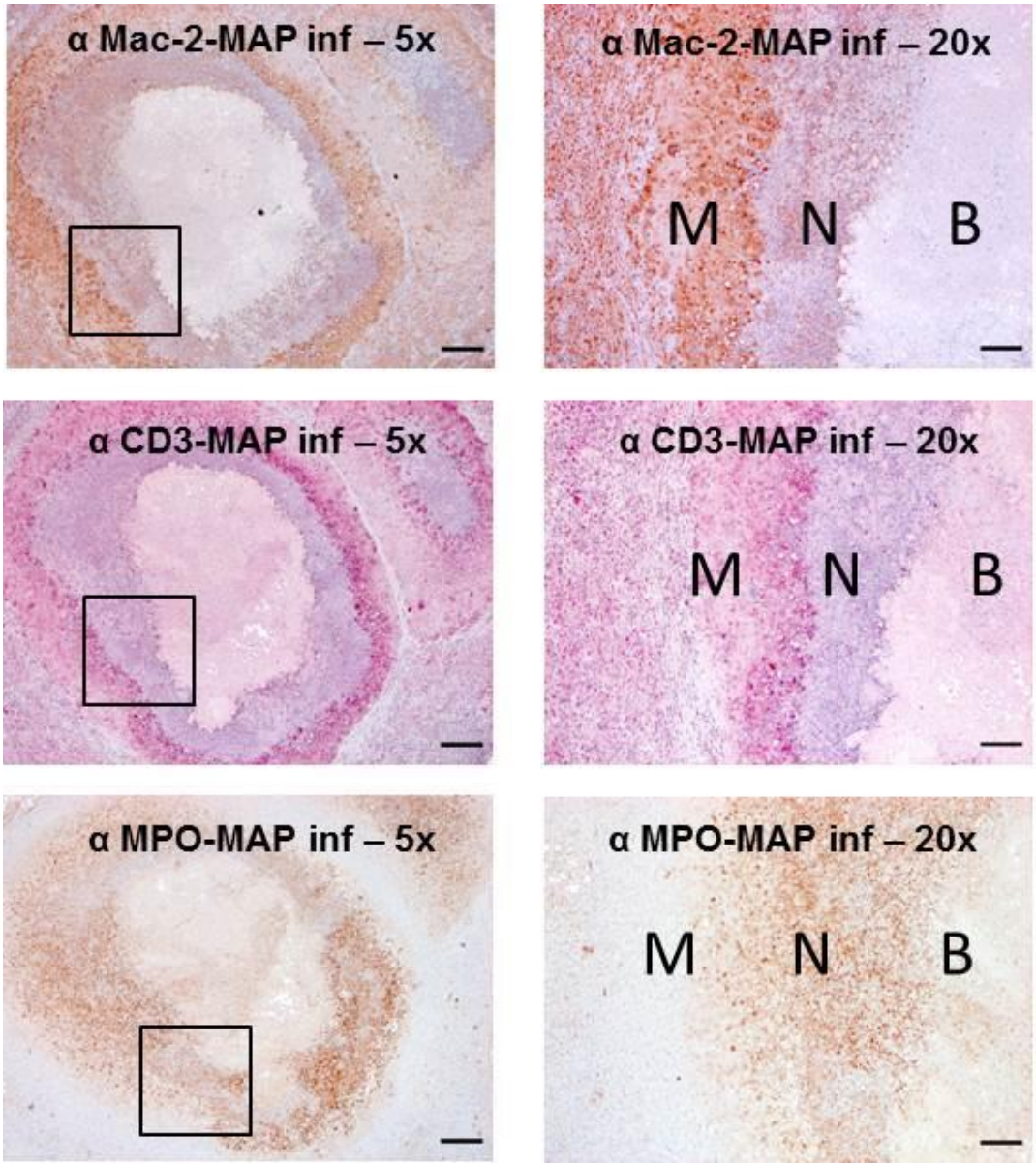

Figure 3.9 Immunohistochemistry in mesenteric tissue.

Accumulation of macrophage (upper), T cells (middle) and neutrophils (bottom) in mesentery were observed at 3 weeks p.i. in MAP infected group by immunohistochemistry (5x magnification in left, 20x magnification in right). Neutrophils (brown), Macrophage (brown) and T cells (red) were visualized by anti-myeloperoxidase (MPO), anti-Mac-2 and anti-CD3. M = T cells and Macrophage zone, N = Neutrophils zone, B = MAP zone. Scale bars, 200 µm (5x) and 50 µm (20x).

3.7 Cellularity of mesenteric lymph nodes

The mesenteric lymph nodes (mLN) are located in the mesenteric tissue and drain the intestine. In order to investigate changes in the cellular composition of mLNs following MAP infection or DSS treatment, we analyzed the immune cells in mLN by flow cytometry at 3 weeks p.i. DSS treatment alone resulted in immigration or accumulation of different types of immune cells in the mLN. Interestingly, reduced numbers of $CD4^+$ and $CD8^+$ T cells were found in mLNs of DSS+MAP animals as compared to DSS+PBS mice (Figure 3.11). Similar results were obtained for macrophages ($CD11b^+Gr1^{lo}Ly6C^{lo}$).

This finding might be explained by retention or death of migratory cells by the presence of MAP in the mesenteric tissue. Conversely, monocytes and granulocytes were found in higher numbers in DSS+MAP mice compared to DSS+PBS. Additionally, dendritic cells and B cells were found to be increased in both DSS treated groups. Together, DSS treatment increases the number of various immune cell populations in mLN but T cell and macrophage proliferation or migration are impaired as a consequence of MAP infection.

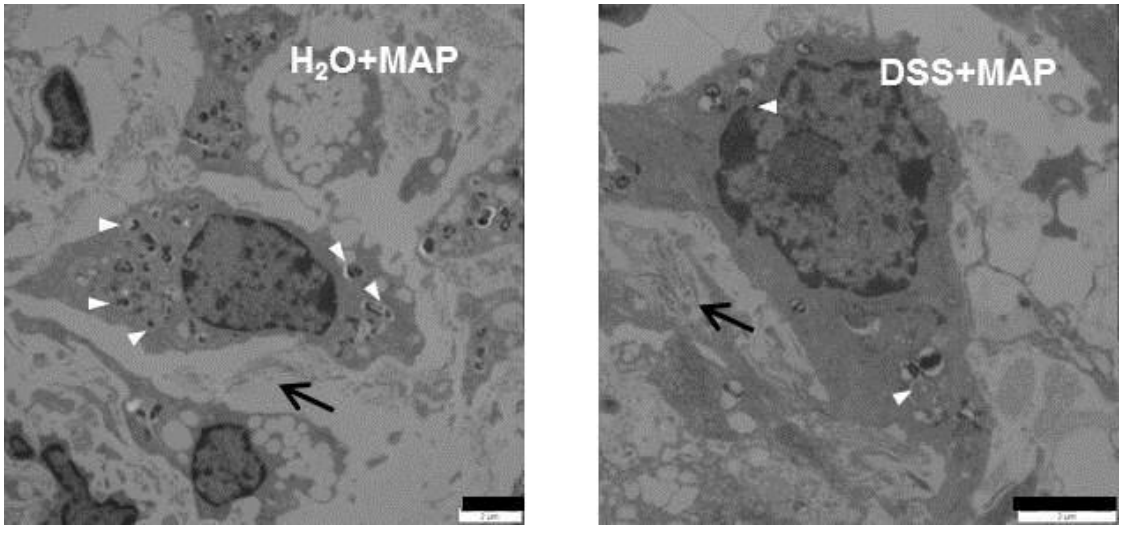

Figure 3.10 Transmission electron microscopic pictures from mesenteric tissue.

TEM visualized mesentery of MAP infected mice at 3 weeks p.i. MAP (white arrowheads) were residing inside of macrophage in both H_2O+MAP (left) and DSS+MAP group (right). Collagen fibers (black arrow) were also observed. Scale bars, 2µm.

3.8 Tropism of MAP to the DSS-treated colon

MAP is known to elicit overt clinical disease in ruminants only after a period of latency. Also, the organ tropism of MAP for the intestinal mucosa is mechanistically still unclear. Hence, we investigated the colonization of MAP in the inflamed colon under our experimental conditions. MAP colonization of colon tissue was significantly higher ($p<0.05$) following DSS treatment (Figure 3.12A). In contrast, only a non-significant colonization was found in the small intestine (Figure 3.12B). This may be explained by the fact that DSS primarily damages the colonic mucosa (Wirtz et al., 2007). Bacteria apparently are being attracted to the damaged mucosal tissue.

Epithelial cell injury after DSS treatment leads to a severe intestinal pathology in the colon. Both DSS-treated groups (DSS+PBS and DSS+MAP) showed high histopathological scores at day 1 p.i.. The score was reduced at 1 week and was even less at 3 weeks p.i.. Strikingly, the colon score of DSS+MAP mice was significantly higher ($p<0.05$) than the score found in DSS+PBS mice at the 3 weeks p.i.. This could be explained by delayed recovery of the colon mucosa due to MAP colonization (Figure 3.13A). At that time point, H&E staining of tissue obtained from DSS+MAP animals revealed moderate infiltration of inflammatory cells and mild epithelial hyperplasia, whereas tissue of DSS+PBS animals only showed low infiltration of inflammatory cells (Figure 3.13B).

In line with the results from the histopathological score, colon tissue of DSS+MAP animals showed significantly higher mRNA levels of IFN-γ (Figure 3.14) in comparison to H_2O+PBS ($p<0.001$), DSS+PBS ($p<0.01$) and H_2O+MAP ($p<0.01$) animals. Interestingly, similar results were also obtained for mRNA of the anti-inflammatory marker IL-10. In contrast, mRNA expression of IL-1ß was increased in colon tissue of all treated groups, DSS+PBS, H_2O+MAP and DSS+MAP in comparison to H_2O+PBS group. Additionally, mRNA expression of TNF-α and IL-6 (data not shown) showed no significant difference between the groups. Taken together, the toxic effect of DSS treatment on the colonic mucosa resulted in higher MAP colonization and delayed tissue recovery possibly due to a higher inflammatory response.

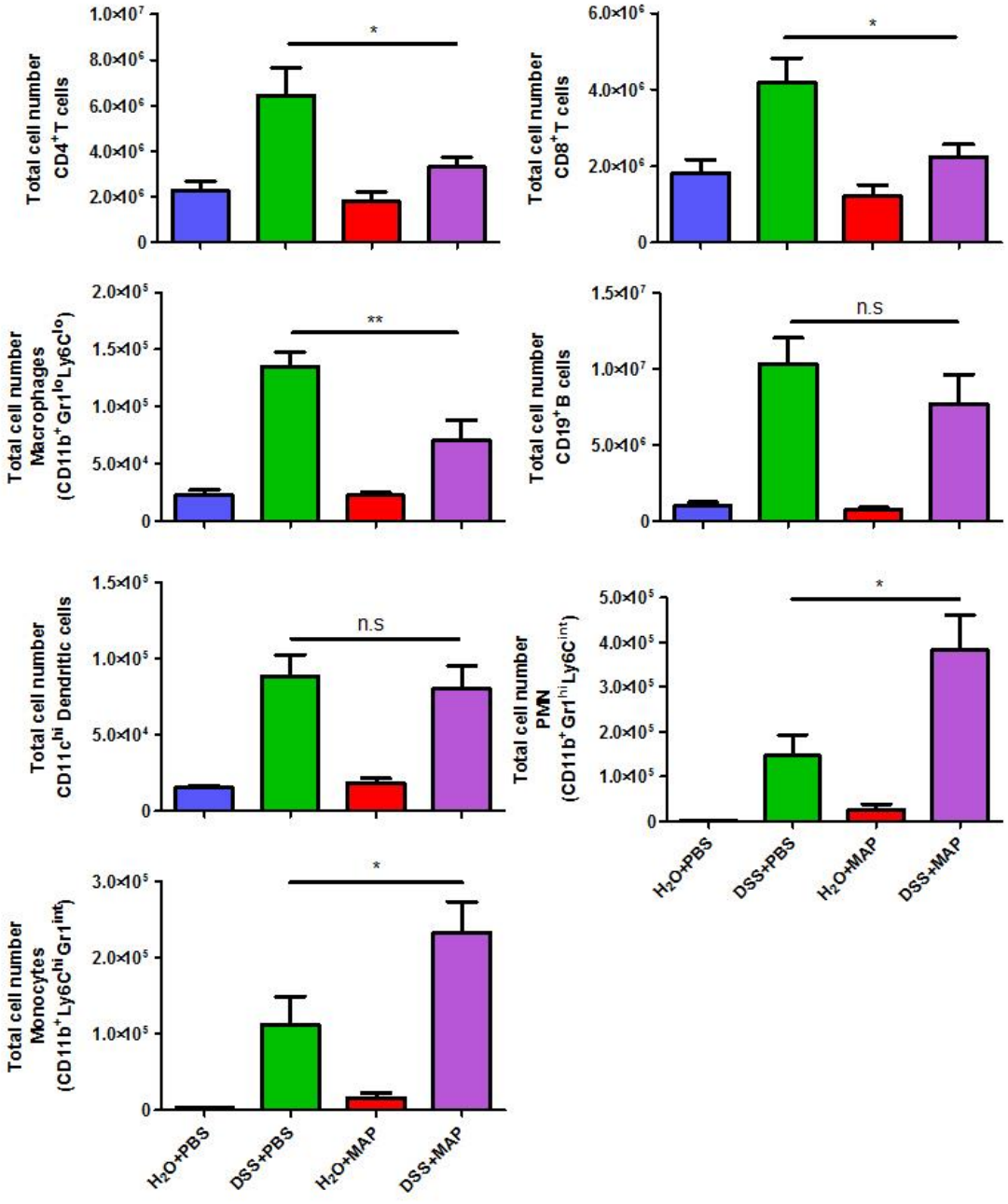

Figure 3.11 Cellularity of mesenteric lymph nodes.

mLN were isolated and stained with DAPI and analyzed by Flow cytometry at 3 weeks p.i. Total number of $CD4^+$ ($CD3^+CD4^+$) and $CD8^+$ ($CD3^+CD8^+$) T cells, $CD19^+$ B cells, dendritic cells ($CD11b^+CD11c^{hi}$), PMN ($CD11b+Gr1^{hi}Ly6C^{int}$), monocytes ($CD11b^+Ly6C^{hi}Gr1^{int}$) and macrophage ($CD11b^+$ $Gr1^{lo}$ $Ly6C^{lo}$) were quantified. Data are from two independent experiments (n=4-5). *p<0.05, **p<0.01, ***p<0.0001, n.s = not significant**.**

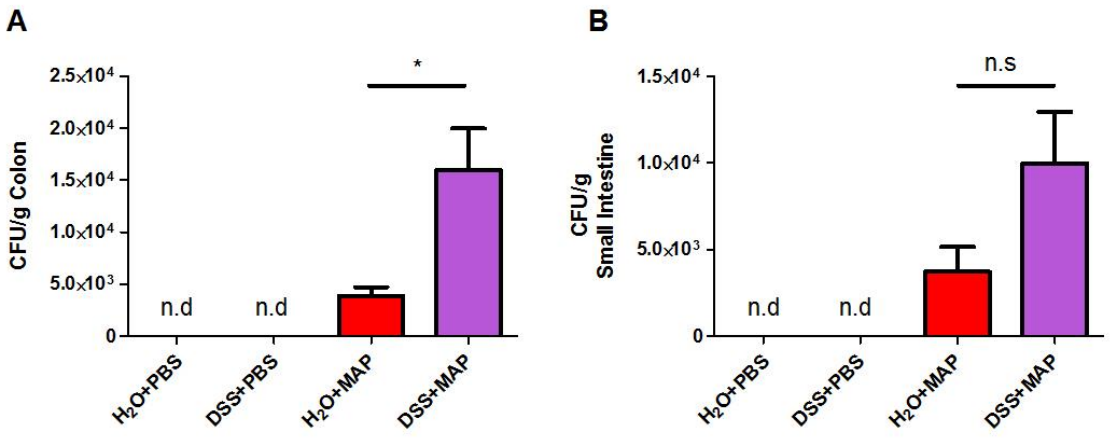

Figure 3.12 MAP had better survival in DSS-induced colon.

A. Bacterial loads in colon and B. small intestine were analyzed at 3 weeks p.i. by plating tissue on Middlebrook agar with antibiotics. Data are representative of at least three independent experiments (n=3-11). *p<0.05, **p<0.01, ***p<0.0001, n.s = not significant**,** n.d = not detectable.

3.9 MAP secondary challenge leads to diarrhea and colitis

As above, 4% DSS was administered in the drinking water of adult female C57BL/6J mice from day 1 until day 5. After two treatment-free days, 10^8 MAP were injected intraperitoneally. Secondary challenge with 10^8 MAP i.p was performed at 5 weeks after first challenge. The five weeks time point was chosen to assure that mice have recovered from MAP first challenge and DSS treatment. The experimental schedule is illustrated in Figure 3.15A. Body weight was measured as a read out for the general health condition (Figure 3.15B). DSS-treated mice infected with MAP for the second time (DSS+MAP+MAP) showed reduction of body weight significantly in comparison to both uninfected DSS-treated (DSS+PBS+PBS) and untreated (H_2O+PBS+PBS) at day 1 after second challenge. They started to regain weight at 4 days after secondary challenge. In contrast, DSS-treated mice infected with MAP for the first time (DSS+PBS+MAP) showed reduction of body weight at 1 day p.i and recovered at day 2 p.i. (Figure 3.15C). Extended weight recovery was also observed in mice without DSS treatment in mice infected with MAP for the second time

(H_2O+MAP+MAP) in comparison to mice without DSS treatment MAP infected for the first time (H_2O+PBS+MAP).

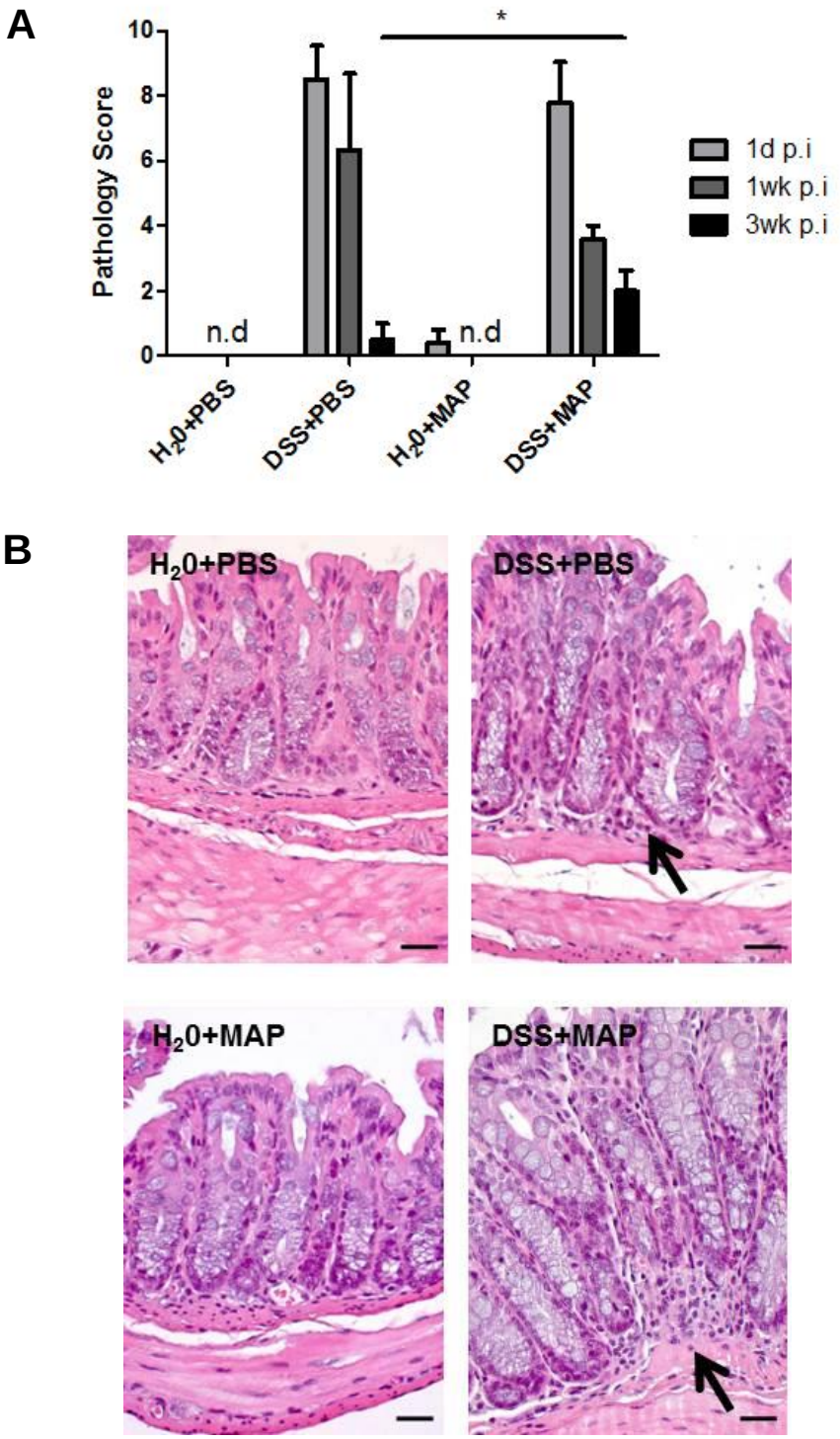

Figure 3.13 MAP showed delayed recovery of DSS-induced colon.

A. Histology changes in the colon were analyzed at day 1, 1 week and 3 weeks p.i. B. H&E staining of colon tissue sections at 3 weeks p.i. Scale bars, 25 µm. H_2O+PBS (upper left) and H_2O+MAP (bottom left) showed normal tissue. DSS+MAP (bottom right) showed mild invasion of

inflammatory cells (black arrow) and mild epithelial hyperplasia. DSS+PBS showed low invasion of inflammatory cells. Data are representative of at least two independent experiments (n=4-5). *p<0.05, **p<0.01, ***p<0.0001, n.d = not detectable.

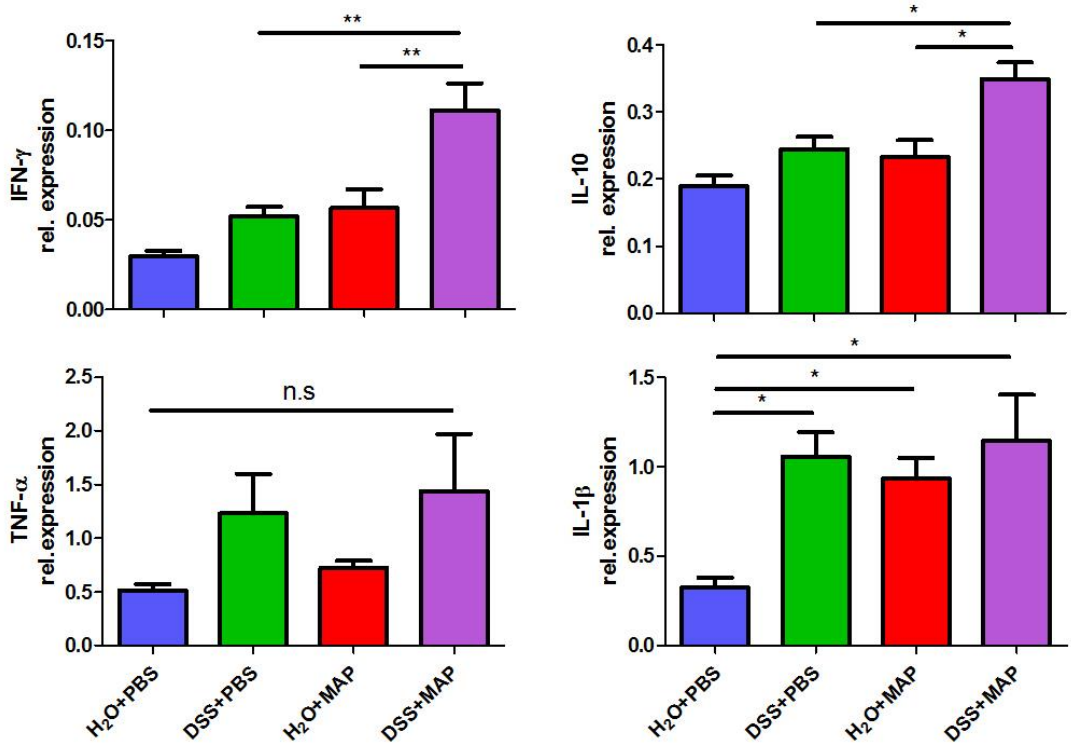

Figure 3.14 Higher inflammatory response in DSS-induced MAP infected mice at 3 weeks p.i.

mRNA expression of IFN-γ (upper left), IL-10 (upper right), TNF-α (bottom left) and IL-1β (bottom right) relative to RPS9 from colon at 3 weeks p.i. (n=4-5). *p<0.05, **p<0.01, n.s = not significant, n.d = not detectable.

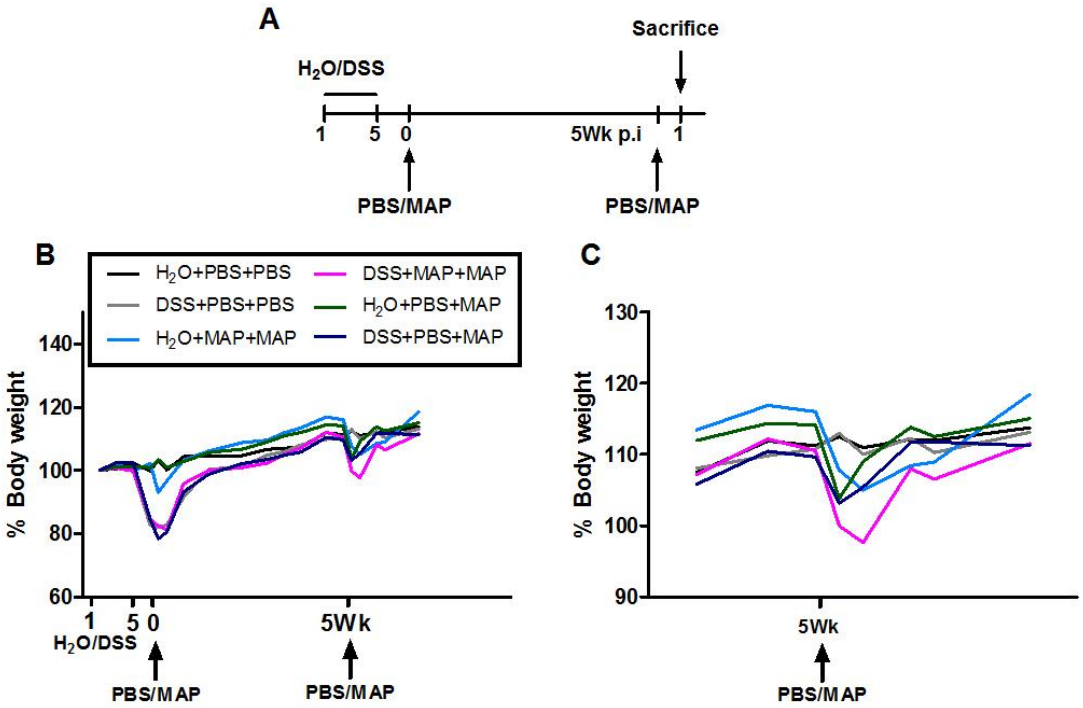

Figure 3.15 Experimental set-up and body weight monitoring.

A. Overview of the experimental schedule. H_2O or 4% DSS were administered to the drinking water from day 1 until day 5, followed by normal drinking water afterwards. PBS or 10^8 CFU MAP in 200 µL i.p. was administered two days after DSS treatment finished (day 0). At 5 weeks p.i, PBS or 10^8 CFU MAP in 200 µL was administered i.p.. Mice were sacrificed at day 1 after secondary challenge. B. Weight change during experiment, C. weight change after secondary challenge, expressed as percentage change from day 1 of DSS treatment. C. The graph shown is only from 5 week after first challenge. The results shown are representative of more than three independent experiments (n=4-5).

Interestingly, both MAP infected group H_2O+MAP+MAP and DSS+MAP+MAP showed reduction of fluid absorption in colon which is a sign of mild diarrhea at day 1 after secondary challenge (Figure 3.16A). Strikingly, reduction of colon length was observed only in DSS+MAP+MAP mice at day 1 after secondary challenge which can be taken as a sign of colitis (Figure 3.16B). Additionally, the colon histology score of DSS+MAP+MAP mice was significantly higher than the score found in DSS+PBS+PBS mice at day 1 after secondary infection (Figure 3.16C). At that time point, H&E staining of tissue obtained from DSS+MAP+MAP animals revealed high infiltration of inflammatory cells and severe epithelial hyperplasia, whereas tissue of DSS+PBS+PBS and

Results

H_2O+MAP+MAP animals only showed low infiltration of inflammatory cells (Figure 3.17). These results suggest that there is a different immune response between first and second infection. DSS-treated MAP infected mice showed stronger immune response after secondary infection. This can be concluded from diarrhea, reduction of colon length and high histology score of the colon.

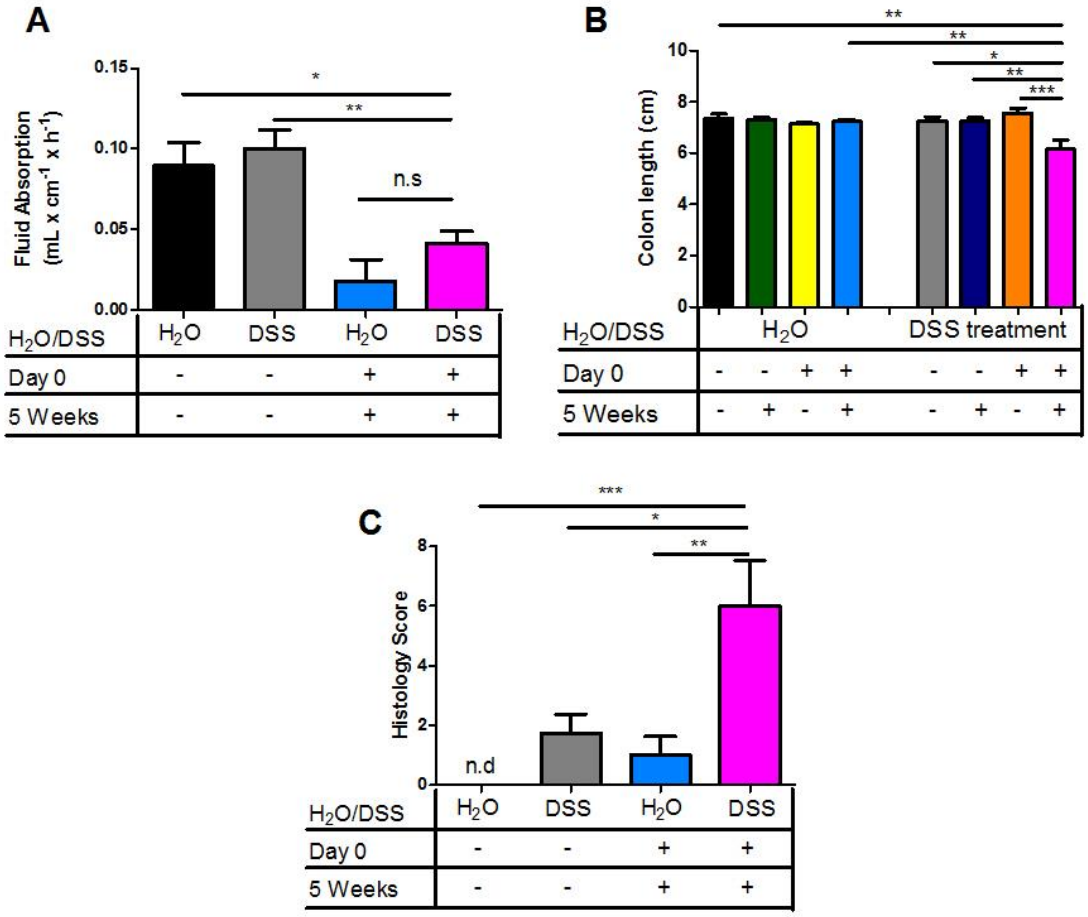

Figure 3.16 MAP secondary challenge leads to diarrhea and colitis.

Fluid absorption from colon in mL x cm^{-1} x $hours^{-1}$ (n=5). B. Upon the autopsy at one day after secondary challenge, colon length was measured. Colon lengths in cm (n=3-5) C. Histology score of the colon were analyzed at one day after secondary challenge (n=3-5). Graph show a representative of at least two independent experiments. *, P<0.05; **, p<0.01; ***,p<0.001, n.s = not significant, one-way ANOVA with Tukey's post test.

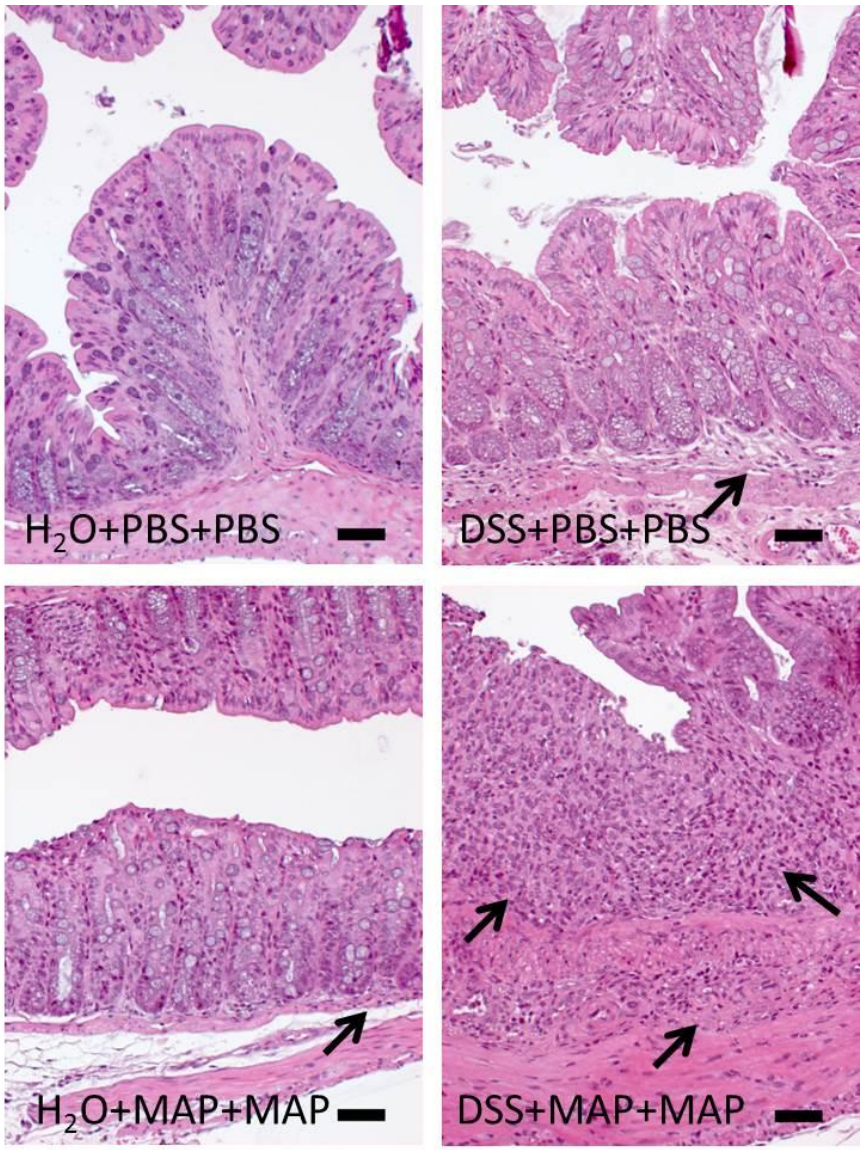

Figure 3.17 H&E staining colon tissue section at day 1 after secondary challenge.

H&E staining of colon tissue sections at day 1 after secondary challenge. Scale bars, 25 µm. H_2O+PBS+PBS (upper left) showed normal tissue. H_2O+MAP+MAP (bottom left) and DSS+PBS+PBS (upper right) showed low infiltration of inflammatory cells (black arrow). DSS+MAP+MAP (bottom right) showed high invasion of inflammatory cells (black arrow) and severe epithelial hyperplasia.

3.10 Elevated cytokines level after secondary challenge

Since a marked immune response was observed in mice after secondary challenge, it was interesting to know whether cytokines and chemokines were induced under these circumstances. Therefore, we collected sera and pooled them from each group at 6 hours after secondary challenge and measured the cytokines and chemokines levels using cytokines and chemokines multiplex assay. Interestingly, nearly all cytokines and chemokines were upregulated in both H_2O+MAP+MAP and DSS+MAP+MAP groups (Table 3.2).

To confirm the result, we collected sera at 2, 6 and 24 hours after secondary challenge. Dramatically elevated levels of TNF-α were observed at 2 hours after secondary challenge in both H_2O+MAP+MAP and DSS+MAP+MAP groups (Figure 3.18A). The TNF-α levels decreased gradually afterwards. IFN-γ levels elevated at 2 hours, reached the peak at 6 hours and decreased at 24 hours after secondary challenge (Figure 3.18B). The same kinetics of TNF-α and IFN-γ levels were also observed from colon supernatant (Figure 3.18C-D).

3.11 DSS+MAP treated mice exhibit increased leukocytes in mLN

The mesenteric lymph nodes (mLN) are located in the mesenteric tissue and drain the intestine. In order to investigate changes in the cellular composition of mLNs following MAP infection and/or DSS treatment, mLN leukocytes were stained and analyzed by flow cytometry at day 1 after secondary challenge. The gating strategy was shown in Figure 3.19.

Interestingly, the frequency of $CD19^+$ B cells, dendritic cells ($CD11b^+CD11c^{hi}$) and PMN ($CD11b^+Ly6G^{hi}Ly6C^{lo}$) were increased in DSS+MAP+MAP group in comparison to other groups, which has not been observed in H_2O+MAP+MAP group (Figure 3.20). The increasing composition of those cells is caused by secondary challenge, since there was no increasing composition of those cells in DSS-treated infected MAP which did not receive a secondary challenge (DSS+MAP+PBS).

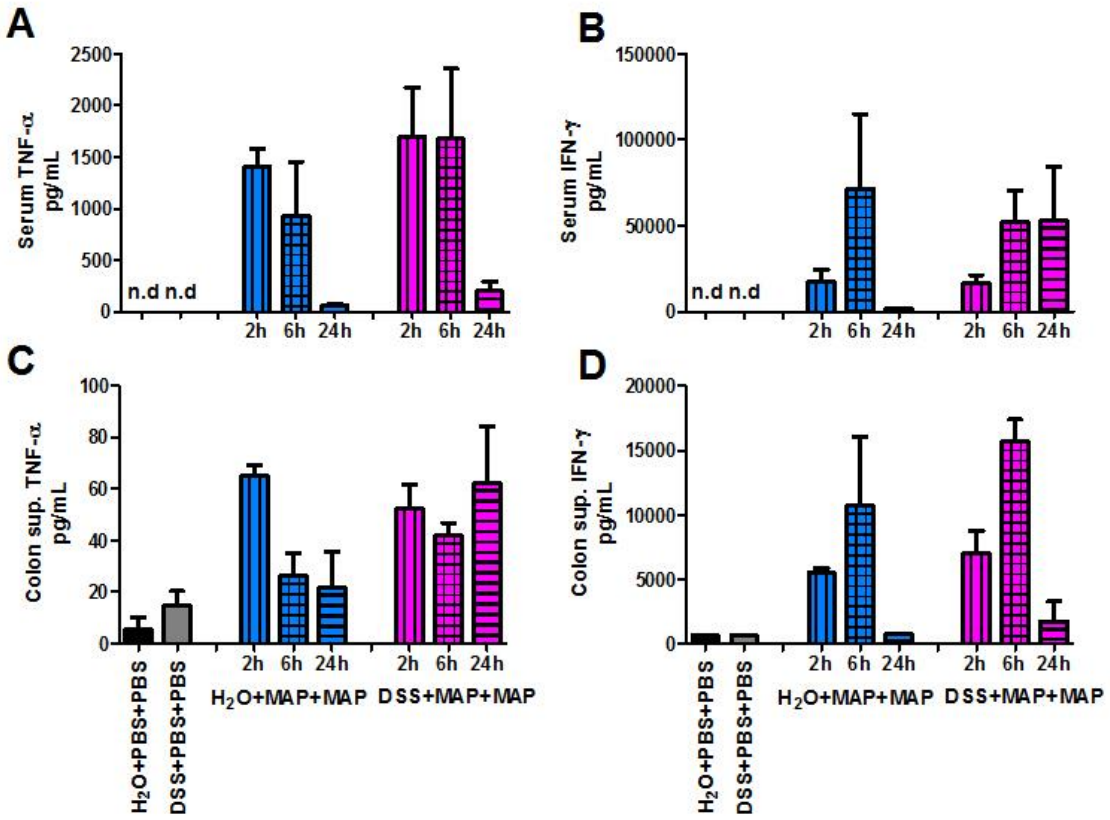

Figure 3.18 Elevated cytokines level after secondary challenge.

Kinetics of TNF-α (A&C) and IFN-γ (B&D) at 2, 6 and 24 hours after secondary challenge (n=3-5). (A-B) Cytokines level in serum (C-D) Secretion of cytokines into the supernatant of overnight cultured from colon. n.d = not detectable.

For inflammatory monocytes ($CD11b^{+}Ly6C^{hi}Ly6G^{int}$) and macrophages ($CD11b^{+}Ly6G^{lo}Ly6C^{lo}F4/80^{hi}$), increased frequency were observed in DSS+MAP+MAP in comparison to H_2O+PBS+PBS group. Additionally, no difference was seen between all groups in $CD4^{+}$ and $CD8^{+}$ T cells (Figure 3.20). However, the total cell numbers were found to be increased in both DSS+MAP+MAP and DSS+MAP+PBS. This leads to increase all leukocytes populations such as B cells, dendritic cells, inflammatory monocytes, PMN, macrophages, $CD4^{+}$ and $CD8^{+}$ T cells (Figure 3.21). Thus, combination of DSS treatment and MAP infection cause an increase in the number of cells in mLN.

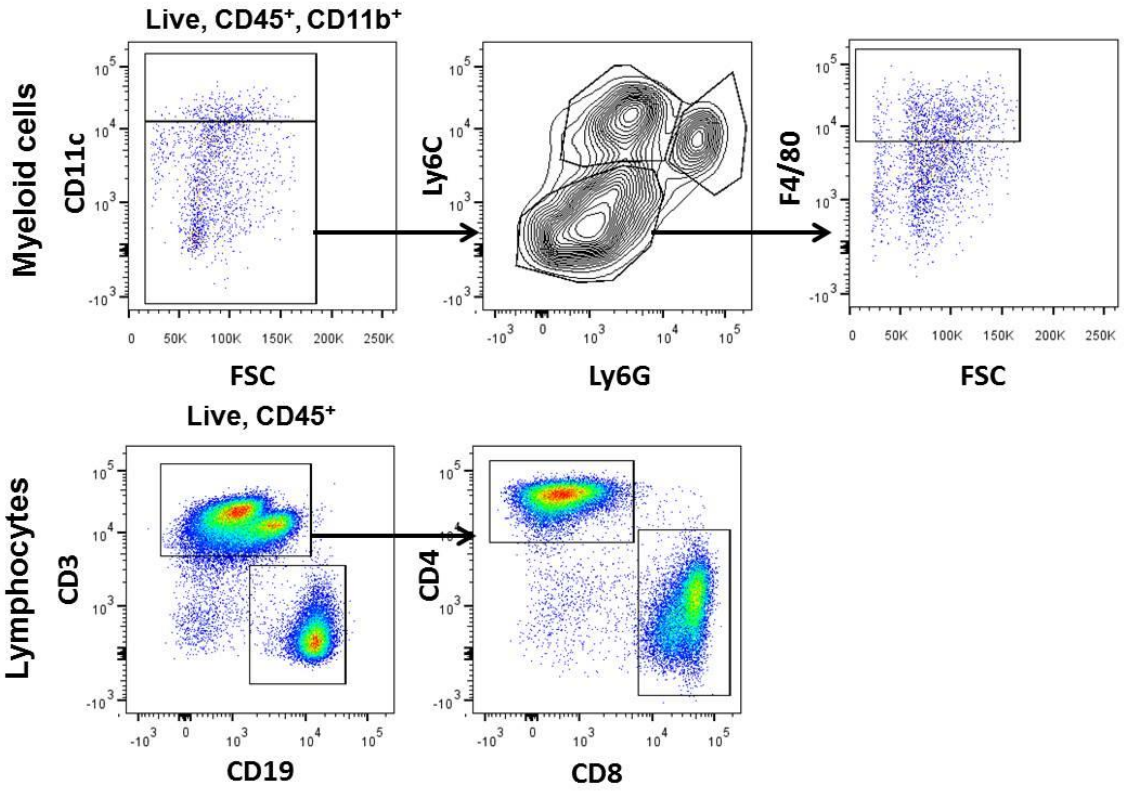

Figure 3.19 Flow cytometry gating strategy for myeloid cells and lymphocytes from mLN and colonic lamina propria.

Myeloid cells from live cells, $CD45^+$ and $CD11b^+$ consist of dendritic cells ($CD11b^+$ $CD11c^{hi}$),PMN ($CD11b^+Ly6G^{hi}Ly6C^{int}$), inflammatory monocytes ($CD11b^+Ly6C^{hi}Ly6G^{int}$) and macrophages ($CD11b^+Ly6G^{lo}Ly6C^{lo}F4/80^{hi}$). Lymphocytes from live cells, $CD45^+$ consist of $CD19^+$ B cells, $CD4^+$ ($CD3^+CD4^+$) and $CD8^+$ ($CD3^+CD8^+$) T cells.

3.12 Role of $CD4^+$ T cells in DSS+MAP mice colon after secondary challenge

To understand the underlying cause of reduction of colon length in DSS+MAP+MAP mice after secondary challenge described above, a detailed analysis of colon leukocytes composition was carried out by flow cytometry. The gating strategy was shown in Figure 3.19. No difference could be observed in $CD8^+$ T cells, $CD19^+$ B cells, macrophages ($CD11b^+Ly6G^{lo}Ly6C^{lo}F4/80^{hi}$) and dendritic cells ($CD11b^+CD11c^{hi}$) (Figure 3.22). Interestingly, $CD4^+$ T cells showed significantly high frequency only in DSS+MAP+MAP in comparison to all other groups (Figure 3.22).

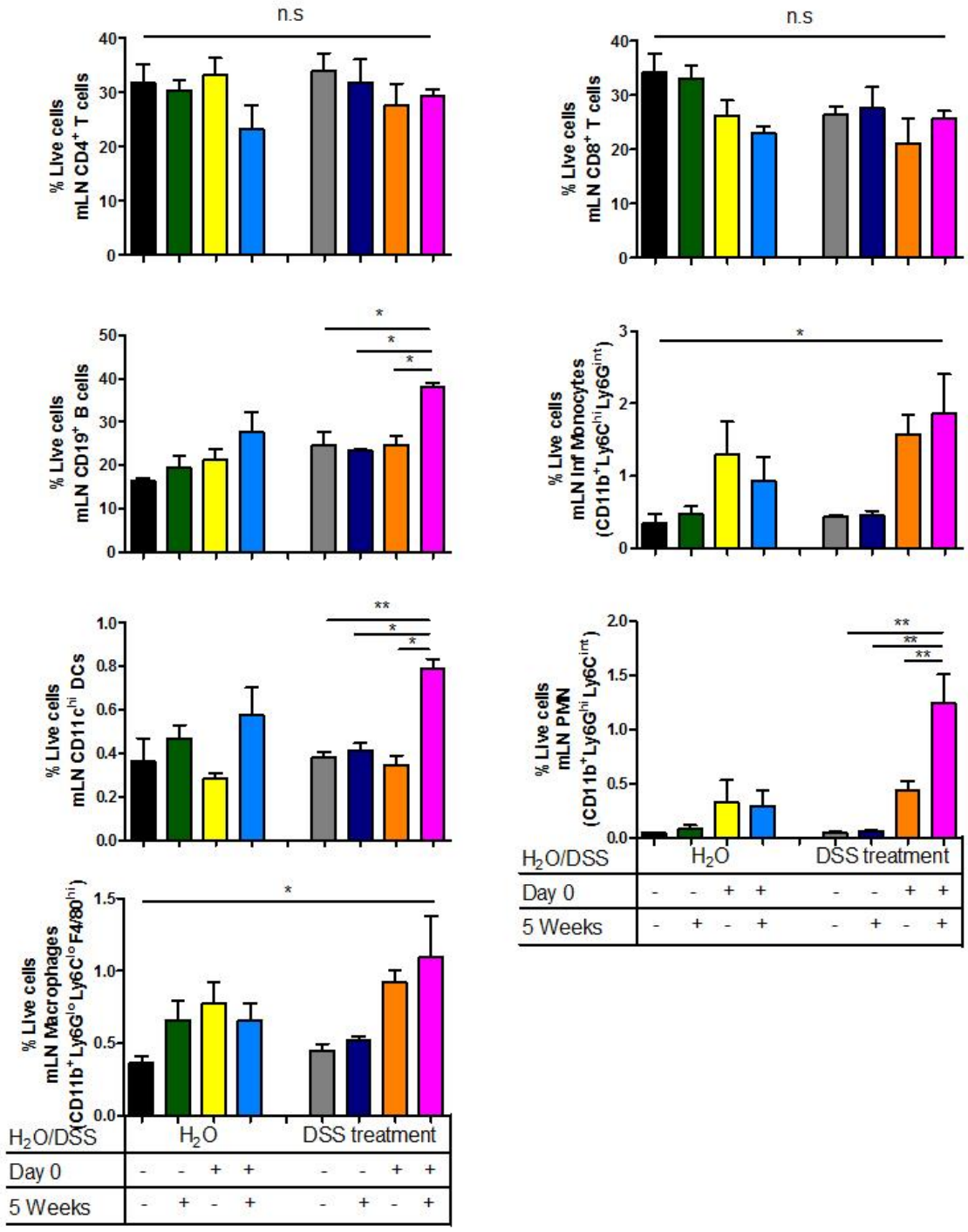

Figure 3.20 Frequency of leukocytes in mLN at day 1 after secondary challenge.

Frequency of $CD19^+$ B cells, $CD4^+$ ($CD3^+CD4^+$) and $CD8^+$ ($CD3^+CD8^+$) T cells. dendritic cells ($CD11b^+$ $CD11c^{hi}$),PMN ($CD11b^+Ly6G^{hi}Ly6C^{int}$), inflammatory monocytes ($CD11b^+Ly6C^{hi}Ly6G^{int}$) and macrophages ($CD11b^+Ly6G^{lo}Ly6C^{lo}F4/80^{hi}$) in mesenteric lymph nodes (n=3-5). Graph show a representative of at least two independent experiments. *, P<0.05; **, p<0.01; ***,p<0.001, n.s = not significant, one-way ANOVA with Tukey's post test.

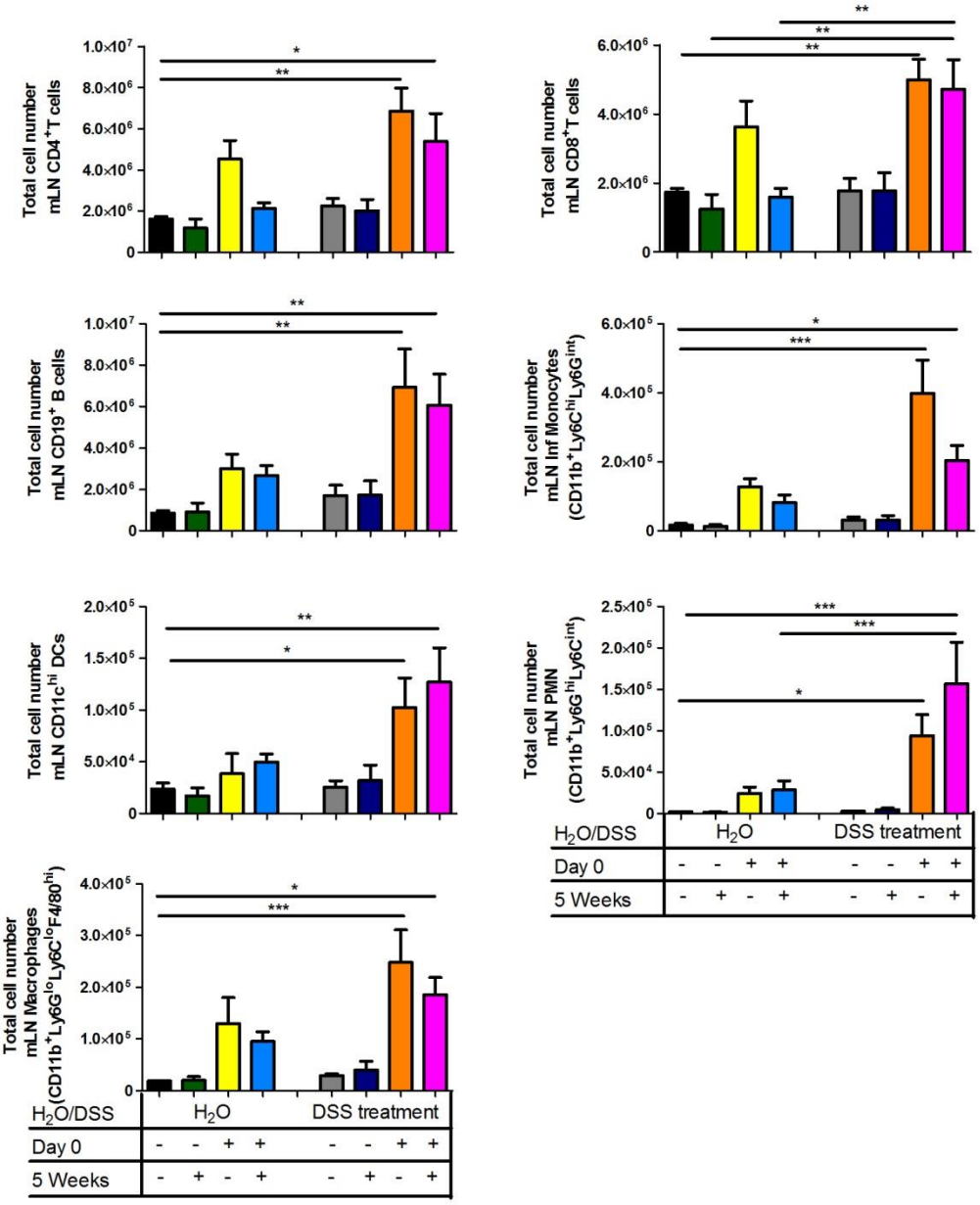

Figure 3.21 DSS+MAP treated mice exhibit increased leukocytes in mLN at day 1 after secondary challenge.

Flow cytometry on leukocytes in mLN at day 1 after secondary challenge. Total cell numbers of $CD19^+$ B cells, $CD4^+$ ($CD3^+CD4^+$) and $CD8^+$ ($CD3^+CD8^+$) T cells, dendritic cells ($CD11b^+$ $CD11c^{hi}$),PMN ($CD11b^+Ly6G^{hi}Ly6C^{int}$), inflammatory monocytes ($CD11b^+Ly6C^{hi}Ly6G^{int}$) and macrophages ($CD11b^+Ly6G^{lo}Ly6C^{lo}F4/80^{hi}$) in mesenteric lymph nodes (n=3-5). Graph show a representative of at least two independent experiments. *, P<0.05; **, p<0.01; ***,p<0.001, one-way ANOVA with Tukey's post test.

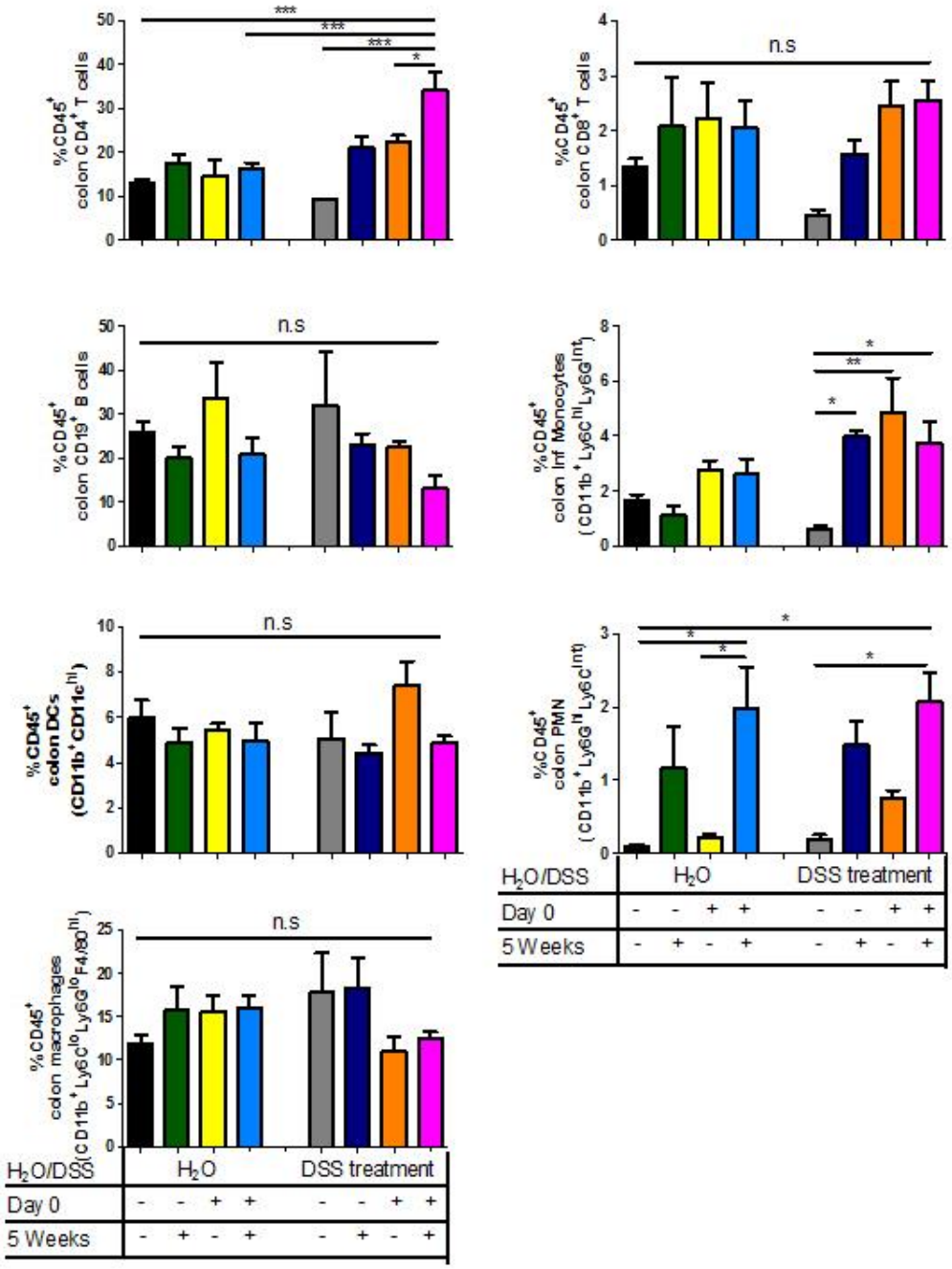

Figure 3.22 Flow cytometry on leukocytes in colonic lamina propria at day 1 after secondary challenge.

Frequency of CD19$^+$ B cells, CD4$^+$ (CD3$^+$CD4$^+$) and CD8$^+$ (CD3$^+$CD8$^+$) T cells, dendritic cells (CD11b$^+$ CD11c^{hi}),PMN (CD11b$^+$Ly6G^{hi}Ly6C^{int}), inflammatory monocytes (CD11b$^+$Ly6C^{hi}Ly6G^{int}) and macrophages (CD11b$^+$Ly6G^{lo}Ly6C^{lo}F4/80^{hi}) in colonic lamina propria (n=3-5). *, P<0.05; **, p<0.01; ***,p<0.001, n.s = not significant, one-way ANOVA with Tukey's post test.

Additionally, we observed high frequency of PMN ($CD11b^{+}Ly6G^{hi}Ly6C^{int}$) in all infected groups. Inflammatory monocytes ($CD11b^{+}Ly6C^{hi}Ly6G^{int}$) were increased in all DSS-treated MAP infected groups.

Next, we investigated the role of adaptive immunity in inducing colitis after secondary challenge with MAP. DSS-treated MAP infected $RAG2^{-/-}$ mice were challenged with MAP ip and sacrificed at day 1 after secondary challenge. Interestingly, we could not observe any reduction of colon length in those mice (Figure 3.23A) indicating that cells of the adaptive immune system are responsible.

To assess the key player in this phenomenon, $CD4^{+}$T cells or $CD8^{+}$T cells from C57BL/6 WT mice were depleted using anti-CD4 or CD8 antibodies two days before secondary challenge (Figure 3.23B). Strikingly, reduction of colon length was not observed in depleted $CD4^{+}$ T cells mice (Figure 3.23C). Conversely, $CD8^{+}$ T cells depleted mice still showed a reduction of colon length. Additionally, there is no colon length reduction in DSS+MAP+PBS, DSS+PBS+MAP, H_2O+MAP+PBS and H_2O+PBS+MAP (Figure 3.23C). Along the same line, colon histology score of depleted $CD4^{+}$ T cells mice showed significantly lower score in comparison to depleted $CD8^{+}$ T cells and WT mice (Figure 3.23D). Moderate infiltration of inflammatory cells and mild epithelial hyperplasia could be observed from DSS+MAP+MAP WT and $CD8^{+}$ T cells depleted mice, whereas tissues from DSS+MAP+MAP $CD4^{+}$ T cells depleted mice, DSS+PBS+PBS, DSS+PBS+MAP and DSS+MAP+PBS showed only low infiltration of inflammatory cells (Figure 3.24).

3.13 MAP specific pathogenicity after secondary challenge

To investigate MAP specific tropism in comparison to other mycobacteria species, we infected DSS-treated mice with closely related mycobacteria species *M. avium* ssp. *avium* (MAA) or *M. avium* ssp. *hominissuis* (MAH). At 5 week after the first challenge, secondary challenge with the same mycobacteria was carried out (Figure 3.25A).

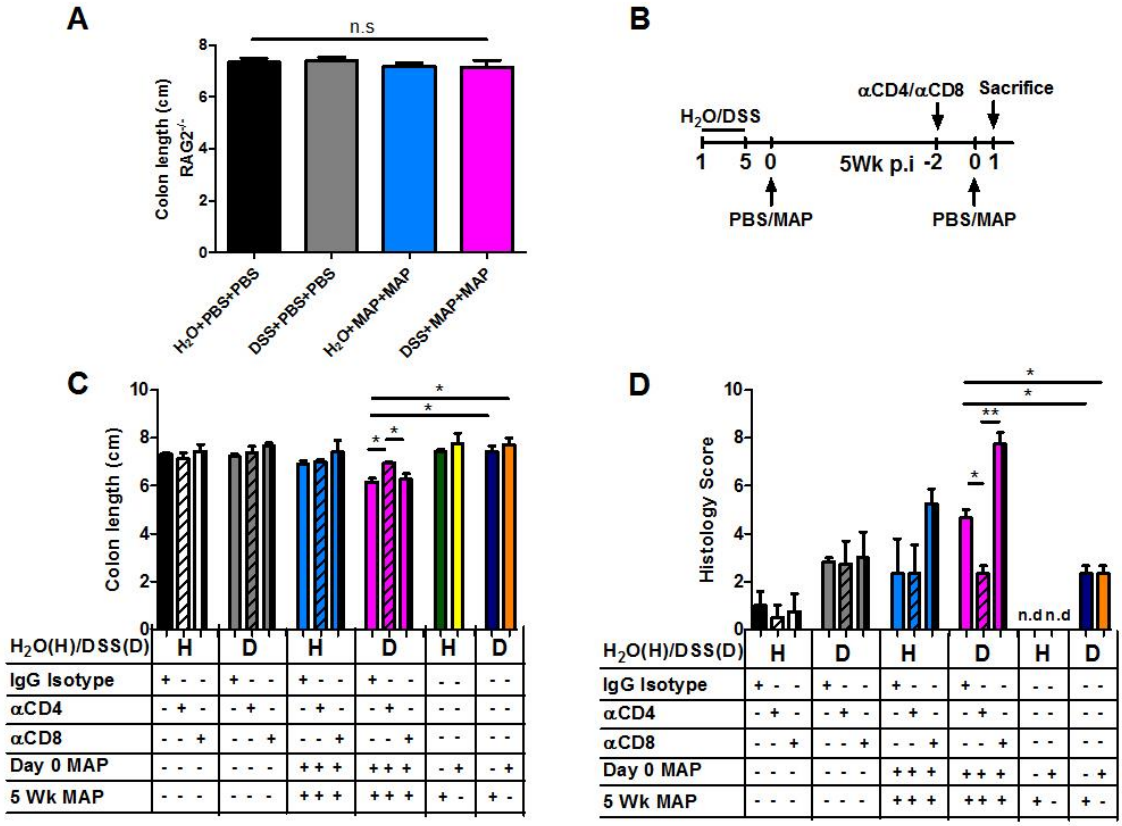

Figure 3.23 Role of CD4$^+$ T cells in colitis.

A. Upon the autopsy at one day after secondary challenge, colon length of RAG$^{-/-}$ mice was measured. Colon lengths in cm (n=4-6). B. Experimental scheme for CD4 and CD8 T cells depletion. H_2O or 4% DSS were administered to the drinking water from day 1 until day 5, followed by normal drinking water afterwards. PBS or 10^8 CFU MAP in 200 µL i.p. was administered two days after DSS treatment finished (day 0). IgG isotype, CD4 or CD8 antibody were administered two days before secondary challenge. At 5 weeks p.i, PBS or 10^8 CFU MAP in 200 µL was administered i.p.. Mice were sacrificed at day 1 after secondary challengeC. Colon length of CD4 or CD8 depleted and IgG Isotype control mice were measured (n=3-4). D. Histology score of the colon were analyzed at one day after secondary challenge (n=3-5). Graph show a representative of at least two independent experiments. *, P<0.05; **, p<0.01; ***,p<0.001, one-way ANOVA with Tukey's post test.

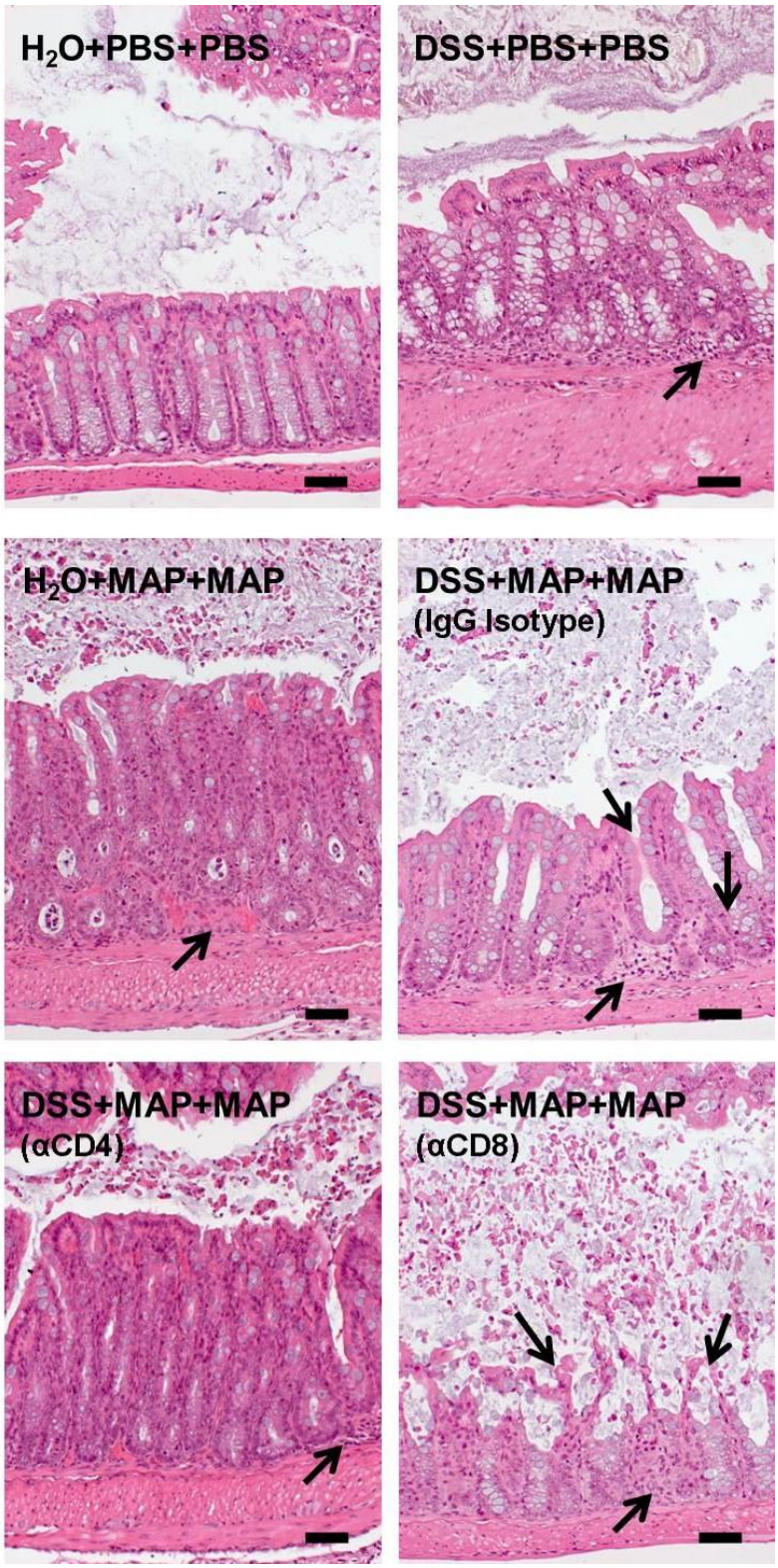

Figure 3.24 H&E staining colon tissue section in $CD4^+$ or $CD8^+$ T cells depleted mice.

H&E staining of colon tissue sections at day 1 after secondary challenge. Scale bars, 25 µm. H_2O+PBS+PBS (upper left) showed normal tissue. DSS+PBS+PBS (upper right),

H_2O+MAP+MAP (middle left) and DSS+MAP+MAP depleted CD4+ T cells (bottom left) showed low infiltration of inflammatory cells (black arrow). DSS+MAP+MAP IgG isotype (middle right) and DSS+MAP+MAP depleted CD8+ T cells (bottom right) showed moderate invasion of inflammatory cells (black arrow) and mild epithelial hyperplasia.

All infected mice showed enlargement of total liver weight in comparison to uninfected groups (Figure 3.25B). Interestingly, mice infected with MAA and MAH showed larger total spleen weight in comparison to MAP infected group (Figure 3.25C). The most important finding is that only DSS-treated MAP infected mice showed reduction of colon length after secondary challenge with the same mycobacteria, neither in DSS-treated MAA nor in DSS-treated MAH after secondary challenge (Figure 3.25D). These results strongly suggested that such bacteria exhibit differential pathogenicity which might be due to a differential tissue tropism. Colitis could only be induced in DSS-treated MAP infected mice after secondary infection.

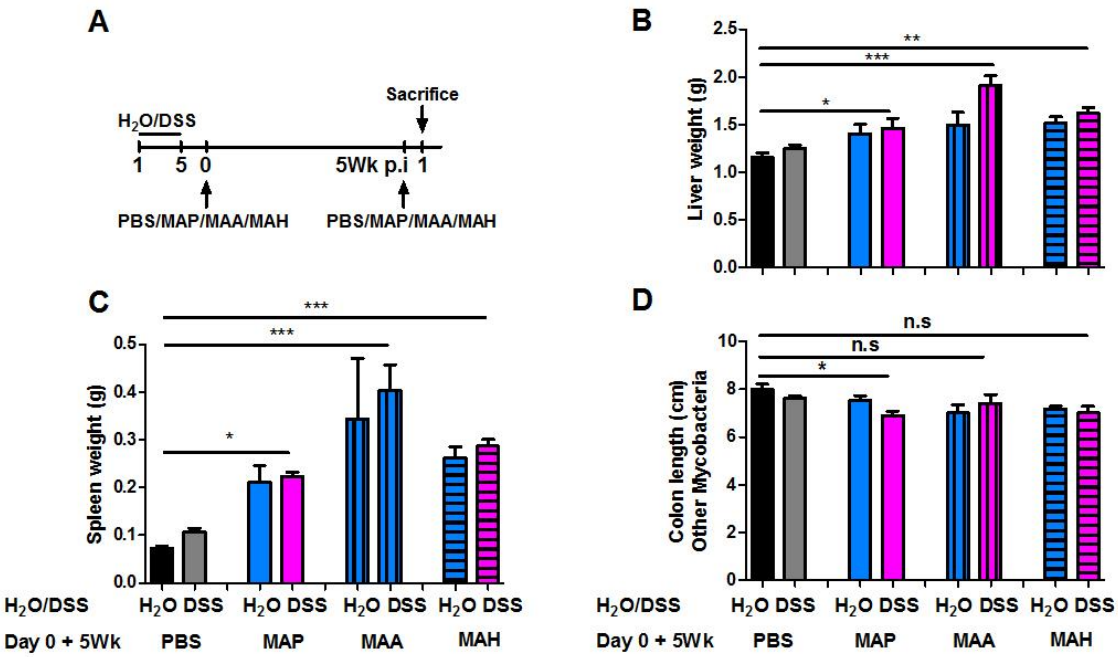

Figure 3.25 MAP specific tropism after secondary challenge.

A. Experimental scheme. H_2O or 4% DSS were administered to the drinking water from day 1 until day 5, followed by normal drinking water afterwards. PBS or 10^8 CFU MAP, MAA or MAH in 200 µL i.p. was administered two days after DSS treatment finished (day 0). At 5 weeks p.i, PBS or 10^8 CFU MAP, MAA or MAH in 200 µL was administered i.p.. Mice were sacrificed at day 1 after secondary challenge. B. Total liver weight in Gram. C. Total spleen weight in Gram. D. Colon length of MAP, MAA and MAH infected group at day 1 after secondary challenge with the

same mycobacteria species (n=3-5). Graph show a representative of at least two independent experiments. *, P<0.05; **, p<0.01; ***,p<0.001, n.s = not significant, one-way ANOVA with Tukey's post test.

3.14 The importance of TLR2 in DSS+MAP mice after secondary challenge

TLR2 play important role for immune activation against mycobacterial infection. To investigate the role of TLR2 in present experimental set-up, DSS-treated MAP infected TLR2$^{-/-}$ mice were challenged with MAP i.p at 5 week after first infection and sacrificed at day 1 after secondary challenge. Significantly larger livers were found in H_2O+MAP+MAP and DSS+MAP+MAP in TLR2$^{-/-}$ mice at day 1 after secondary challenge (Figure 3.26A). Along the same line, enlargement of spleen was observed in H_2O+MAP+MAP and DSS+MAP+MAP in TLR2$^{-/-}$ mice at day 1 after secondary challenge (Figure 3.26B). Interestingly, there was no reduction of colon length in TLR2$^{-/-}$ mice while it could be observed in WT DSS+MAP+MAP group (Figure 3.26C).

Taken together, CD4^{+} T cells are the important key player in causing colitis in DSS-treated MAP infected mice after secondary challenge. The mechanism might be via TLR2 signaling which is known as the important factor in immune response against mycobacterial infection. Colitis phenomena after secondary challenge show the specific tropism of MAP that could not be seen in other closely related mycobacteria species.

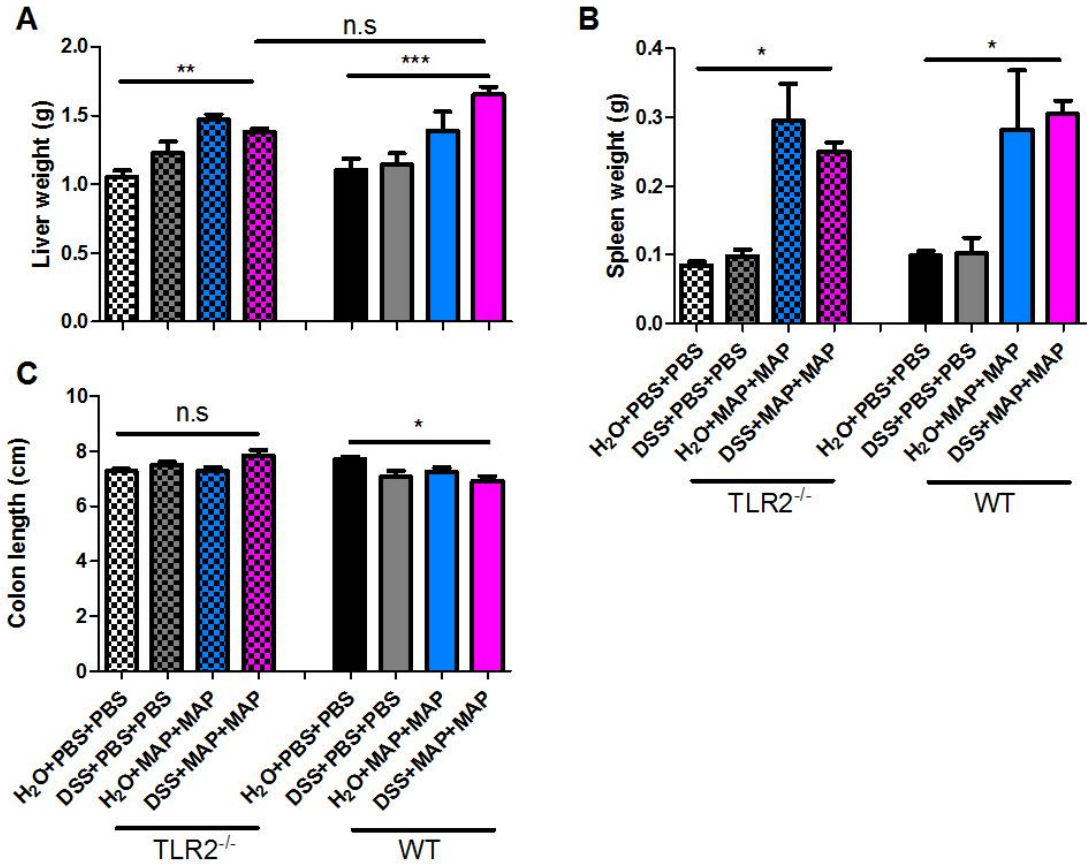

Figure 3.26 The importance of TLR2 for inducing colitis in DSS-treated MAP infected mice after secondary challenge.

(A-C) Upon the autopsy at one day after secondary challenge of TLR2$^{-/-}$ mice, colon length, liver and spleen weight were measured. A. Total liver weight in Gram. B. Total spleen weight in Gram. C. Colon length of TLR2$^{-/-}$ mice at day 1 after secondary challenge (n=3-5). Graph show a representative of at least two independent experiments. *, P<0.05; **, p<0.01; ***,p<0.001, n.s = not significant, one-way ANOVA with Tukey's post test.

Table 3.1 Cytokines and chemokines multiplex assay at 2h and 24h p.i

Note: OOR = out of range

	H_20 + PBS 2h	DSS + PBS 2h	H_20 + MAP 2h	DSS + MAP 2h	H_20 + PBS 24h	DSS + PBS 24h	H_20 + MAP 24h	DSS + MAP 24h
IL-1α	13,36	18,96	38,3	20,11	22,75	17,3	36,17	53,13
IL-1β	27,28	130,37	142,71	142,71	45,50	117,68	130,37	380,71
IL-2	5,60	9,85	8,76	10,91	7,07	11,95	12,46	31,7
IL-3	OOR <	OOR <	0,37	0,12	OOR <	0,58	OOR <	1,87
IL-4	OOR <	0,52	2,38	1,48	OOR <	1,10	0,52	3,42
IL-5	14,55	9,46	125,56	14,55	9,46	10,79	15,73	30,46
IL-6	8,79	32,95	1252,32	873,86	7,73	9,52	67,28	86,68
IL-9	1,39	31,93	74,59	74,59	22,62	22,62	40,89	147,89

	H_20 + PBS 0h	DSS + PBS 0h	H_20 + MAP 0h	DSS + MAP 0h	H_20 + PBS 6h	DSS + PBS 6h	H_20 + MAP 6h	DSS + MAP 6h
IL-10	17,49	20,07	501,99	92,25	18,78	22,65	20,07	88,27
IL-12 (p40)	156,73	60,3	395,91	178,53	87,12	40,29	37,56	55,37
IL-12 (p70)	23,37	22,4	52,4	40,92	16,27	28,81	24,01	81,64
IL-13	35,66	47,9	93,22	84,94	23,49	43,82	76,68	185,11
IL-17	70,93	34,16	36,28	44,42	39,14	32,91	45,89	106,84
Eotaxin	112,92	54,92	307,72	181,24	54,92	45,98	120,78	266,63
G-CSF	112,65	3760,78	1536,84	4551,74	62,07	2521,65	26360,02	20367,3
GM-CSF	11,87	OOR <	72,44	75	OOR <	55,56	61,53	127,23
IFN-g	1,83	1,90	4,45	3,57	3,5	3,5	2,46	7,93
KC	132,02	289,8	2753,54	3252,66	23,51	222,38	790,71	726,32
MCP-1	73,69	123,9	2037,3	1614,44	71,67	114,49	189,47	227,26
MIP-1a	5,09	7,75	124,94	46,94	5,75	6,15	98,9	131,35
MIP-1b	10	16,84	239,37	105,27	10	21,89	16,84	43,41
RANTES	27,1	8,67	31,61	15,38	23,47	8,34	26,43	8,76
TNF-α	1128,09	849,65	5586,55	1238,83	1017,01	1238,83	849,65	2872,55

Table 3.2 Cytokines and chemokines multiplex assay at 0 and 6h after secondary challenge.

	H_20 + PBS+PBS	DSS + PBS+PBS	H_20 + MAP +MAP 2h	DSS + MAP +MAP 2h	H_20 + MAP +MAP 24h	DSS + MAP +MAP 24h
IL-1α	14,7	6,1	1,16	10,49	72,11	73,58
IL-1β	27,28	27,28	90,99	45,50	667,15	457,52
IL-2	4,67	4,67	6,49	11,43	8284,91	9110,05
IL-3	OOR <	OOR <	OOR <	OOR <	3,16	3,02
IL-4	0,08	0,08	0,91	OOR <	3,93	4,10
IL-5	38,84	18,59	12,71	9,46	496,5	259,48
IL-6	2,48	2,34	2,91	3,48	8948,15	OOR >
IL-9	22,62	OOR <	OOR <	17,77	129,2	169,9
IL-10	17,49	8,53	6	12,36	350,41	449,54
IL-12(p40)	77,24	55,17	189,15	219,78	841,72	1169,19
IL-12(p70)	20,47	13,34	14,32	17,24	69,38	83,26
IL-13	15,43	7,44	27,53	60,21	235,72	218,82
IL-17	34,66	24,8	19,22	26,59	336,4	180,62
Eotaxin	112,92	45,98	OOR <	36,76	2245,66	5007,7
G-CSF	148,21	208,14	49,56	970,22	16694,29	28297,56
GM-CSF	11,87	OOR <	OOR <	OOR <	112,3	129,9
IFN-g	2,32	0,45	2,74	2,74	1505,6	2467,31
KC	24,72	10,02	20,73	50,78	8048,34	7671,89
MCP-1	75,69	65,42	166,46	117,67	10854	11987,42
MIP-1a	2,22	0,94	4,70	9,09	215,64	227,95
MIP-1b	12,83	8,52	9,27	13,51	274,63	518,22
RANTES	14,73	11,8	41,95	39,53	391,88	502,89
TNF-α	793,64	339,9	681,24	961,33	5005,62	4209,94

4 Discussion

DSS-induced colitis is a commonly used murine model to study inflammatory bowel disease of humans. Symptoms such as diarrhea, bloody feces, mucosal ulceration, shortening of colon length and weight loss occur both in DSS treated mice and humans suffering from IBD (Wirtz et al., 2007). The chemical DSS exerts a direct cytotoxic effect on enterocytes and the protective mucus layer resulting in barrier damage and translocation of commensal bacteria associated with an inflammatory response (Johansson et al., 2013; Saleh and Elson, 2011). For the induction of DSS colitis, the adaptive immune system does not play an essential role. In contrast, the innate immune system i.e. TLR and the inflammasome are required for tissue repair and protection from colitis (Saleh and Elson, 2011). In addition, intestinal mononuclear phagocytes such as macrophages and dendritic cells (Qualls et al., 2006) showed a suppressive influence on DSS-induced colitis thus supporting the critical role of the innate immune system in this model. Even though the adaptive immunity does not play an essential role in this model, both T helper (Th)1 and Th2 cells have been shown the influence at the later phases to the disease (Dieleman et al., 1998). DSS-induced colitis therefore appeared to be a suitable system to test the hypothesis that MAP infection is exacerbating an existing colitis. Indeed, MAP infection led to a more pronounced reduction in body weight and delayed recovery from DSS-induced mucosal damage.

The reduction of body weight after MAP administration might be due to the increased levels of cytokines, such as TNF-α in serum. These increased cytokine levels were expected since MAP contains several PAMPs that are able to elicit strong innate immune stimulation. However, under inflammatory condition by DSS administration, kinetics of cytokines production was altered with TNF-α as one of the most obvious and probably one of the most deleterious examples.

Exacerbation of DSS inflammation by MAP could also be confirmed by the analysis of individual organs. The spleen weight was significantly enhanced in DSS+MAP mice although the bacterial burden was comparable with the H_2O+MAP control group. Spleen enlargement was most likely due to an increased influx, activation or even expansion of myeloid cells. Similarly, the liver was enlarged in DSS+MAP animals in the absence of an increased bacterial count. Granuloma formation was observed in both DSS and non DSS treated MAP infected animals. However, the granuloma in liver of DSS+MAP animals were more frequent and larger as compared to the granuloma found in mice only infected with MAP. Again, increased numbers of myeloid cells were detected. Granuloma formation contributes to restrict tissue spread of mycobacteria. On the other hand, intracellular infection of macrophages within granulomas supports mycobacterial survival and persistence in the host (Saunders and Britton, 2007). Cytokines and immune cells, particularly T cells are required for the formation of such structures (Cooper et al., 1993; Saunders et al., 2002). Since DSS treatment not only allows microbial translocation through the damaged barrier but also activates immune cells, it might also support the formation of larger granuloma in liver.

Mice treated with DSS and infected with MAP produced stronger antibody reactions. Increased total serum IgG was observed and also MAP specific IgG showed significantly higher levels. Interestingly, a specific IgG response against MAP was also observed in children and adults with Crohn's disease (Verdier et al., 2013). Conversely, in ruminants antibodies against MAP are rarely detectable before clinically overt disease (Stabel, 1998). This might be due to immune evasion mechanisms of the bacteria which might differentially regulated in different species. Future investigations will have to follow the antibody titers in more detail over an extended time after infection, since three weeks might be too early for the evasion mechanisms to be effective in a chronic MAP infection.

A recent review suggested that large numbers of MAP might be found in the mesenteric tissue of Crohn's disease patients. MAP might infect endothelial cells and proliferate within them. This might cause focal obstruction within vessels leading to neo-angiogenesis and 'creeping fat' of mesenteric tissue as

observed in individuals with CD and JD (Pierce, 2009). Our study confirmed the presence of large numbers of MAP in the mesenteric tissue associated with granuloma formation and tissue destruction as well as thickening of mesentery. However, a more detailed analysis revealed that MAP resided predominantly in tissue macrophages in contrast to the postulated residence in endothelial cells (Pierce, 2009).

As discussed above, DSS treatment and MAP infection acts as ‘double hit’. This could exacerbate the disease since the immune system is confronted with two problems. However, we found that macrophages and both $CD4^+$ and $CD8^+$ T cells in the mLN of DSS+MAP treated mice were reduced compared to DSS+PBS treated animals. This might be due to cell death induced by the presence of MAP in mesentery or other means of bacterial immune evasion (Zur Lage et al., 2003).

A very important finding of this study was that animals of the DSS+MAP group showed an enhanced colonization of the colon by MAP. The bacteria might be attracted directly by signals of the damaged cells or by the inflammation. Most likely, MAP may use myeloid cells like monocytes/macrophages as Trojan horses to reach the inflamed tissue. This would also explain why the colon as primary target organ of DSS-induced tissue damage is most heavily colonized by MAP.

The mucosal damage itself may help MAP to better survive and persist within colonic tissue. The presence of MAP or MAP infected macrophages in the colon on the other hand might impair the healing process and thus explain the observed delay in tissue recovery. Alternatively, MAP could directly induce tissue destruction and delay mucosal tissue recovery. This is supported by the high expression of IFN-γ an important cytokine of the anti-mycobacterial host defense. Apparently, the presence of higher bacterial counts increased the IFN-γ expression. On the other hand, high expression of the anti-inflammatory cytokine IL-10 might be needed to ameliorate and protect from excessive tissue damage due to an overshooting immune response (Couper et al., 2008). Interestingly, one study showed complete removal of IL-10 leads to uncontrolled

inflammatory responses and disease progression in *Mycobacterium tuberculosis* infection (Higgins et al., 2009).

The different body weight pattern after first and secondary challenge might be due to the altered immune response after a secondary infection. A specific memory immune response is expected to elicit a stronger response. The reduction of body weight after secondary challenge with MAP might be due to the increased levels of cytokines and/or chemokines. Since TLR2 was also shown to be involved most likely the stronger response is elicited by a cross talk between the innate and the specific immune system. The innate immune activation activates a specific adaptive immune response that generates cytokines and chemokines storm.

Strikingly, clinical symptoms of CD and JD became apparent in our mouse MAP infection model. Diarrhea as well as a reduction colon length were observed after secondary challenge. A reduction of fluid absorption in colon was observed as well after secondary challenge with MAP. From previous studies, it was known that administration of anti-CD3 antibody leads to high fluid secretion or diarrhea. In this model, anti-CD3 injection causes systemic cytokine release and acute TNF-dependent diarrhea (Clayburgh et al., 2005; Musch et al., 2002). Hence, we hypothesized that after secondary challenge with MAP, adaptive immunity, T cells in particular, causes cytokines release which leads to reduction of fluid absorption or diarrhea. Nevertheless, there is no difference in both DSS-treated or untreated MAP infected after secondary challenge, neither from fluid absorption, nor TNF-α and IFN-γ level in serum and colon supernatant cytokines production. This might be because DSS-treated MAP infected colon is more sensitive to any trigger which leads to colitis after secondary challenge, whereas it is not the case in untreated MAP infected colon.

DSS treatment and MAP infection could exacerbate the disease since the immune system deal with two problems. Flow cytometry based analysis results from mesenteric lymph nodes showed increasing total number of leukocytes in DSS+MAP+MAP and DSS+MAP+PBS. This result suggested there is continuously immune activation and proliferation in the draining lymph nodes

due to chronic MAP infection and inflammation in the intestine. The phenotype supports the hypothesis that MAP could exacerbate the existing colitis.

A very important finding in this study was the observation of reduction of colon length only in DSS-treated MAP infected group after secondary challenge. $CD4^+$ T cell are the key players for this phenomenon. In mycobacteria infection, $CD4^+$ T cells were shown to have an important role in antibacterial protection (Ehlers and Schaible, 2012). The presence of $CD4^+$ T cells accelerates granulomatous response because of it enhances the production of TNF-α and IFN-γ at the site of infection (Hänsch et al., 1996). On the other hand, $CD4^+$ T cells also important in inducing colitis. Clonal T cell populations that are highly specific for intestinal bacterial antigen can induce colitis (Kullberg et al., 2003). $CD4^+$ T cell with high expression of CD45RB could induce a pathogenic Th1 response that leads to colitis (Powrie et al., 1994). Based on those finding, it was speculated that after secondary infection, MAP specific $CD4^+$T cells were activated and proliferated. This leads to production of effector T cells which then induce colitis.

Additionally, the increasing frequency of PMN in all groups that were infected at 5 week time point showed the recruitment of PMN during the acute phase of MAP infection. In contrast, increasing frequency of colonic inflammatory monocytes in all DSS-treated MAP infected groups showed that there is more immune activation. Recruitment of inflammatory monocytes is essential for controlling and clearance bacterial infection (Shi and Pamer, 2011). Under these conditions, the host is not only facing MAP but also bacterial translocation from intestine.

MAP showed different pathogenicity compared to the closely related mycobacteria species, such as MAA and MAH. Although both species showed higher immune activation from total liver and spleen weight, only MAP showed reduction of colon length after secondary challenge. This might be because only MAP has a correlation with JD and also CD which are inflammatory bowel disease in animals and human. This might be exerted by a differential tissue tropism which however needs to be demonstrated.

Discussion

An interesting finding in the present study is that no reduction of colon length in TLR2 deficient mice was observed after secondary challenge. This might be a clue for the mechanism of $CD4^+$ T cells reactivation in MAP infection. Previous study showed an importance of TLR2 in $CD4^+$ T cells induction or reactivation during mycobacteria infection (Heldwein et al., 2003). Based on that, the reactivation of $CD4^+$ T cells might need TLR2 signaling to become activated.

In conclusion, the present study provides evidence that MAP infection might exacerbate and prolong an existing inflammatory intestinal disease. Several aspects described for JD and CD such as the presence of MAP in macrophages of the mesenteric tissue or strong inflammation of the colonic mucosa were also observed in present model. Stronger immune responses were observed in MAP infection of inflamed tissue after secondary challenge. TLR2 appears to be necessary from the reactivation of $CD4^+$ T cells. This activation then leads to induction of colitis and diarrhea which are the clinical symptoms of JD and CD. Thus, the presented model might facilitate a more in-depth analysis of the association of MAP with intestinal mucosal inflammation including the underlying molecular mechanisms in the future.

.

5 Summary

In current study, it was hypothesized that MAP might not be the causative agent of CD, but exacerbating an already existing disease. Secondly, due to long disease progression from sub-clinical phase to the clinical phase and ubiquitous exposure of animals to environmental MAP, it was further hypothesized that infected animals will reveal the clinical symptoms after secondary exposure to MAP. This might be also the case in CD. Based on both hypotheses, dextran sulfate sodium-induced colitis was combined with MAP infection.

The exacerbation due to the infection was evident from the increasing liver and spleen weight after infection in DSS-treated MAP infected mice. In addition, higher number and larger liver granuloma were observed in that group. Furthermore, higher numbers of viable bacteria were found in the colon of DSS+MAP mice in comparison to untreated MAP infected mice. Interestingly, the tissue recovery was delayed in DSS+MAP in comparison to DSS-treated uninfected mice. Additionally, large numbers of MAP were found in mesentery that caused large granuloma and necrotic regions. Thus, according to the original hypothesis MAP infection indeed exacerbates the existing inflammation.

Upon secondary infection, DSS-treated MAP infected mice came down with diarrhea. Colitis was also observed. Both of which are also the clinical symptoms of JD and CD. An increased frequency of $CD4^+$ T cell in the colon and the prevention of colitis by depletion of $CD4^+$ T cells demonstrate the importance of $CD4^+$ T cells in the pathogenesis of MAP infection after secondary challenge. Interestingly, specific activity of MAP was found when other mycobacteria were compared and failed to induce similar effects. This might be due to a specific tissue tropism of MAP. Furthermore, reduction of colon length could not be observed in TLR2 deficient mice suggesting an involvement of innate receptors during reactivation of potentially MAP specific $CD4^+$ T cells.

Summary

Taken together, these results are consistent with the previous hypothesis that MAP exacerbates the existing colitis. Thus, the mouse model presented here reflects histopathological aspects of JD and might in the long run help to understand a possible association between MAP and CD in humans.

6 Appendix

6.1 Abbreviation

µg: microgram

µl: microliter

^{o}C: degree Celcius

AIDS: Acquired Immune Deficiency Syndrome

APC: antigen presenting cells

APC: allophycocyanin

ATG16L: Autophagy-related protein 16-1

BCG: Bacillus Calmette-Guérin

bp: basepairs

BSA: bovine serum albumin

C: cytosine

CARD: caspase-activating recruitment domain

CD: cluster of differentiation

CD: Crohn´s diseases

CFU: colony forming unit

Cm: centimeter

Cy: Cyianine

ddH_2O: double distilled water

DC: dendritic cells

DNA: deoxyribonucleic acid

DSS: Dextran Sulfate Sodium

DTT: dichlorodiphenyltrichloroethane

EDTA: Ethylenediaminetetraacetic acid

ELISA: Enzyme Linked Immunosorbent Assay

et al.: and others

FCS: Fetal Calf Serum

FITC: fluorescein isothiocyanate

FoxP3: Forkhead-Box-Protein P3

G: guanine

G-CSF: Gronulocytes-stimulating factor

GM-CSF: colony-stimulating factor

GWAS: genome-wide association studies

h.: hours

H&E: hematoxylin and eosin

HEK: Human Embryonic Kidney

HEPES: 4-(2-hydroxyethyl)-1-piperazineethanesulfonic acid

Appendix

i.p.: intraperitoneal

IBD: inflammatory bowel disease

IFN: interferon

Ig: Immunoglobulin

IL: interleukin

IS: Insertion Element

IMDM: Iscove's Modified Dulbecco's Medium

JD: Johne´s disease

KC: Keratinocyte-Derived Chemokine

l: liter

LAM: lipoarabinomannan

LM: Lipomannan

LPS: Lipopolysaccharide

Ly6: lymphocytes antigen 6 complex

M: molar

MAA: Mycobacterium avium ssp. avium

MAC: Mycobacterium avium complex

MAH : Mycobacterium avium ssp. hominissuis

MAP: Mycobacterium avium ssp. paratuberculosis

MCP-1: monocyte chemoattractant protein-1

mg: milligram

MHC-I: major histocompatibility complex class one

MHC-II: major histocompatibility complex class two

MIP: macrophage inflammatory protein

ml: milliliter

mLN: mesenteric lymph nodes

mm: millimeter

mM: millimolar

MPO: myeloperoxidase

MTB: Mycobacterium tuberculosis

NOD: nucleotide oligomerization domain

NK: Natural killer

n.d: not detectable

n.s: not significant

PAMPs: Pathogen-associated molecular patterns

PBMC: peripheral blood mononuclear cells

PBS: Phosphate buffered saline

PCR: polymerase chain reaction

PE: Phycoerythrin

PerCP: peridinin chlorophyll protein

p.i: post infection

PMN: Polymorphonuclear

RAG: recombination activating gene

Appendix

RANTES: Regulated on Activation Normal T Cell Expressed and Secreted

RPMI: Roswell Park Memorial Institute

RNA: Ribonucleic Acid

STAT3: Signal Transducer and Activator of Transcription 3

TGFβ: Transforming Growth Factor-β

TLR: Toll-like receptor

TNF: Tumor Necrosis Factor

w.k: week

ZN: Ziehl Neelsen

6.2 References

Abubakar, I., D. Myhill, S.H. Aliyu, and P.R. Hunter. 2008. Detection of Mycobacterium avium subspecies paratuberculosis from patients with Crohn's disease using nucleic acid-based techniques: A systematic review and meta-analysis. *Inflammatory Bowel Diseases*. 14:401-410 410.1002/ibd.20276.

Baumgart, D.C., and W.J. Sandborn. 2007. Inflammatory bowel disease: clinical aspects and established and evolving therapies. *The Lancet*. 369:1641-1657.

Bermudez, L.E., M. Petrofsky, S. Sommer, and R.G. Barletta. 2010. Peyer's patch-deficient mice demonstrate that Mycobacterium avium subsp. paratuberculosis translocates across the mucosal barrier via both M cells and enterocytes but has inefficient dissemination. *Infection and immunity*. 78:3570-3577.

Bruijnesteijn van Coppenraet, L.E.S., P.E.W. Haas, J.A. Lindeboom, E.J. Kuijper, and D. Soolingen. 2008. Lymphadenitis in children is caused by Mycobacterium avium hominissuis and not related to ‘bird tuberculosis’. *Eur J Clin Microbiol Infect Dis*. 27:293-299.

Bull, T.J., E.J. McMinn, K. Sidi-Boumedine, A. Skull, D. Durkin, P. Neild, G. Rhodes, R. Pickup, and J. Hermon-Taylor. 2003. Detection and verification of Mycobacterium avium subsp. paratuberculosis in fresh ileocolonic mucosal biopsy specimens from individuals with and without Crohn's disease. *Journal of clinical microbiology*. 41:2915-2923.

Cadwell, K., K.K. Patel, N.S. Maloney, T.C. Liu, A.C. Ng, C.E. Storer, R.D. Head, R. Xavier, T.S. Stappenbeck, and H.W. Virgin. 2010. Virus-plus-susceptibility gene interaction determines Crohn's disease gene Atg16L1 phenotypes in intestine. *Cell*. 141:1135-1145.

Appendix

Carta, T., J. Álvarez, J.M. Pérez de la Lastra, and C. Gortázar. 2013. Wildlife and paratuberculosis: A review. *Research in Veterinary Science*. 94:191-197.

Cerf-Bensussan, N., and V. Gaboriau-Routhiau. 2010. The immune system and the gut microbiota: friends or foes? *Nature reviews. Immunology*. 10:735-744.

Chassaing, B., and A. Darfeuille-Michaud. 2011. The commensal microbiota and enteropathogens in the pathogenesis of inflammatory bowel diseases. *Gastroenterology*. 140:1720-1728.

Chiodini, R.J., and C.D. Buergelt. 1993. Susceptibility of Balb/c, C57/B6 and C57/B10 mice to infection with Mycobacterium paratuberculosis. *Journal of comparative pathology*. 109:309-319.

Chiodini, R.J., W.M. Chamberlin, J. Sarosiek, and R.W. McCallum. 2012. Crohn's disease and the mycobacterioses: A quarter century later. Causation or simple association? *Critical reviews in microbiology*. 38:52-93.

Chiodini, R.J., H.J. Van Kruiningen, W.R. Thayer, and J.A. Coutu. 1986. Spheroplastic phase of mycobacteria isolated from patients with Crohn's disease. *Journal of clinical microbiology*. 24:357-363.

Cho, J.H. 2008. The genetics and immunopathogenesis of inflammatory bowel disease. *Nature reviews. Immunology*. 8:458-466.

Clarke, C.J. 1997. The pathology and pathogenesis of paratuberculosis in ruminants and other species. *Journal of comparative pathology*. 116:217-261.

Clayburgh, D.R., T.A. Barrett, Y. Tang, J.B. Meddings, L.J. Van Eldik, D.M. Watterson, L.L. Clarke, R.J. Mrsny, and J.R. Turner. 2005. Epithelial myosin light chain kinase–dependent barrier dysfunction mediates T cell activation–induced diarrhea in vivo. *The Journal of Clinical Investigation*. 115:2702-2715.

Collins, M.T. 1997. Mycobacterium paratuberculosis: A Potential Food-Borne Pathogen? *Journal of Dairy Science*. 80:3445-3448.

Consortium, T.W.T.C.C. 2007. Genome-wide association study of 14,000 cases of seven common diseases and 3,000 shared controls. *Nature*. 447:661-678.

Cooper, A.M., D.K. Dalton, T.A. Stewart, J.P. Griffin, D.G. Russell, and I.M. Orme. 1993. Disseminated tuberculosis in interferon gamma gene-disrupted mice. *The Journal of experimental medicine*. 178:2243-2247.

Cosma, C.L., D.R. Sherman, and L. Ramakrishnan. 2003. THE SECRET LIVES OF THE PATHOGENIC MYCOBACTERIA. *Annual review of microbiology*. 57:641-676.

Appendix

Couper, K.N., D.G. Blount, and E.M. Riley. 2008. IL-10: The Master Regulator of Immunity to Infection. *The Journal of Immunology*. 180:5771-5777.

Dieleman, Palmen, Akol, Bloemena, PeÑA, Meuwissen, and R. Van. 1998. Chronic experimental colitis induced by dextran sulphate sodium (DSS) is characterized by Th1 and Th2 cytokines. *Clinical & Experimental Immunology*. 114:385-391.

Dorhoi, A., S.T. Reece, and S.H.E. Kaufmann. 2011. For better or for worse: the immune response against Mycobacterium tuberculosis balances pathology and protection. *Immunological Reviews*. 240:235-251.

Ehlers, S., and U.E. Schaible. 2012. The granuloma in tuberculosis: dynamics of a host-pathogen collusion. *Frontiers in immunology*. 3:411.

Falkinham, J.O., C.D. Norton, and M.W. LeChevallier. 2001. Factors Influencing Numbers of Mycobacterium avium, Mycobacterium intracellulare, and Other Mycobacteria in Drinking Water Distribution Systems. *Applied and environmental microbiology*. 67:1225-1231.

Feller, M., K. Huwiler, R. Stephan, E. Altpeter, A. Shang, H. Furrer, G.E. Pfyffer, T. Jemmi, A. Baumgartner, and M. Egger. 2007. Mycobacterium avium subspecies paratuberculosis and Crohn's disease: a systematic review and meta-analysis. *The Lancet infectious diseases*. 7:607-613.

Ferwerda, G., B.J. Kullberg, D.J. de Jong, S.E. Girardin, D.M.L. Langenberg, R. van Crevel, T.H.M. Ottenhoff, J.W.M. Van der Meer, and M.G. Netea. 2007. Mycobacterium paratuberculosis is recognized by Toll-like receptors and NOD2. *Journal of leukocyte biology*. 82:1011-1018.

Franke, A., D.P.B. McGovern, J.C. Barrett, K. Wang, G.L. Radford-Smith, T. Ahmad, C.W. Lees, T. Balschun, J. Lee, R. Roberts, C.A. Anderson, J.C. Bis, S. Bumpstead, D. Ellinghaus, E.M. Festen, M. Georges, T. Green, T. Haritunians, L. Jostins, A. Latiano, C.G. Mathew, G.W. Montgomery, N.J. Prescott, S. Raychaudhuri, J.I. Rotter, P. Schumm, Y. Sharma, L.A. Simms, K.D. Taylor, D. Whiteman, C. Wijmenga, R.N. Baldassano, M. Barclay, T.M. Bayless, S. Brand, C. Buning, A. Cohen, J.-F. Colombel, M. Cottone, L. Stronati, T. Denson, M. De Vos, R. D'Inca, M. Dubinsky, C. Edwards, T. Florin, D. Franchimont, R. Gearry, J. Glas, A. Van Gossum, S.L. Guthery, J. Halfvarson, H.W. Verspaget, J.-P. Hugot, A. Karban, D. Laukens, I. Lawrance, M. Lemann, A. Levine, C. Libioulle, E. Louis, C. Mowat, W. Newman, J. Panes, A. Phillips, D.D. Proctor, M. Regueiro, R. Russell, P. Rutgeerts, J. Sanderson, M. Sans, F. Seibold, A.H. Steinhart, P.C.F. Stokkers, L. Torkvist, G. Kullak-Ublick, D. Wilson, T. Walters, S.R. Targan, S.R. Brant, J.D. Rioux, M. D'Amato, R.K. Weersma, S. Kugathasan, A.M. Griffiths, J.C. Mansfield, S. Vermeire, R.H. Duerr, M.S.

Appendix

Silverberg, J. Satsangi, S. Schreiber, J.H. Cho, V. Annese, H. Hakonarson, M.J. Daly, and M. Parkes. 2010. Genome-wide meta-analysis increases to 71 the number of confirmed Crohn's disease susceptibility loci. *Nature genetics*. 42:1118-1125.

Ghosh, P., C.-w. Wu, and A.M. Talaat. 2013. Key Role for the Alternative Sigma Factor, SigH, in the Intracellular Life of Mycobacterium avium subsp. paratuberculosis during Macrophage Stress. *Infection and immunity*. 81:2242-2257.

Grant, I.R. 2005. Zoonotic potential of Mycobacterium avium ssp. paratuberculosis: the current position. *Journal of Applied Microbiology*. 98:1282-1293.

Grant, I.R., H.J. Ball, S.D. Neill, and M.T. Rowe. 1996. Inactivation of Mycobacterium paratuberculosis in cows' milk at pasteurization temperatures. *Applied and environmental microbiology*. 62:631-636.

Green, E.P., M.L.V. Tizard, M.T. Moss, J. Thompson, D.J. Winterbourne, J.J. McFadden, and J. Hermon-Taylor. 1989. Sequence and characteristics or IS900, an insertion element identified in a human Crohn's disease isolate or Mycobacterium paratuberculosis. *Nucleic Acids Research*. 17:9063-9073.

Greenstein, R.J. 2003. Is Crohn's disease caused by a mycobacterium? Comparisons with leprosy, tuberculosis, and Johne's disease. *The Lancet infectious diseases*. 3:507-514.

Greenstein, R.J., and M.T. Collins. Emerging pathogens: is Mycobacterium avium subspecies paratuberculosis zoonotic? *The Lancet*. 364:396-397.

Hänsch, H.C.R., D.A. Smith, M.E.A. Mielke, H. Hahn, G.J. Bancroft, and S. Ehlers. 1996. Mechanisms of granuioma formation in murine Mycobacterium avium infection: the contribution of CD4+ T cells. *International Immunology*. 8:1299-1310.

Harris, N.B., and R.G. Barletta. 2001. Mycobacterium avium subsp. paratuberculosisin Veterinary Medicine. *Clinical Microbiology Reviews*. 14:489-512.

Heldwein, K.A., M.D. Liang, T.K. Andresen, K.E. Thomas, A.M. Marty, N. Cuesta, S.N. Vogel, and M.J. Fenton. 2003. TLR2 and TLR4 serve distinct roles in the host immune response against Mycobacterium bovis BCG. *Journal of leukocyte biology*. 74:277-286.

Hermon-Taylor, J., and T. Bull. 2002. Crohn's disease caused by Mycobacterium avium subspecies paratuberculosis: a public health tragedy whose resolution is long overdue. *J Med Microbiol*. 51:3-6.

Appendix

Higgins, D.M., J. Sanchez-Campillo, A.G. Rosas-Taraco, E.J. Lee, I.M. Orme, and M. Gonzalez-Juarrero. 2009. Lack of IL-10 alters inflammatory and immune responses during pulmonary Mycobacterium tuberculosis infection. *Tuberculosis (Edinburgh, Scotland)*. 89:149-157.

Hostetter, J.M., E.M. Steadham, J.S. Haynes, T.B. Bailey, and N.F. Cheville. 2002. Cytokine effects on maturation of the phagosomes containing Mycobacteria avium subspecies paratuberculosis in J774 cells. *FEMS Immunology & Medical Microbiology*. 34:127-134.

Johansson, M.E.V., H. Sjovall, and G.C. Hansson. 2013. The gastrointestinal mucus system in health and disease. *Nat Rev Gastroenterol Hepatol*. 10:352-361.

Kappelman, M.D., S.L. Rifas–Shiman, K. Kleinman, D. Ollendorf, A. Bousvaros, R.J. Grand, and J.A. Finkelstein. 2007. The Prevalence and Geographic Distribution of Crohn's Disease and Ulcerative Colitis in the United States. *Clinical gastroenterology and hepatology : the official clinical practice journal of the American Gastroenterological Association*. 5:1424-1429.

Kirkland, D., A. Benson, J. Mirpuri, R. Pifer, B. Hou, Anthony L. DeFranco, and F. Yarovinsky. 2012. B Cell-Intrinsic MyD88 Signaling Prevents the Lethal Dissemination of Commensal Bacteria during Colonic Damage. *Immunity*. 36:228-238.

Kuehnel, M.P., R. Goethe, A. Habermann, E. Mueller, M. Rohde, G. Griffiths, and P. Valentin-Weigand. 2001. Characterization of the intracellular survival of Mycobacterium avium ssp. paratuberculosis: phagosomal pH and fusogenicity in J774 macrophages compared with other mycobacteria. *Cellular Microbiology*. 3:551-566.

Kullberg, M.C., J.F. Andersen, P.L. Gorelick, P. Caspar, S. Suerbaum, J.G. Fox, A.W. Cheever, D. Jankovic, and A. Sher. 2003. Induction of colitis by a CD4+ T cell clone specific for a bacterial epitope. *Proceedings of the National Academy of Sciences*. 100:15830-15835.

Li, M.O., and R.A. Flavell. 2008. Contextual Regulation of Inflammation: A Duet by Transforming Growth Factor-^{2} and Interleukin-10. *Immunity*. 28:468-476.

Loftus, E.V. 2004. Clinical epidemiology of inflammatory bowel disease: incidence, prevalence, and environmental influences. *Gastroenterology*. 126:1504-1517.

Lybeck, K.R., M. Løvoll, T.B. Johansen, I. Olsen, A.K. Storset, and M. Valheim. 2013. Intestinal Strictures, Fibrous Adhesions and High Local Interleukin-10

Appendix

Levels in Goats Infected Naturally with Mycobacterium avium subsp. paratuberculosis. *Journal of comparative pathology*. 148:157-172.

Maynard, C.L., and C.T. Weaver. 2009. Intestinal Effector T Cells in Health and Disease. *Immunity*. 31:389-400.

Merkal, R., and W. McCullough. 1982. A new mycobactin, mycobactin J, fromMycobacterium paratuberculosis. *Current Microbiology*. 7:333-335.

Merkal, R.S., and B.J. Curran. 1974. Growth and Metabolic Characteristics of Mycobacterium paratuberculosis. *Applied Microbiology*. 28:276-279.

Millar, D., J. Ford, J. Sanderson, S. Withey, M. Tizard, T. Doran, and J. Hermon-Taylor. 1996. IS900 PCR to detect Mycobacterium paratuberculosis in retail supplies of whole pasteurized cows' milk in England and Wales. *Applied and environmental microbiology*. 62:3446-3452.

Momotani, E., D.L. Whipple, A.B. Thiermann, and N.F. Cheville. 1988. Role of M Cells and Macrophages in the Entrance of Mycobacterium paratuberculosis into Domes of Ileal Peyer's Patches in Calves. *Veterinary Pathology Online*. 25:131-137.

Musch, M.W., L.L. Clarke, D. Mamah, L.R. Gawenis, Z. Zhang, W. Ellsworth, D. Shalowitz, N. Mittal, P. Efthimiou, Z. Alnadjim, S.D. Hurst, E.B. Chang, and T.A. Barrett. 2002. T cell activation causes diarrhea by increasing intestinal permeability and inhibiting epithelial Na+/K+-ATPase. *The Journal of Clinical Investigation*. 110:1739-1747.

Mutwiri, G.K., D.G. Butler, S. Rosendal, and J. Yager. 1992. Experimental infection of severe combined immunodeficient beige mice with Mycobacterium paratuberculosis of bovine origin. *Infection and immunity*. 60:4074-4079.

Olsen, I., Ó.G. Sigurðardóttir, and B. Djønne. 2002. Paratuberculosis with special reference to cattle A review. *Veterinary Quarterly*. 24:12-28.

Over, K., P.G. Crandall, C.A. O'Bryan, and S.C. Ricke. 2011. Current perspectives on Mycobacterium avium subsp. paratuberculosis, Johne's disease, and Crohn's disease: a Review. *Critical reviews in microbiology*. 37:141-156.

Pierce, E.S. 2009. Where are all the Mycobacterium avium subspecies paratuberculosis in patients with Crohn's disease? *PLoS pathogens*. 5:e1000234.

Pott, J., T. Basler, C.U. Duerr, M. Rohde, R. Goethe, and M.W. Hornef. 2009. Internalization-dependent recognition of Mycobacterium avium ssp.

paratuberculosis by intestinal epithelial cells. *Cellular Microbiology*. 11:1802-1815.

Powrie, F., R. Correa-Oliveira, S. Mauze, and R.L. Coffman. 1994. Regulatory interactions between CD45RBhigh and CD45RBlow CD4+ T cells are important for the balance between protective and pathogenic cell-mediated immunity. *The Journal of experimental medicine*. 179:589-600.

Qualls, J.E., A.M. Kaplan, N. van Rooijen, and D.A. Cohen. 2006. Suppression of experimental colitis by intestinal mononuclear phagocytes. *Journal of leukocyte biology*. 80:802-815.

Rioux, J.D., R.J. Xavier, K.D. Taylor, M.S. Silverberg, P. Goyette, A. Huett, T. Green, P. Kuballa, M.M. Barmada, L.W. Datta, Y.Y. Shugart, A.M. Griffiths, S.R. Targan, A.F. Ippoliti, E.J. Bernard, L. Mei, D.L. Nicolae, M. Regueiro, L.P. Schumm, A.H. Steinhart, J.I. Rotter, R.H. Duerr, J.H. Cho, M.J. Daly, and S.R. Brant. 2007. Genome-wide association study identifies new susceptibility loci for Crohn disease and implicates autophagy in disease pathogenesis. *Nature genetics*. 39:596-604.

Sakaguchi, S., N. Sakaguchi, M. Asano, M. Itoh, and M. Toda. 1995. Immunologic self-tolerance maintained by activated T cells expressing IL-2 receptor alpha-chains (CD25). Breakdown of a single mechanism of self-tolerance causes various autoimmune diseases. *The Journal of Immunology*. 155:1151-1164.

Saleh, M., and C.O. Elson. 2011. Experimental inflammatory bowel disease: insights into the host-microbiota dialog. *Immunity*. 34:293-302.

Sartor, R.B. 2006. Mechanisms of Disease: pathogenesis of Crohn's disease and ulcerative colitis. *Nat Clin Pract Gastroenterol Hepatol*. 3:390-407.

Saunders, B.M., and W.J. Britton. 2007. Life and death in the granuloma: immunopathology of tuberculosis. *Immunology and cell biology*. 85:103-111.

Saunders, B.M., A.A. Frank, I.M. Orme, and A.M. Cooper. 2002. CD4 is required for the development of a protective granulomatous response to pulmonary tuberculosis. *Cellular immunology*. 216:65-72.

Schulze-Röbbecke, R., and K. Buchholtz. 1992. Heat susceptibility of aquatic mycobacteria. *Applied and environmental microbiology*. 58:1869-1873.

Selby, W.S. 2004. Mycobacterium avium subspecies paratuberculosis bacteraemia in patients with inflammatory bowel disease. *Lancet*. 364:1013-1014.

Appendix

Shi, C., and E.G. Pamer. 2011. Monocyte recruitment during infection and inflammation. *Nature reviews. Immunology*. 11:762-774.

Singh, A.K., B. Riederer, M. Chen, F. Xiao, A. Krabbenhöft, R. Engelhardt, O. Nylander, M. Soleimani, and U. Seidler. 2010. The switch of intestinal Slc26 exchangers from anion absorptive to HCO3− secretory mode is dependent on CFTR anion channel function. *American Journal of Physiology - Cell Physiology*. 298:C1057-C1065.

Sohal, J.S., S.V. Singh, P. Tyagi, S. Subhodh, P.K. Singh, A.V. Singh, K. Narayanasamy, N. Sheoran, and K. Singh Sandhu. 2008. Immunology of mycobacterial infections: With special reference to Mycobacterium avium subspecies paratuberculosis. *Immunobiology*. 213:585-598.

Souza, C.D., O.A. Evanson, and D.J. Weiss. 2006. Regulation by Jun N-terminal kinase/stress activated protein kinase of cytokine expression in Mycobacterium avium subsp paratuberculosis–infected bovine monocytes. *American Journal of Veterinary Research*. 67:1760-1765.

Spurr, A.R. 1969. A low-viscosity epoxy resin embedding medium for electron microscopy. *Journal of Ultrastructure Research*. 26:31-43.

Stabel, J.R. 1998. Johne's Disease: A Hidden Threat. *Journal of Dairy Science*. 81:283-288.

Sung, N., and M.T. Collins. 1998. Thermal Tolerance of Mycobacterium paratuberculosis. *Applied and environmental microbiology*. 64:999-1005.

Valentin-Weigand, P., and R. Goethe. 1999. Pathogenesis of Mycobacterium avium subspecies paratuberculosis infections in ruminants: still more questions than answers. *Microbes and Infection*. 1:1121-1127.

Veazey, R.S., D.W. Horohov, J.L. Krahenbuhl, H.W. Taylor, J.L. Oliver, and T.G. Snider Iii. 1996. Differences in the kinetics of T cell accumulations in C3HHeN (Bcg-resistant) and C57BL6 (Bcg-susceptible) mice infected with Mycobacterium paratuberculosis. *Comparative Immunology, Microbiology and Infectious Diseases*. 19:289-304.

Verdier, J., L. Deroche, M. Allez, C. Loy, F. Biet, C.C. Bodier, S. Bay, C. Ganneau, T. Matysiak-Budnik, J.M. Reyrat, M. Heyman, N. Cerf-Bensussan, F.M. Ruemmele, and S. Ménard. 2013. Specific IgG Response against *Mycobacterium avium paratuberculosis* in Children and Adults with Crohn's Disease. *PLoS ONE*. 8:e62780.

Weiss, D.J., O.A. Evanson, D.J. McClenahan, M.S. Abrahamsen, and B.K. Walcheck. 2001. Regulation of Expression of Major Histocompatibility Antigens by Bovine Macrophages Infected withMycobacterium avium subsp.

paratuberculosis orMycobacterium avium subsp. avium. *Infection and immunity*. 69:1002-1008.

Whitlock, R.H., and C. Buergelt. 1996. Preclinical and clinical manifestations of paratuberculosis (including pathology). *The Veterinary clinics of North America. Food animal practice*. 12:345-356.

Wirtz, S., C. Neufert, B. Weigmann, and M.F. Neurath. 2007. Chemically induced mouse models of intestinal inflammation. *Nature protocols*. 2:541-546.

Woo, S.-R., J.A. Heintz, R. Albrecht, R.G. Barletta, and C.J. Czuprynski. 2007. Life and death in bovine monocytes: The fate of Mycobacterium avium subsp. paratuberculosis. *Microbial Pathogenesis*. 43:106-113.

Wu, C.-w., M. Livesey, S.K. Schmoller, E.J.B. Manning, H. Steinberg, W.C. Davis, M.J. Hamilton, and A.M. Talaat. 2007. Invasion and Persistence of Mycobacterium avium subsp. paratuberculosis during Early Stages of Johne's Disease in Calves. *Infection and immunity*. 75:2110-2119.

Zigmond, E., C. Varol, J. Farache, E. Elmaliah, Ansuman T. Satpathy, G. Friedlander, M. Mack, N. Shpigel, Ivo G. Boneca, Kenneth M. Murphy, G. Shakhar, Z. Halpern, and S. Jung. 2012. Ly6Chi Monocytes in the Inflamed Colon Give Rise to Proinflammatory Effector Cells and Migratory Antigen-Presenting Cells. *Immunity*. 37:1076-1090.

Zur Lage, S., R. Goethe, A. Darji, P. Valentin-Weigand, and S. Weiss. 2003. Activation of macrophages and interference with CD4+ T-cell stimulation by Mycobacterium avium subspecies paratuberculosis and Mycobacterium avium subspecies avium. *Immunology*. 108:62-69.

6.3 List of Figures

Appendix

6.4 List of Tables

CURRICULUM VITAE

Personal Information

Name:	Abdulhadi Suwandi
Date of Birth:	11.12.1982
Place of Birth:	Bandung, Indonesia
Nationality:	indonesia
Address:	Magdeburgstr. 32, 38124 Braunschweig

Educational Background

07.2010 – 12.2013	PhD student in Molecular Immunology at Helmholtz-Zentrum für Infektionsforschung, Braunschweig
03.2009 – 09.2009	Master thesis in research group Immunregulation at Center for Regenerative Therapies Dresden, Dresden (Dr. Karsten Kretschmer)
10.2007 - 09.2009	Master Programm in Molecular Bioengineering at Technische Universität Dresden, Dresden (Master of Science)
10.2005 – 05.2007	Apothecary Profession Programm in Department of Pharmacy at Bandung Institute of Technology, Bandung Indonesia (Pharmacist).
01.2005 – 08.2005	Bachelor thesis in research group Pharmaceutical Biotechnology at Bandung Institute of Technology, Bandung, Indonesia (Dr. Debbie S. Retnoningrum).
08.2001-09.2005	Bachelor in Pharmacy in Department of Pharmacy at Bandung Institute of Technology, Bandung, Indonesia (Bachelor of Science)
1998 – 2001	High School at Taruna Bakti, Bandung, Indonesia

Publications

Suwandi, A., Bargen, I., Roy, B., Pils, M.C., Krey, M., Zur Lage, S., Basler, T., Rohde, M., Falk, C.S., Hornef, M.W., Goethe, R., Weiß, S.: Experimental colitis is exacerbated by concomitant infection with *Mycobacterium avium* subsp. *paratuberculosis* (submitted).

Suwandi, A., Bargen, I., Pils, M.C., Krey, M., Zur Lage, S., Singh, A.K., Basler, T., Falk, C.S., Seidler, U., Hornef, M.W., Goethe, R., Weiß, S.: Role of CD4+ T cells inducing colitis after secondary challenge with *Mycobacterium avium* subsp. *paratuberculosis* in mice (in preparation).

Koc, A., Bargen, I., **Suwandi, A**., Rodenfeld, M., Tschuschner, A., Rath, T., Gerlach, G.G., Hornef, M.W., Goethe, R., Weiss, S., Roeb, E.: Systemic and mucosal immune reactivity upon *Mycobacterium avium ssp. paratuberculosis* infection in mice (in revision).

Meissner, T., Basler, T., Meens, J., Eckelt, E., Heinzmann, J., **Suwandi, A**., Oelemann, W., Trenkamp,S., Holst, O., Gerlach, G.F., Goethe, R. : Investigation of an isogenic *Mycobacterium avium ssp. paratuberculosis* mptD mutant reveals novel insights into the role of lipid metabolism for adaptation to the host environment (submitted).

Acknowledgement

First of all, I would like to give special thanks to Allah Subhanahu wa ta'ala who has given me patience, health, energy, peace and power to meet the challenges of higher education and to succeed.

Second, I would like to thank to my supervisor Dr. Siegfried Weiss who has given me the opportunity to become his student, his support for my study and personal life.

I would like to thank my thesis committee member and also collaborator Prof. Mathias W. Hornef and Prof. Ralph Goethe for giving me lots of input for the project and also make me not to lose my faith to the project.

I also would like to thank the whole Molecular Immunology group, especially Martina Krey, Imke Bargen and Susanne Zur Lage for their help and support. Tina Basler and the members of ZooMAP consortium for their support and help. The HZI Graduate School that gave me opportunity to learn a lot about the infection biology field.

Importantly, I would like to thank my family, my wife Dina who is always support me and being patient. My children, Fathurrahmaan and Fathiya Rahiim who always become my inspiration and energy.